UNCLASSIFIED

AD NUMBER
AD893021
LIMITATION CHANGES

TO:

Approved for public release; distribution is unlimited.

FROM:

Distribution authorized to U.S. Gov't. agencies only; Test and Evaluation; MAR 1972. Other requests shall be referred to Air Force Armament Laboratory, DLGC, Eglin AFB, FL 32542.

AUTHORITY
afatl ltr, 20 nov 1975

THIS PAGE IS UNCLASSIFIED

AEDC-TR-72-47
AFATL-TR-72-57

cy.2

SEPARATION CHARACTERISTICS OF THE REDESIGNED LAU-61/A ROCKET LAUNCHER FROM THE F-4C AIRCRAFT AT MACH NUMBERS FROM 0.53 TO 0.94

R. A. Paulk

ARO, Inc.

March 1972

This document has been approved for public release its distribution is unlimited. *Rev TAB 76-6, D+d 12 march, 1976*

PROPULSION WIND TUNNEL FACILITY

ARNOLD ENGINEERING DEVELOPMENT CENTER

AIR FORCE SYSTEMS COMMAND

ARNOLD AIR FORCE STATION, TENNESSEE

NOTICES

SEPARATION CHARACTERISTICS OF THE REDESIGNED LAU-61/A ROCKET LAUNCHER FROM THE F-4C AIRCRAFT AT MACH·NUMBERS FROM 0.53 TO 0.94

R. A. Paulk
ARO, Inc.

FOREWORD

The work reported herein was sponsored by the Air Force Armament Laboratory (DLGC/Bob Hume), Armament Development and Test Center, Air Force Systems Command (AFSC), under Program Element 64602F, Project 2592, Task 04.

The test results presented were obtained by ARO, Inc. (a subsidiary of Sverdrup & Parcel and Associates, Inc.), contract operator of the Arnold Engineering Development Center (AEDC), AFSC, Arnold Air Force Station, Tennessee, under Contract F40600-72-C-0003. The test was conducted from January 7 to 14, 1972, under ARO Project No. PC0231. The manuscript was submitted for publication on February 22, 1972.

This technical report has been reviewed and is approved.

George F. Garey   Frank J. Passarello
Lt Colonel, USAF   Colonel, USAF
AF Representative, PWT   Acting Director
Directorate of Test   Directorate of Test

ABSTRACT

A captive-trajectory store separation test was conducted using 0.05-scale models of the F-4C aircraft and the redesigned LAU-61/A rocket launcher (full and empty). The stores were launched from the Multiple Ejection Rack and the Triple Ejection Rack from the centerline pylon and the right-wing inboard pylon, respectively. For the redesigned LAU-61/A the support lugs will be shifted forward either 6 or 3 in. Both positions were used in these tests. The tests were run at Mach numbers 0.53 to 0.94 and at the parent-aircraft angle of attack to give level flight at a simulated altitude of 5000 ft. At selected conditions some of the trajectories were obtained for both constant and time-variant ejector forces.

CONTENTS

APPENDIXES

I. ILLUSTRATIONS

Figure

NOMENCLATURE

BL   Aircraft buttock line from plane of symmetry, in., model scale

b   Store reference dimension, 1.308 ft, full scale

C_m Store pitching-moment coefficient, referenced to the store cg, pitching
            moment/$q_\infty Sb$

C_{m_q}	Store pitch-damping derivative, $dC_m/d(qb/2V_\infty)$
C_n	Store yawing-moment coefficient, referenced to the store cg, yawing moment/$q_\infty Sb$
C_{n_r}	Store yaw-damping derivative, $dC_n/d(rb/2V_\infty)$
E-1, E-2	Time-variant ejector force functions
E-3	Constant ejector force
FS	Aircraft fuselage station, in., model scale
I_{xx}	Full-scale moment of inertia about the store X_B axis, slug-ft^2
I_{yy}	Full-scale moment of inertia about the store Y_B axis, slug-ft^2
I_{zz}	Full-scale moment of inertia about the store Z_B axis, slug-ft^2
M_∞	Free-stream Mach number
$\overline{m}$	Full-scale store mass, slugs
p_∞	Free-stream static pressure, psfa
q	Store angular velocity about the Y_B axis, radians/sec
q_∞	Free-stream dynamic pressure, $0.7\, p_\infty M_\infty^2$, psf
r	Store angular velocity about the Z_B axis, radians/sec
S	Store reference area, 1.344 ft^2, full scale
t	Real trajectory time from initiation of trajectory, sec
V_∞	Free-stream velocity, ft/sec
WL	Aircraft waterline from reference horizontal plane, in., model scale
X	Separation distance of the store cg parallel to the flight axis system X_F direction, ft, full scale measured from the prelaunch position
X_{cg}	Full-scale cg location, ft, from nose of store
X_L	Ejector piston location relative to the store cg, positive forward of store cg, ft, full scale

Y   Separation distance of the store cg parallel to the flight-axis system Y_F direction, ft, full scale measured from the prelaunch position

Z   Separation distance of the store cg parallel to the flight-axis system Z_F direction, ft, full scale measured from the prelaunch position

a Parent-aircraft model angle of attack relative to the free-stream velocity vector, deg

θ Angle between the store longitudinal axis and its projection in the X_F-Y_F plane, positive when store nose is raised as seen by pilot, deg

ψ Angle between the projection of the store longitudinal axis in the X_F-Y_F plane and the X_F axis, positive when the store nose is to the right as seen by the pilot, deg

FLIGHT-AXIS SYSTEM COORDINATES

Directions

X_F Parallel to the free-stream wind vector, positive direction is forward as seen by the pilot

Y_F Perpendicular to the X_F and Z_F directions, positive direction is to the right as seen by the pilot

Z_F In the aircraft plane of symmetry, perpendicular to the free-stream wind vector, positive direction is downward as seen by the pilot

The flight-axis system origin is coincident with the aircraft cg and remains fixed with respect to the parent aircraft during store separation. The X_F, Y_F, and Z_F coordinate axes do not rotate with respect to the initial flight direction and attitude.

STORE BODY-AXIS SYSTEM COORDINATES

Directions

X_B Parallel to the store longitudinal axis, positive direction is upstream in the prelaunch position

Y_B Perpendicular to the store longitudinal axis, and parallel to the flight-axis system X_F-Y_F plane when the store is at zero roll angle, positive direction is to the right as seen by the pilot when the store is at zero yaw and roll angles

Z_B Perpendicular to both the X_B and Y_B axes, positive direction is downward as seen by the pilot when the store is at zero pitch and roll angles.

The store body-axis system origin is coincident with the store cg and moves with the store during separation from the parent airplane. The X_B, Y_B, and Z_B coordinate axes rotate with the store in pitch, yaw, and roll so that mass moments of inertia about the three axes are not time-varying quantities.

SECTION I
INTRODUCTION

This investigation was conducted in the Aerodynamic Wind Tunnel (4T) of the Propulsion Wind Tunnel Facility (PWT) to obtain captive-trajectory store separation data for the redesigned LAU-61/A rocket launcher from the F-4C aircraft. The full and empty LAU-61/A rocket launchers have been previously certified for separation from the F-4C and other military aircraft. However, the recent requirement of heavier warheads on the rockets has caused a forward shift of the cg of the full launcher resulting in excessive loading and structural failure of the forward support lug on the LAU-61/A. To reduce the load on the forward lug the lugs will be moved forward either 3 or 6 in. on the redesigned launcher. This gives a more favorable distribution of the full launcher weight relative to the lugs. This redesign will require recertification of the launcher. Thus, the purpose of the test was to obtain separation data for use as an aid in recertifying the rocket launcher.

This test was conducted using 0.05-scale models of the F-4C aircraft and redesigned LAU-61/A full and empty launchers. The parent-aircraft model was attached to the main tunnel support system, and the store model was mounted on a strain-gage balance attached to the Captive Trajectory Support (CTS) system. The store models were separated from the Multiple Ejection Rack (MER) and the Triple Ejection Rack (TER) on the centerline and right-wing inboard stations, respectively. Data were obtained for a Mach number range from 0.53 through 0.94 for the angle of attack required for unaccelerated level flight at a simulated altitude of 5000 ft. The ejector forces were either constant for a given distance or time-variant functions provided by the Air Force Armament Laboratory.

SECTION II
APPARATUS

2.1 TEST FACILITY

Tunnel 4T is a closed-loop, continuous flow, variable density tunnel in which the Mach number can be varied from 0.1 to 1.3. At all Mach numbers, the stagnation pressure can be varied from 300 to 3700 psfa. The test section is 4 ft square and 12.5 ft long with perforated, variable porosity (0.5- to 10-percent-open) walls. It is completely enclosed in a plenum chamber from which the air can be evacuated, allowing part of the tunnel airflow to be removed through the perforated walls of the test section.

For store separation testing, two separate and independent support systems are used to support the models. The parent aircraft model is inverted in the test section and supported by an offset sting attached to the main pitch sector. The store model is supported by the CTS which extends down from the tunnel top wall and provides store movement (six degrees of freedom) independent of the parent-aircraft model. An isometric drawing of a typical store separation installation is shown in Fig. 1, Appendix I.

Also shown in Fig. 1 is a block diagram of the computer control loop used during captive trajectory testing. The analog system and the digital computer work as an integrated unit and, utilizing required input information, control the store movement during a trajectory. Store positioning is accomplished by use of six individual d-c electric motors. Maximum translational travel of the CTS is ±15 in. from the tunnel centerline in the lateral and vertical directions and 36 in. in the axial direction. Maximum angular displacements are ±45 deg in pitch and yaw and ±360 deg in roll. A more complete description of the test facility can be found in Ref. 1. A schematic showing the test section details and the location of the models in the tunnel is shown in Fig. 2.

2.2 TEST ARTICLES

The test articles were 0.05-scale models of the F-4C aircraft and redesigned LAU-61/A full and empty rocket launchers. The LAU-61/A rocket launcher is geometrically similar to the LAU-69/A rocket launcher. However, the LAU-61/A is heavier than the LAU-69/A and is constructed differently. Separation characteristics of the LAU-69/A from the F-4C were obtained in a previous test (Ref. 2). A sketch showing the basic dimensions of the F-4C parent model is presented in Fig. 3. Details and dimensions of the centerline and inboard pylons are shown in Fig. 4, the 370-gal fuel tank and outboard pylon are shown in Fig. 5, the TER and MER are shown in Figs. 6 and 7, respectively, and sketches of the redesigned LAU-61/A models are shown in Figs. 8 and 9.

The redesigned LAU-61/A empty metric model is shown in Fig. 9a. The lugs are shifted forward 0.30 and 0.15 in. (model scale) from the standard location. The nose section is drilled to simulate the empty launcher tubes. The air passing through the launcher tubes passes through the balance cavity. A thin sheet of Mylar® (0.00025 in. thick) is wrapped around the balance to prevent the air from impinging upon the balance.

The F-4C parent model is geometrically similar to the full-scale aircraft except for some modifications incident to wind tunnel installations and CTS operation. The tail section was removed to reduce the interference between the CTS support and the aircraft. The parent model was inverted and attached by a 20-deg offset sting to the main sting support system (Fig. 2). The TER and MER were mounted on the right-wing inboard and centerline pylons, respectively, and were aligned with the 30-in. suspension lug positions as indicated in Figs. 4, 6, and 7. The MER was installed in the aft position as indicated by the dimension 2.685 in. in Fig. 7. For the forward shifted MER this dimension is 3.836 in. Figure 10 shows the numbering sequence of the TER and MER stations and the roll orientations of the stores mounted on each of the launch positions. Figure 11 shows a typical tunnel installation photograph of the parent aircraft and store model. In Fig. 11 there is shown only a right-wing 370-gal fuel tank. In an attempt to reduce parent dynamics a 370-gal fuel tank was added to the left wing shortly after testing of the full store began. This had no influence upon the trajectories. For this test the engine inlets were open to allow flow through the engine cavities.

2.3 INSTRUMENTATION

An integrally built 3-in. offset sting and a five-component strain-gage balance were attached to the CTS support system. This sting-balance system was used for all the empty store launches from the TER and MER and the full store launches from the MER. A six-component strain-gage balance attached to a 3-in. offset sting with roll capability was used for the full store launches from the inboard TER. This sting reduced somewhat the store model dynamics as the sting was substantially stiffer than the previous sting; it also reduced the available trajectory as it reached a sting-to-parent contact point sooner because of its larger diameter.

Translational and angular positions of the store were obtained from CTS analog outputs, and parent-model angle of attack was determined by an angular position indicator on the main pitch sector. The right-wing and centerline pylons contained a touch wire system which enabled the store to be accurately positioned for launch. The system was also wired to automatically stop the CTS motion and give a visual indication if the store or sting support makes contact with any surface other than the touch wire.

SECTION III
TEST DESCRIPTION

3.1 TEST CONDITIONS

Store separation trajectory data were obtained at Mach numbers 0.53, 0.62, 0.70, 0.78, 0.86, and 0.94. All trajectories were run at a dynamic pressure of 500 psf except three trajectories of the full store in Fig. 13e. These trajectories were for $M_\infty = 0.78$, 0.86, and 0.94, and were run at $q_\infty = 300$ psf. The dynamic pressure was reduced in an attempt to reduce the full store model dynamics. The tunnel conditions were held constant at the desired settings while data for each trajectory were obtained.

Because of the large store angles reached during the trajectories, either mechanical limits or sting-parent model contact usually terminated the trajectories. However, some of the trajectories were of such duration that they were stopped manually after sufficient data were obtained to indicate a trend.

3.2 TRAJECTORY DATA ACQUISTION

To run a store separation trajectory, the test conditions were established in the tunnel and the parent model was pitched to the desired angle of attack. The store model was then angularly oriented to the desired attitude and lowered to a position corresponding to the store carriage location. After the store was set at the desired initial position, operational control of the CTS was switched to the digital computer which controlled the store movement during the trajectory through commands to the CTS analog system (see block diagram, Fig. 1). Data from the wind tunnel, consisting of measured store model forces and moments, wind tunnel operating conditions, and CTS rig positions, were input to the digital computer for use in the full-scale trajectory calculations.

3

The digital computer was programmed to solve the six-degree-of-freedom equations to calculate the angular and linear displacements of the store relative to the parent-aircraft pylon (Ref. 3). In general, the program involves using the last two successive measured values of each static aerodynamic coefficient to predict the magnitude of the coefficients over the next time interval of the trajectory. These predicted values are used to calculate the new position and attitude of the store at the end of the time interval. The CTS is then commanded to move the store model to this new position, and the aerodynamic loads are measured. If these new measurements agree with the predicted values, the process is repeated until a complete trajectory has been obtained.

In applying the wind tunnel data to the calculations of the full-scale store trajectories, the measured forces and moments are reduced to coefficient form and then applied with proper full-scale store dimensions and flight dynamic pressure. Dynamic pressure was calculated using a flight velocity equal to the free-stream velocity component plus the components of store velocity relative to the aircraft, and a density corresponding to the simulated altitude.

The initial portion of each launch trajectory incorporated simulated ejector forces in addition to the measured aerodynamic forces acting on the store. The ejector force was either time variant or constant. The time-variant forces are presented in Figs. 12a and b and are designated E-1 and E-2, respectively. Ejector force E-1 was used for the full launcher separations, and E-2 was used for the empty launcher separations. The constant ejector force was 1100 lb until the store had moved 0.25 ft in Z; then it was terminated. The constant ejector force was designated E-3 and was used for both the full and empty launcher separations. The locations of the applied ejector forces and other full-scale store parameters used in the trajectory calculations are listed in Table I, Appendix II.

3.3 CORRECTIONS

Balance, sting, and support deflections caused by the aerodynamic loads on the store models were accounted for in the data reduction program to calculate the true store-model angles. Corrections were also made for model weight tares to calculate the net aerodynamic forces on the store model.

3.4 PRECISION OF DATA

The trajectory data are subject to error from several sources including tunnel conditions, balance measurements, extrapolation tolerances allowed in the predicted coefficients, computer inputs, and CTS position control, which was ±0.05 in. for the translational settings and ±0.15 deg for angular displacement settings in pitch and yaw. Extrapolation tolerances were ±0.10 for each of the aerodynamic coefficients. The maximum uncertainties in full-scale position data caused by balance precision limitations are given below.

Maximum Trajectory Uncertainties

Model Configuration	t,sec	X,ft	Y,ft	Z,ft	θ,deg	ψ,deg
Empty, five-component balance	0.3	±0.46	±0.16	±0.14	±6.6	±6.6
Full, five-component balance	0.3	±0.07	±0.03	±0.02	±1.3	±1.2
Full, six-component balance	0.3	±0.03	±0.05	±0.03	±1.1	±1.7

SECTION IV
RESULTS AND DISCUSSION

4.1 GENERAL

Trajectories were obtained to determine the safe separation envelopes of the full and empty redesigned LAU-61/A launcher from the F-4C aircraft. Tests were conducted simulating 6- and 3-in. forward shifts of the support lugs on the redesigned launcher. Also tested were two full configurations simulating loads of the 2.75-in. folding-fin rockets with heavy and light warheads. No attempt is made in this report to establish the safe separation envelopes or qualify the store as safe or unsafe for aircraft separation.

The trajectories obtained during the test were for ejector-separated store configurations simulating release from right- and left-wing inboard pylons and the centerline pylon. Separation of the full (light and heavy warheads) and the empty launcher from the TER for configurations 1, 2, and 3 (Table II) are for right-wing simulation; configurations 1, 6, and 7 are for left-wing simulation. Configurations 4 and 5 are special simulations. The trajectories from the MER simulate launches from stations 2, 4, and 6. Because of centerline symmetry, and to simplify the test, trajectories that would have been launched from station 4 were launched from station 6 with a dummy store at station 4. For all trajectories, the MER was in the aft location (Fig. 7). Plots showing the linear displacements of the stores relative to the carriage positions and the angular displacements relative to the flight-axis system are presented in Figs. 13 through 23. Positive X, Y, and Z displacements (as seen by the pilot) are forward, to the right, and down, respectively. Positive changes in θ and ψ (as seen by the pilot) are nose up and nose to the right, respectively. Table I lists the full-scale store parameters used in the trajectory calculations, and Table II describes the aircraft load nomenclature.

4.2 LAU-61/A, FULL

Trajectory data for the full LAU-61/A with heavy warheads, and lugs shifted 6 and 3 in. forward, are presented in Figs. 13 and 14, respectively. For both lug positions the ejector force acts aft of the store cg. This would tend to cause the nose of the store to pitch toward the TER or MER, and because the store is statically unstable, the

aerodynamic force would then tend to keep it pitching. This is demonstrated for the 6-in. lug shift for some of the trajectories shown in Figs. 13c, e, and f, and for the 3-in. lug shift for some of the trajectories shown in Figs. 14a, b, c, and d. Here the stores at $M_\infty \leq 0.62$ pitch nose up, and for the higher Mach numbers the model pitches nose down. Apparently the local flow-field angles are large enough in the remainder of the trajectories (Figs. 13a, b, d, g, h, and i) that the aerodynamic moment overcomes the ejector force moment and causes the stores to pitch nose down.

The store with the lugs shifted only 3 in. has the ejector force aft of the cg 0.455 ft (Table I), but for the 6-in. lug shift the ejector force is aft of the cg 0.205 ft. The effect of lug shift on the translational and rotational movement is treated in Section 4.4.

Trajectory data for the full LAU-61/A with light warheads and lugs shifted 6 and 3 in. forward are presented in Figs. 15 and 16, respectively. For the 6-in. lug shift the ejector force acts forward of the cg 0.195 ft (Table I), and for the 3-in. lug shift the ejector force is aft of the cg 0.0545 ft. In Fig. 15a for the trajectory with $M_\infty = 0.53$ the store has a nose up attitude, but for the remainder of the trajectories in Fig. 15 the stores have a nose down attitude.

For the 3-in. lug shift the trajectories for Mach number 0.53 show that for two configurations (Figs. 16a and b) the stores pitch nose up, but for the remainder of the configurations the stores pitch nose down. It appears that the predominant influence on the trajectories with the full launchers is the local flow field angle, with the ejector force location influencing only the borderline cases where the local flow-field angle is nearly 0 deg relative to the store.

As previously mentioned, the ejector force acts aft of the cg for the full store (heavy warhead) and would be expected to cause the store to yaw toward the TER. Since the store is statically unstable it would then tend to continue yawing toward the TER. This is the case for the trajectories shown in Fig. 13b and g, 14a and d, and most of those in Fig. 13c. The store yawed away from the TER in Fig. 13f, apparently influenced by the local flow field. For the remainder of the configurations (Figs. 13a, d, and e, and 14b and c) the stores were launched from station number 1 and should not be influenced in yaw by the ejector force. For these configurations the stores all yawed positive apparently because of the angle of the local flow field relative to the store.

For the full store (light warhead), the ejector force acts forward of the cg for the 6-in. lug shift and would be expected to cause the store to yaw away from the TER. This is shown in Fig. 15a. In Fig. 15c, however, the store yaws toward the TER apparently as a result of the aerodynamic moment. For the trajectories in Fig. 15b, the store is launched from station number 1 and yaws to the right. For the 3-in. lug shift (Fig. 16), the ejector force acts a small distance (-0.0545 ft) aft of the store cg. The store yaws the same as for the 6-in. lug shift, apparently influenced primarily by the angle of the local flow field.

4.3 LAU-61/A, EMPTY

Trajectory data for the empty LAU-61/A with lugs shifted 6 and 3 in. forward are presented in Figs. 17 and 18, respectively. For both lug positions, the ejector force acts forward of the store cg. The combination of the ejector force moment and the aerodynamic moment causes all of the stores to pitch nose down. The effect of lug shift on the translational and rotational movement is treated in Section 4.4.

The empty LAU-61/A would be expected to yaw away from the TER because the ejector force acts forward of the cg. This is shown in Figs. 17b, c, f, and g and 18a. The stores for all the trajectories except for $M_\infty = 0.78$ yaw away from the TER in Fig. 18d. For Figs. 17a, d, and e, and 18b and c, the store is launched from station number 1 and should not be affected in yaw by the ejector force. For the trajectories in Figs. 17h and i, the store was launched from the MER.

4.4 LUG SHIFT EFFECT

Comparing the trajectories of the models with the 3- and 6-in. lug shift indicates that the lug shift has no effect on the movement of the store cg for the duration of the trajectories. However, the pitch rate of the store is decreased when the lugs are shifted forward 6 in. as compared to the pitch rate for the 3-in. shift.

Typical comparison plots are made in Figs. 19a and b, 20a and b, and 21a and b for the full launcher with heavy and light warhead and the empty launcher, respectively. The decrease of the pitch is of the order of 4 deg for 0.200 sec of trajectory flight time for both positive and negative pitch.

4.5 EJECTOR FORCE EFFECT

Trajectories of the full launcher with heavy warheads for ejector forces E-1 and E-3 (Fig. 12a and Section 3.2) are shown in Fig. 22. Trajectories of the empty launcher for the ejector forces E-2 and E-3 (Fig. 12b and Section 3.2) are shown in Fig. 23. For the full launcher (heavy warhead), there is no apparent effect on translational or rotational movement of the store (Fig. 22) for the duration of the trajectories.

For the empty model, the ejector force E-3 caused the store to move slightly farther in Z for a given time than ejector force E-2 (Fig. 23). All the empty stores pitched negatively for ejector force E-2 and pitched slightly more negative for ejector force E-3 (Fig. 23).

REFERENCES

1. <u>Test Facilities Handbook</u> (Ninth Edition). "Propulsion Wind Tunnel Facility, Vol. 4." Arnold Engineering Development Center, July 1971.

2.   Mansfield, A. C. "Separation Characteristics of the LAU-69/A Rocket Launcher from the F-4C Aircraft at Mach Numbers from 0.29 to 0.78." AEDC-TR-71-228 (AD888694L), October 1971.

3.   Christopher, J. P., and Carleton, W. E. "Captive-Trajectory Store-Separation System of the AEDC-PWT 4-Foot Transonic Tunnel." AEDC-TR-68-200 (AD839743), September 1968.

APPENDIXES
I. ILLUSTRATIONS
II. TABLES
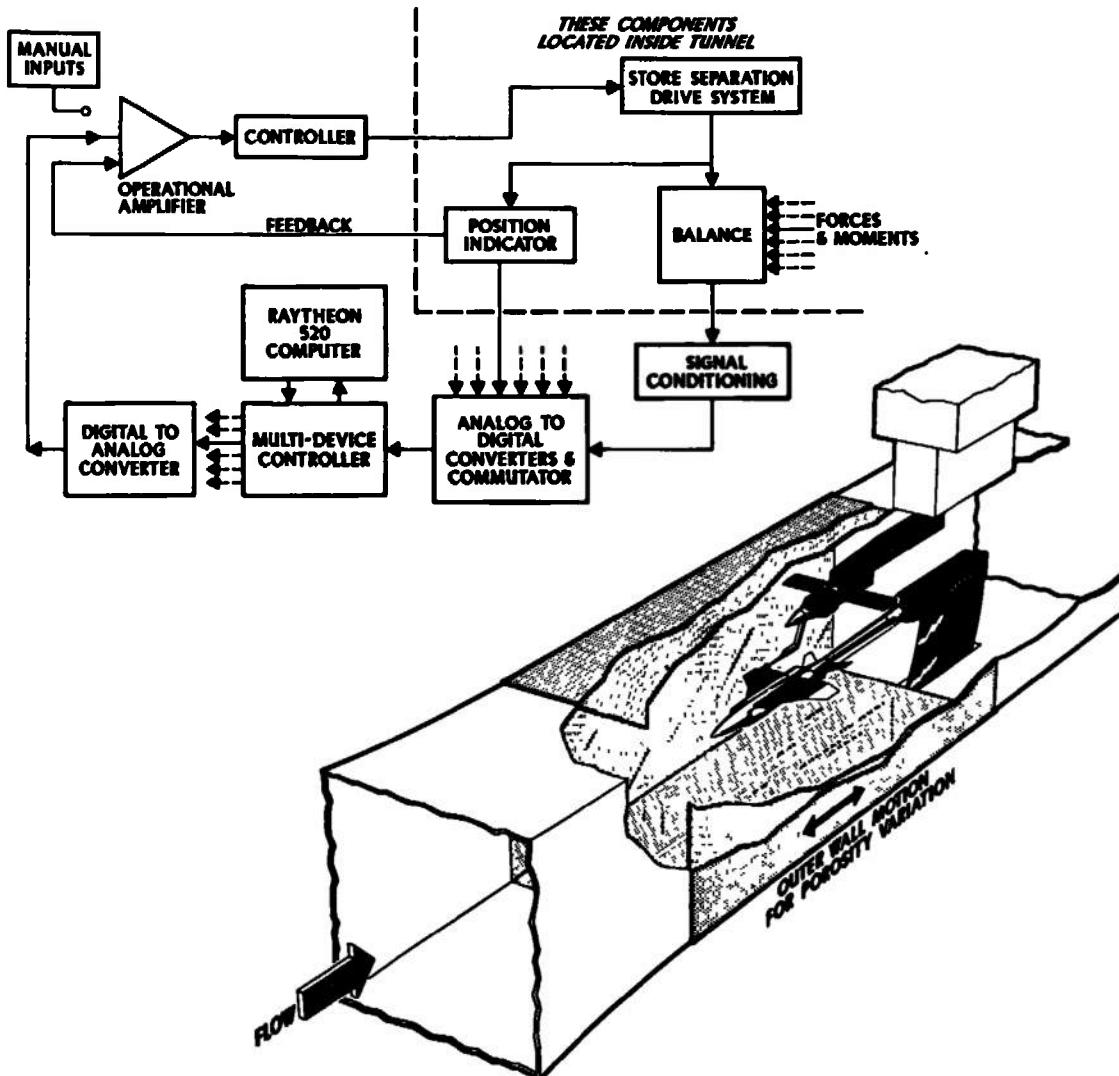
Fig. 1 Isometric Drawing of a Typical Store Separation Installation and a
Block Diagram of the Computer Control Loop

60°

0.500 DIAM

AIRSTREAM SURFACE

0.375

0.375

TYPICAL PERFORATED WALL CROSS SECTION   NOTE: TUNNEL STATIONS AND DIMENSIONS ARE IN INCHES

SOLID AREAS

PERFORATED WALLS (10 % MAXIMUM OPEN AREA)

F-4C MODEL

CTS STING

MAIN SUPPORT

FLOW EXPANSION REGION

STA. 0.0

STA. 36.0

STA. 87.9

STA. 150.0
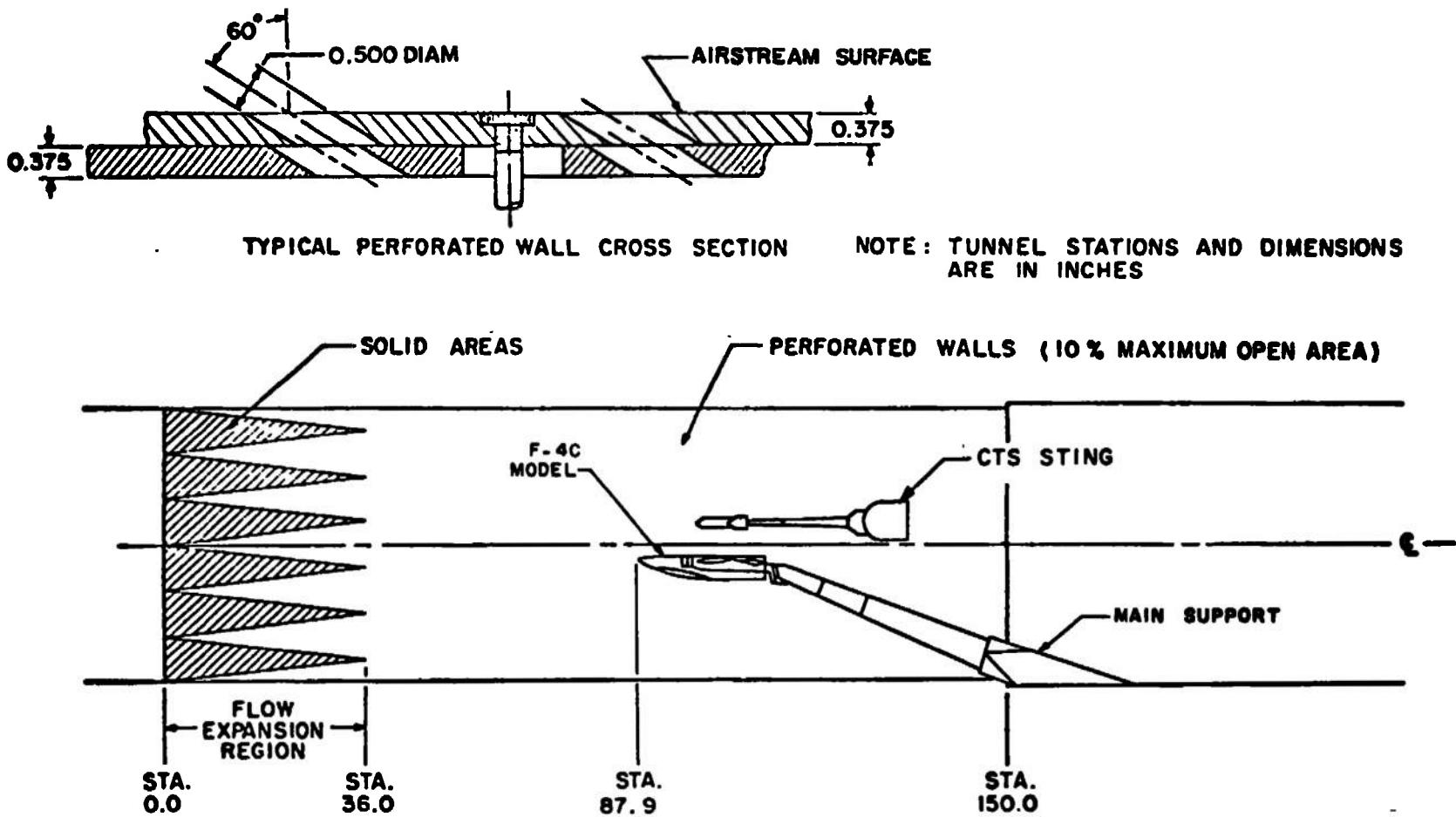
Fig. 2 Schematic of the Tunnel Test Section Showing Model Location

WL 0.000

BL 11.560

BL 6.625

BL4.075

BL - 4.075
INBOARD PYLON

BL - 6.625
OUTBOARD PYLON

BL -11.560

FS - 1.355

FS 0.000

FS 33.166
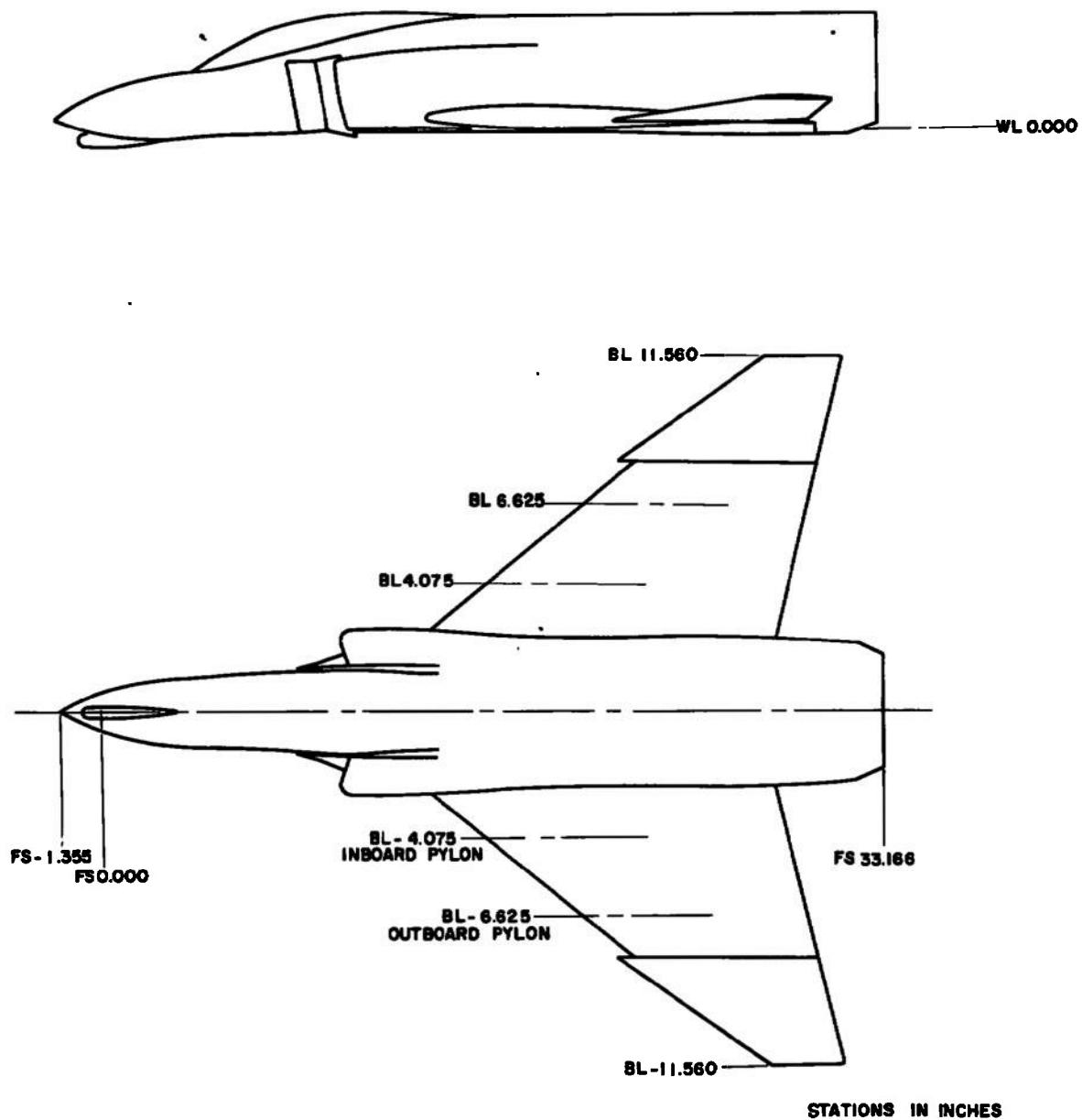
STATIONS IN INCHES

Fig. 3 Sketch of the F-4C Parent-Aircraft Model
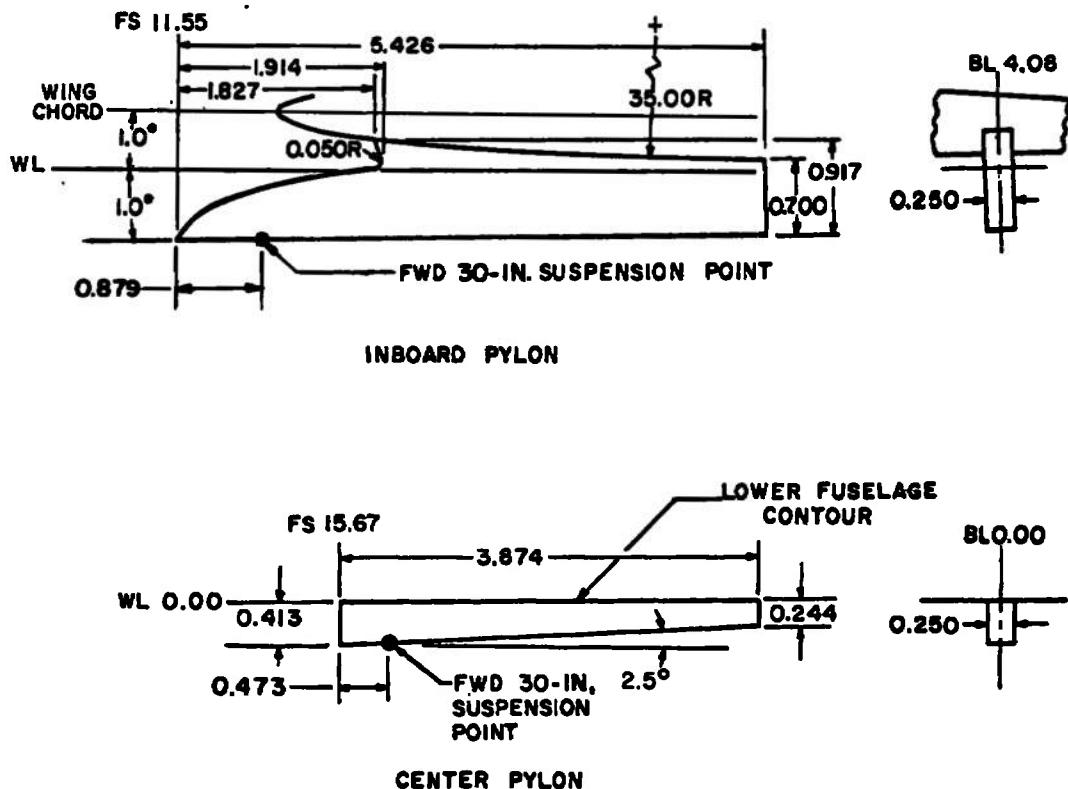
Fig. 4 Details and Dimensions of the F-4C Inboard and Centerline Pylon Models

FS10.65

FS 16.05

BL
6.625

7.5°

0.500

0.480

WL

1.5°

1.300

12.000

STA.
0.0

ALL DIMENSIONS IN INCHES
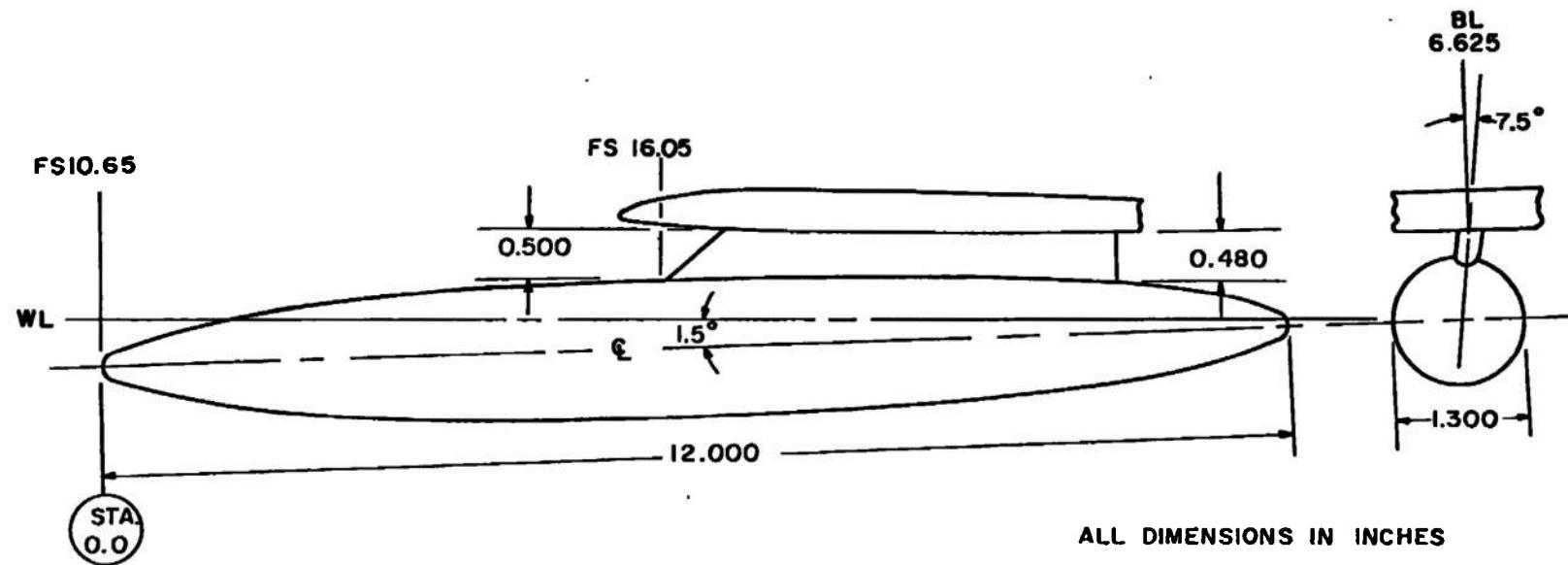
BODY CONTOUR, TYPICAL BOTH ENDS

STATION	BODY DIAM	STATION	BODY DIAM
0.000	0.000	2.500	1.116
0.025	0.100	2.750	1.156
0.050	0.144	3.000	1.190
0.150	0.258	3.250	1.218
0.250	0.340	3.500	1.242
0.500	0.498	3.750	1.260
0.750	0.622	4.000	1.274
1.000	0.724	4.250	1.286
1.250	0.812	4.500	1.294
1.500	0.890	4.750	1.298
1.750	0.958	5.000	1.300
2.000	1.016	6.000	1.300
2.250	1.070		

Fig. 5 Details and Dimensions of the F-4C 370-gal Fuel Tank Model

3.335

2.550

0.920

0.800

A

FWD 30-IN. SUSPENSION POINT

FWD 14-IN. SUSPENSION POINTS

1.320

A

ALL DIMENSIONS IN INCHES

0.326

0.725

0.130

45°

0.345

SECTION A-A
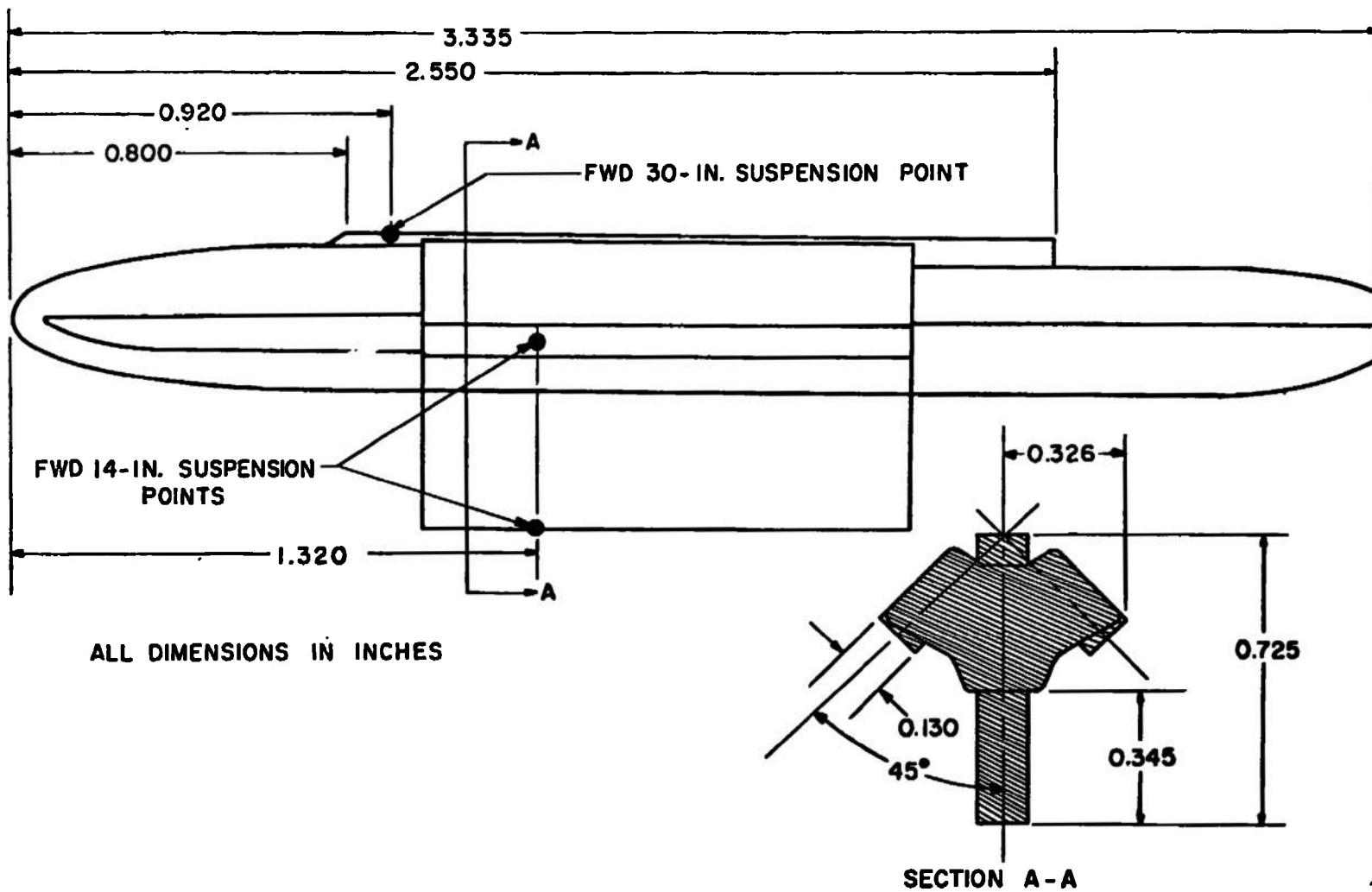
Fig. 6 Details and Dimensions of the TER Model

ALL DIMENSIONS IN INCHES

7.750
6.615
5.735
5.405
2.685
1.915
1.035

FWD 30-IN.
SUSPENSION POINT

FWD 14-IN.
SUSPENSION POINTS

0.062 R

0.326

0.707

0.345

45°

SECTION B-B
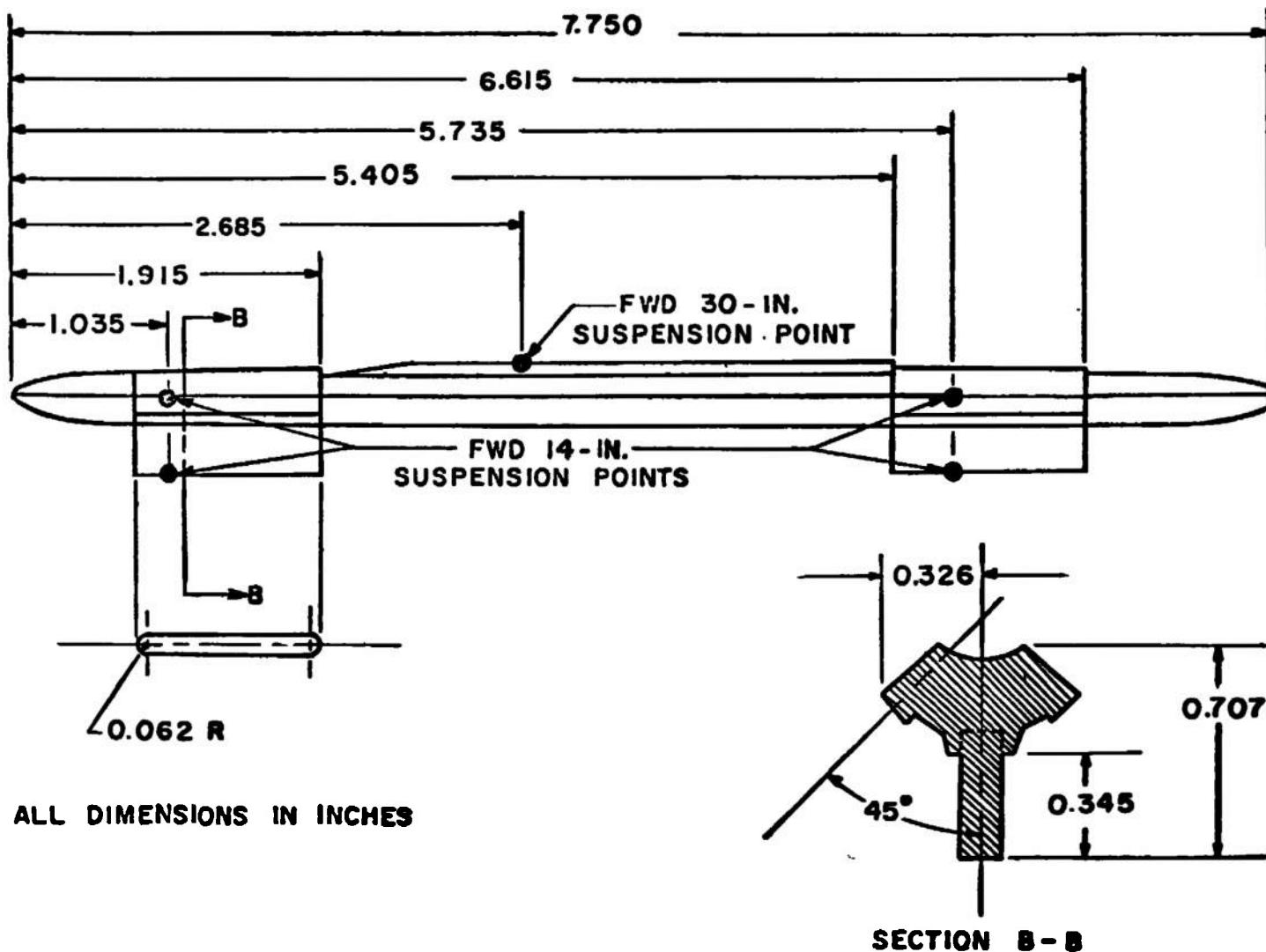
Fig. 7 Details and Dimensions of the MER Model

X	Y
0 026	0 201
0 110	0 372
0 240	0 528
0 400	0 645
0 594	0 734
0 800	0 780
0 950	0 785

ALL DIMENSIONS IN INCHES
A = 1.625, LUGS SHIFTED 3 in. FWD.
A = 1.475, LUGS SHIFTED 6 in. FWD.
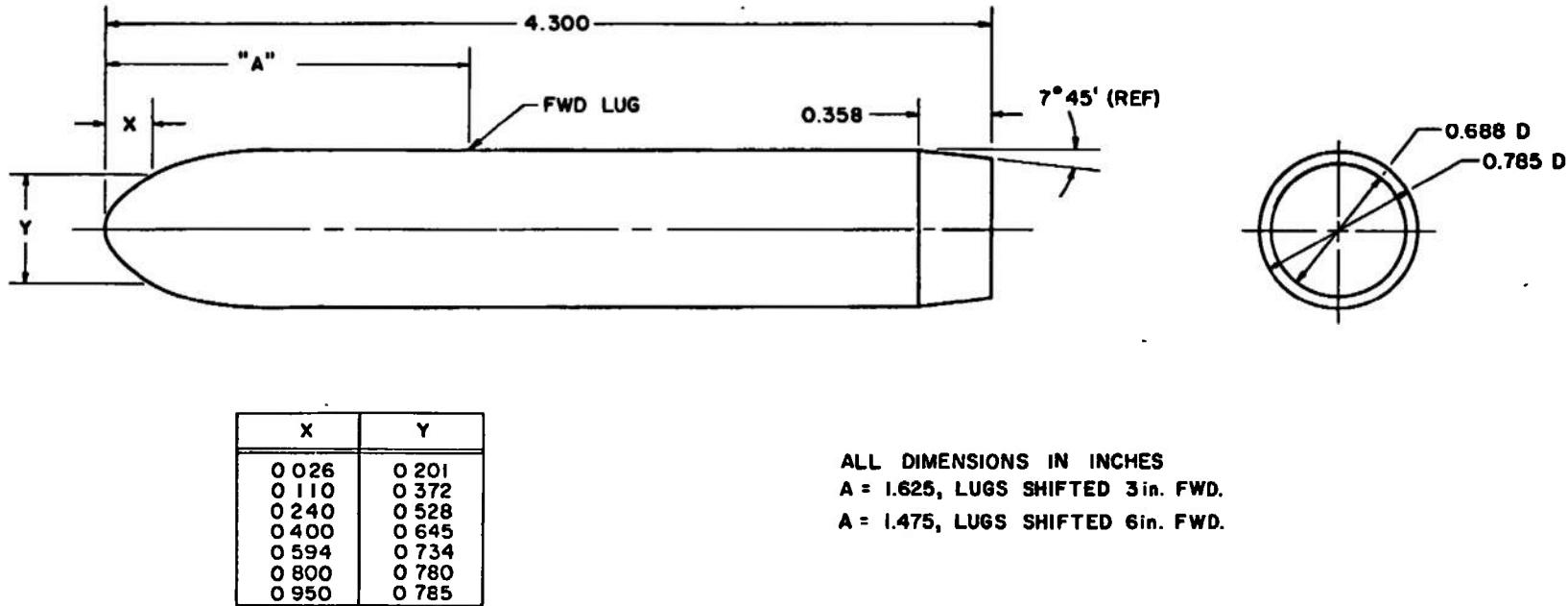
Fig. 8 Details and Dimensions of the Redesigned LAU-61/A Metric and Dummy Rocket Launcher Models (Full)
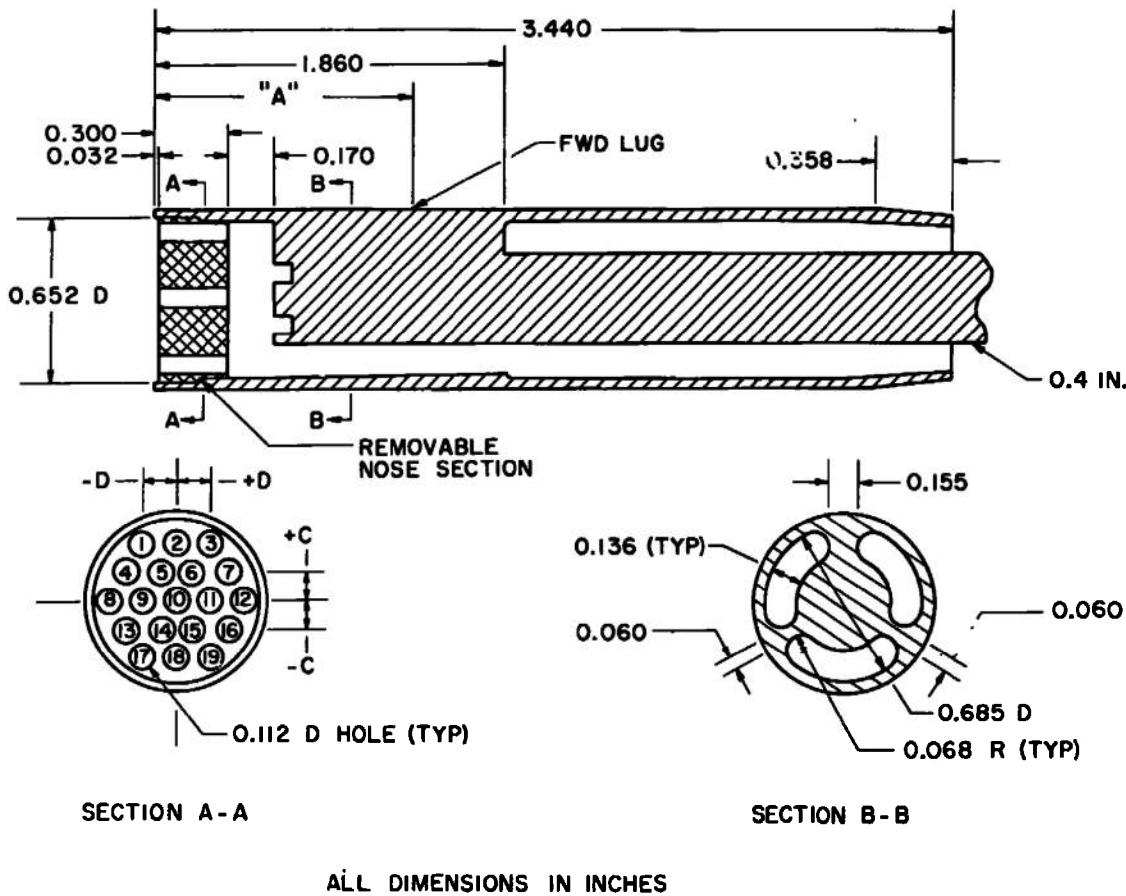
A = 0.765, LUGS SHIFTED 3 in. FWD
A = 0.615, LUGS SHIFTED 6 in. FWD
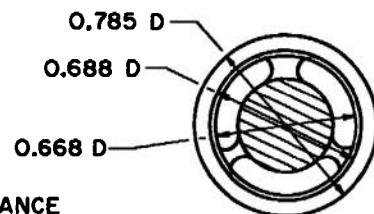
HOLE NO.	C	D
1	0.250	-0.143
2	0.250	0.000
3	0.250	0.143
4	0.125	-0.218
5	0.125	-0.062
6	0.125	0.062
7	0.125	0.218
8	0.000	-0.287
9	0.000	-0.143
10	0.000	0.000
11	0.000	0.143
12	0.000	0.287
13	-0.125	-0.218
14	-0.125	-0.062
15	-0.125	0.062
16	-0.125	0.218
17	-0.250	-0.143
18	-0.250	0.000
19	-0.250	0.143

SECTION A-A

SECTION B-B

ALL DIMENSIONS IN INCHES

a. Metric Model
Fig. 9 Details and Dimensions of the Redesigned LAU-61/A Rocket Launcher Models (Empty)

3.440

"A"

0.032

FWD LUG

0.358

A

0.652 D

A

-D   +D

0.785 D

0.688 D

0.668 D

A = 0.765, LUGS SHIFTED 3 in. FWD
A = 0.615, LUGS SHIFTED 6 in. FWD

+C

-C

0.112 D HOLE (TYP), THROUGH
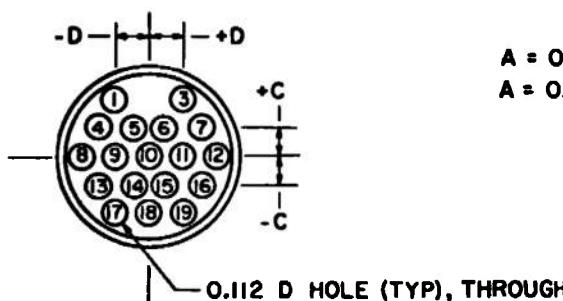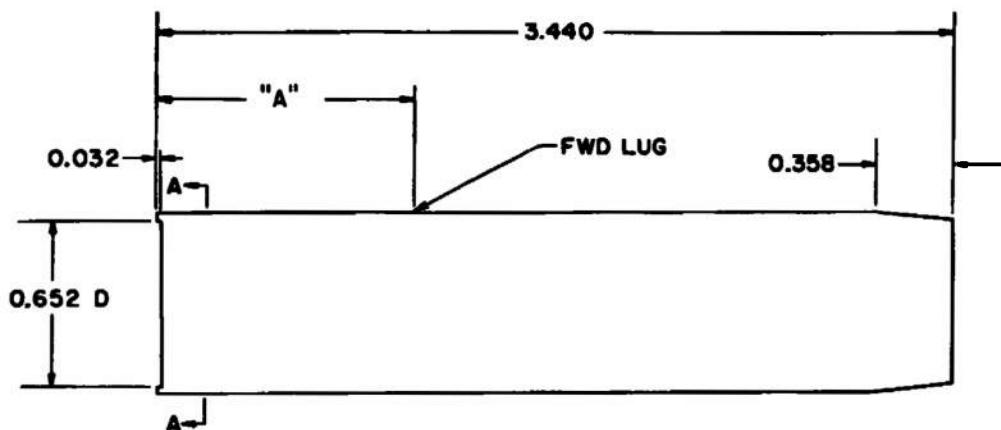
SECTION A - A

ALL DIMENSIONS IN INCHES
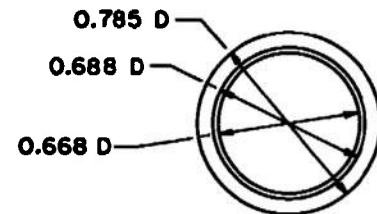
HOLE NO.	C	D
1	0.250	-0.143
3	0.250	0.143
4	0.125	-0.218
5	0.125	-0.062
6	0.125	0.062
7	0.125	0.218
8	0.000	-0.287
9	0.000	-0.143
10	0.000	0.000
11	0.000	0.143
12	0.000	0.287
13	-0.125	-0.218
14	-0.125	-0.062
15	-0.125	0.062
16	-0.125	0.218
17	-0.250	-0.143
18	-0.250	0.000
19	-0.250	0.143

b. Dummy Model
Fig. 9 Concluded
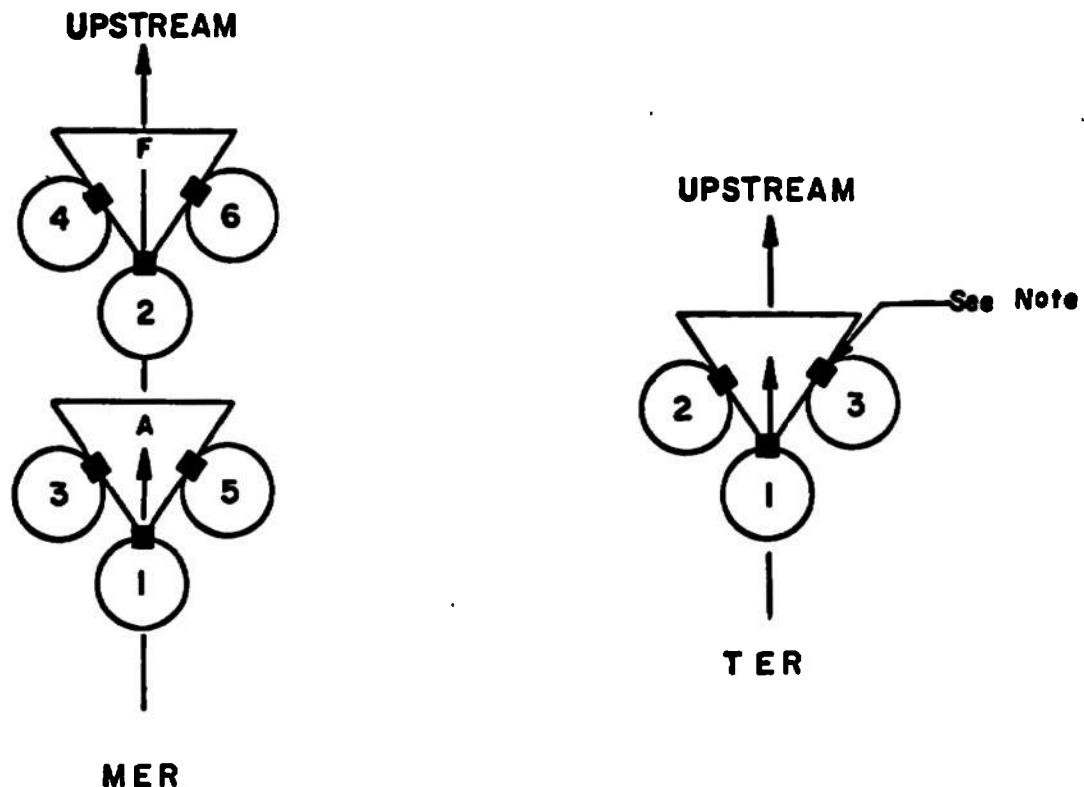
Fig. 10 Schematic of TER and MER Store Stations and Orientations
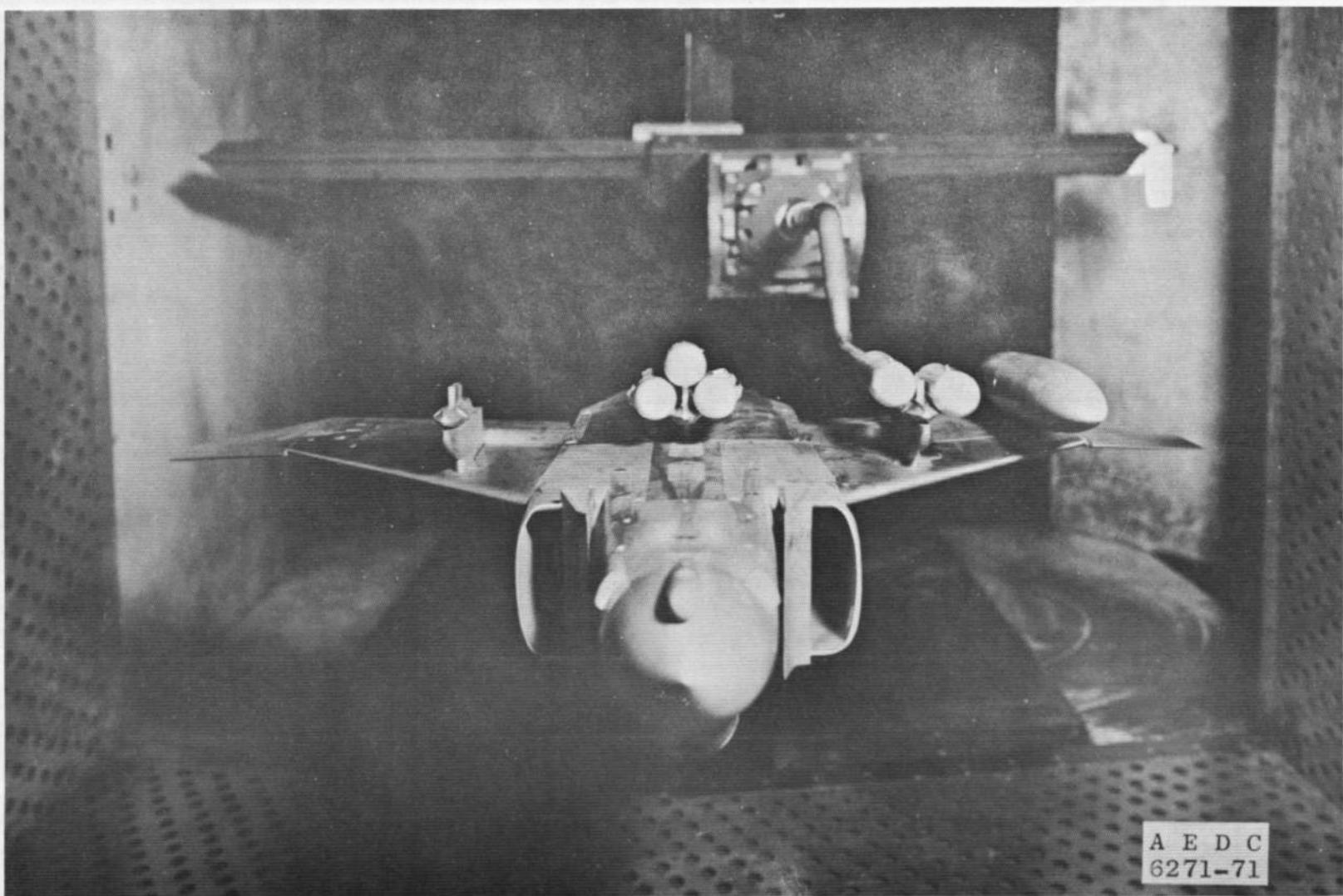
Fig. 11 Tunnel Installation Photograph Showing Parent Aircraft, Store, and CTS
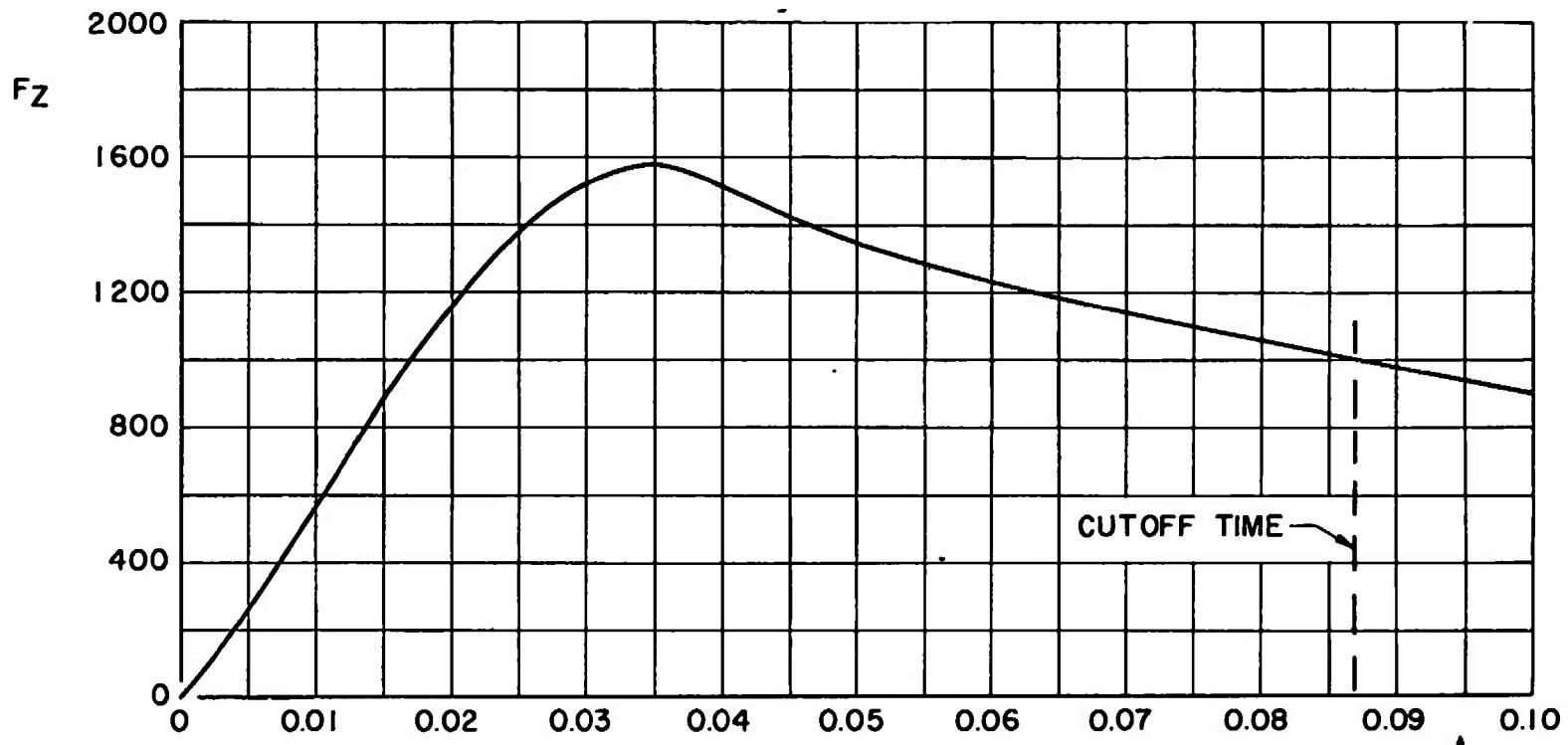
a. E-1 (LAU-61/A, Full)
Fig. 12 TER and MER Ejector Force Functions
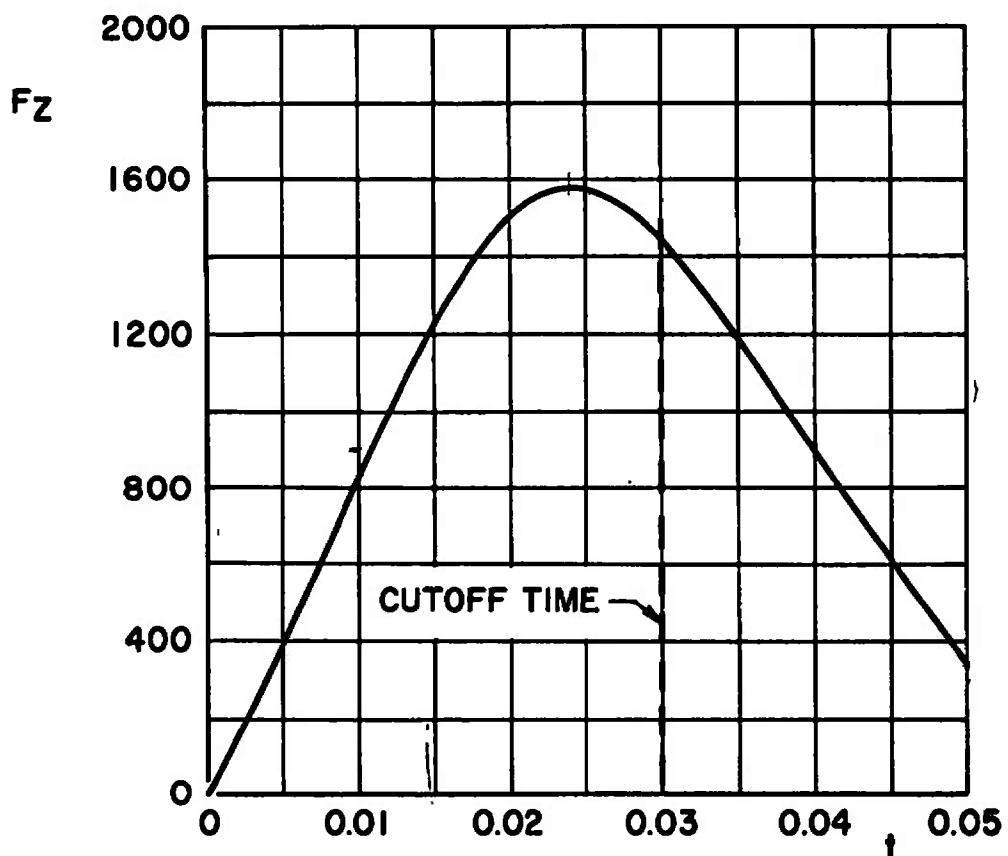
b. E-2 (LAU-61/A, Empty)
Fig. 12 Concluded
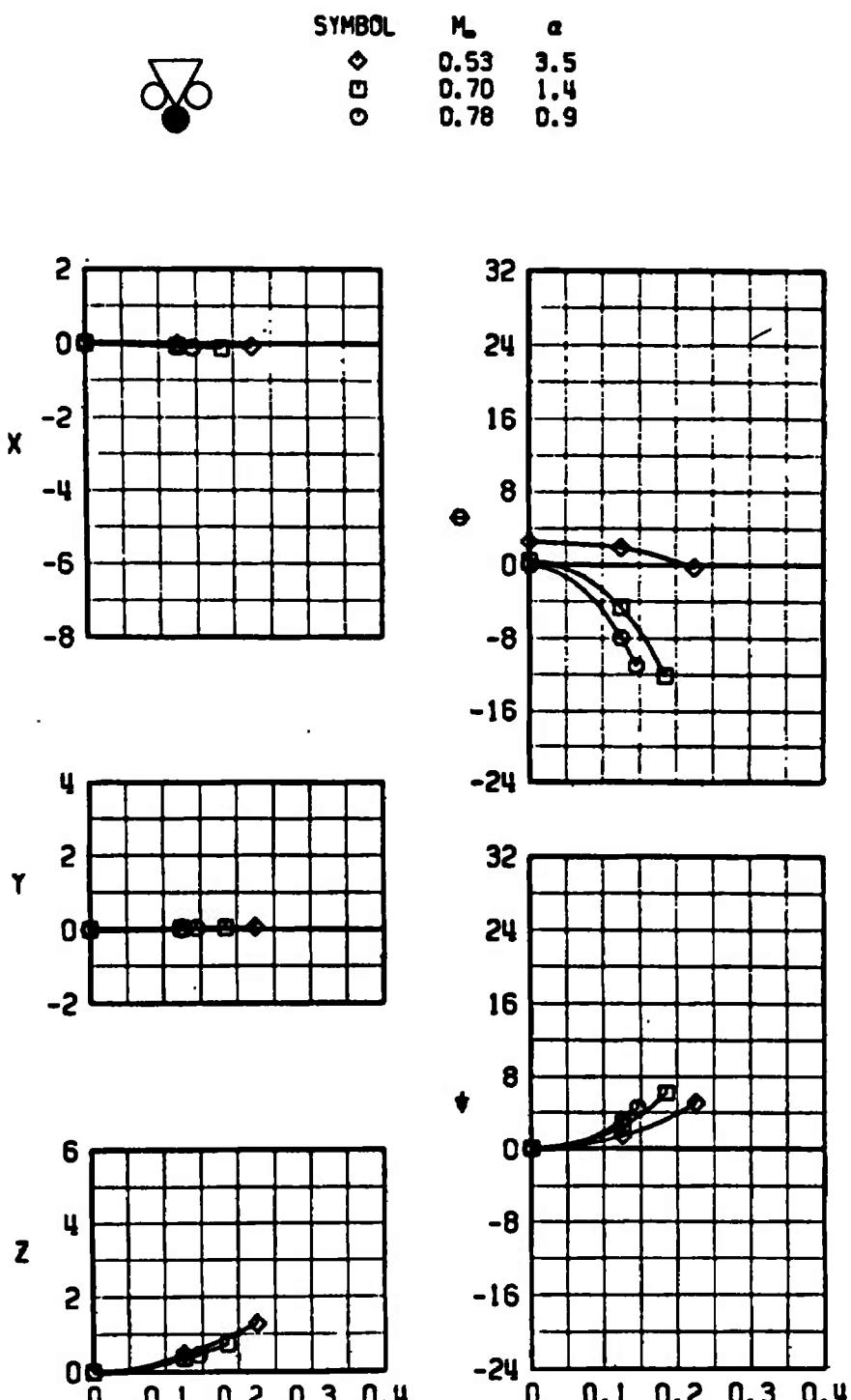
a. TER, Configuration 1H
Fig. 13 Effect of Mach Number on the Separation Characteristics of the
LAU-61/A (Full with the Heavy Warhead and Lugs Shifted 6 in.
Forward) from the Inboard TER and Centerline MER
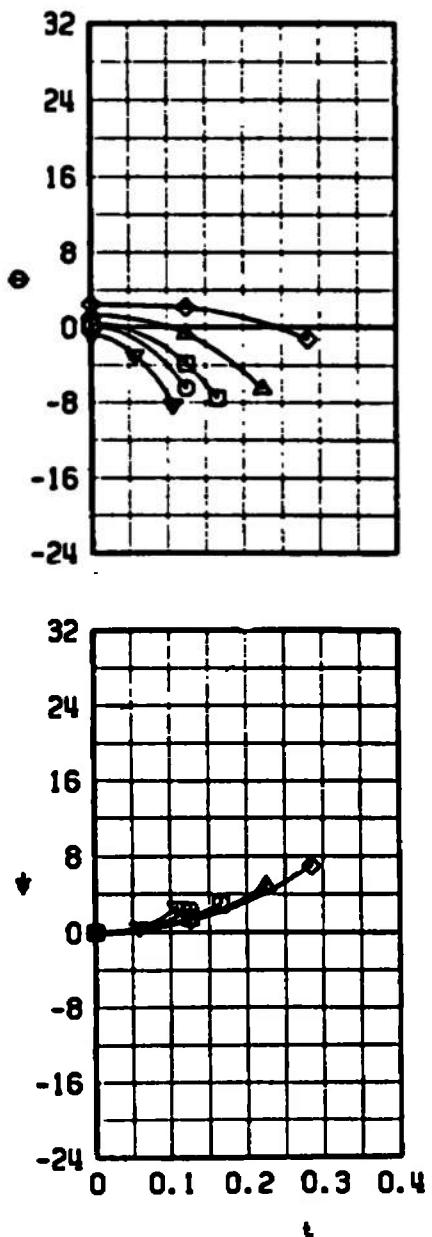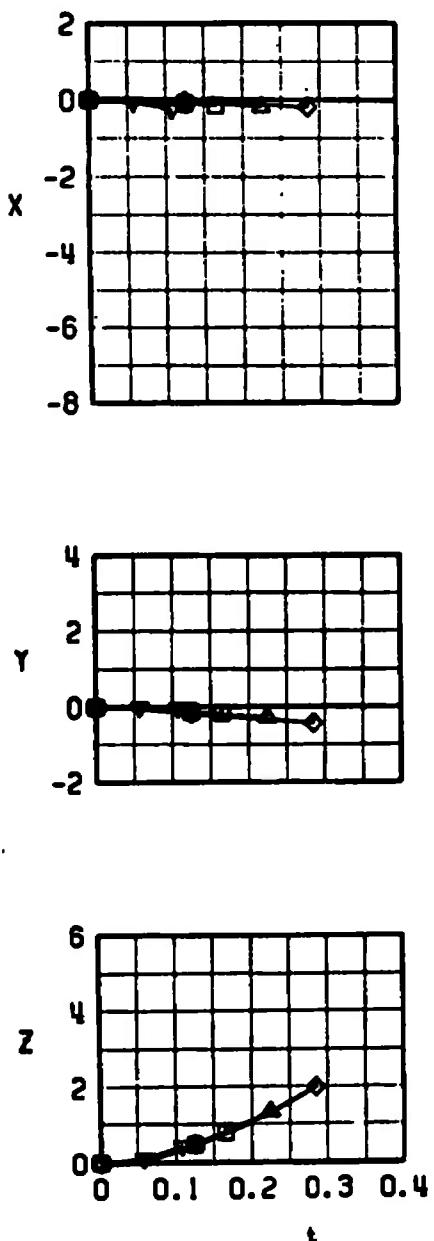
b. TER, Configuration 2H
Fig. 13 Continued

SYMBOL	M_∞	α
◇	0.53	3.5
△	0.62	2.3
▣	0.70	1.4
⊙	0.78	0.9
▽	0.94	0.2
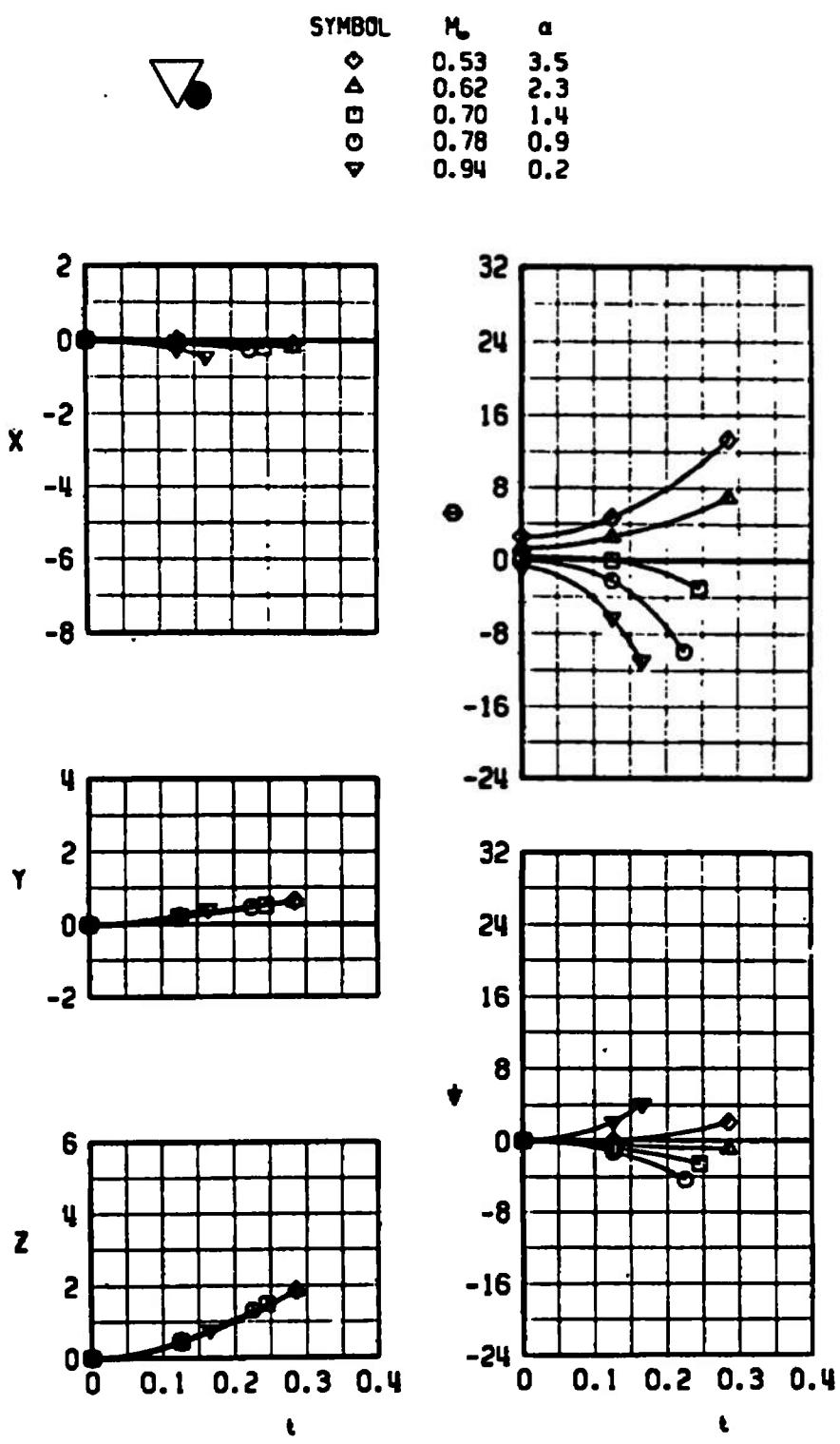
c. TER, Configuration 3H
Fig. 13 Continued

SYMBOL	M_∞	a
△	0.62	2.3
⬒	0.70	1.4
⊙	0.78	0.9
▽	0.94	0.2
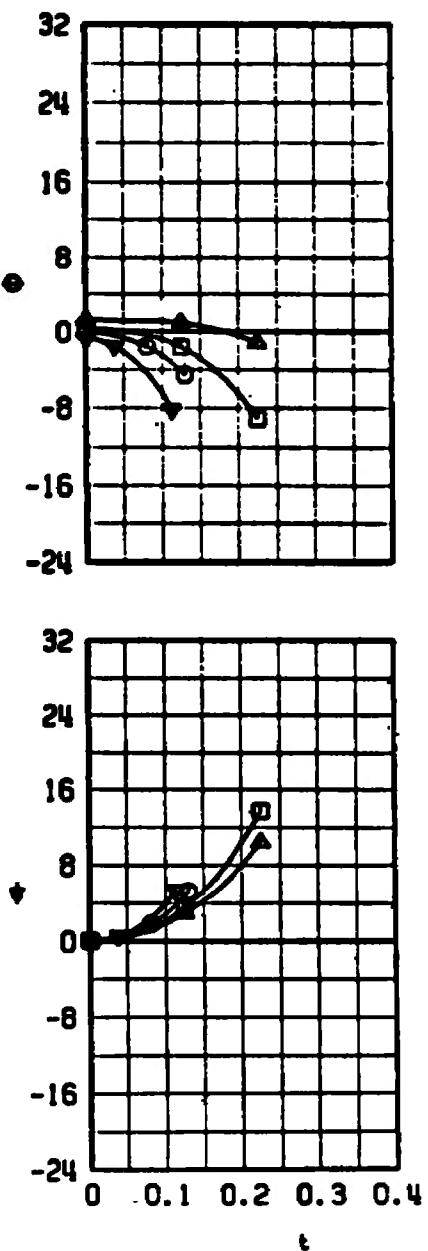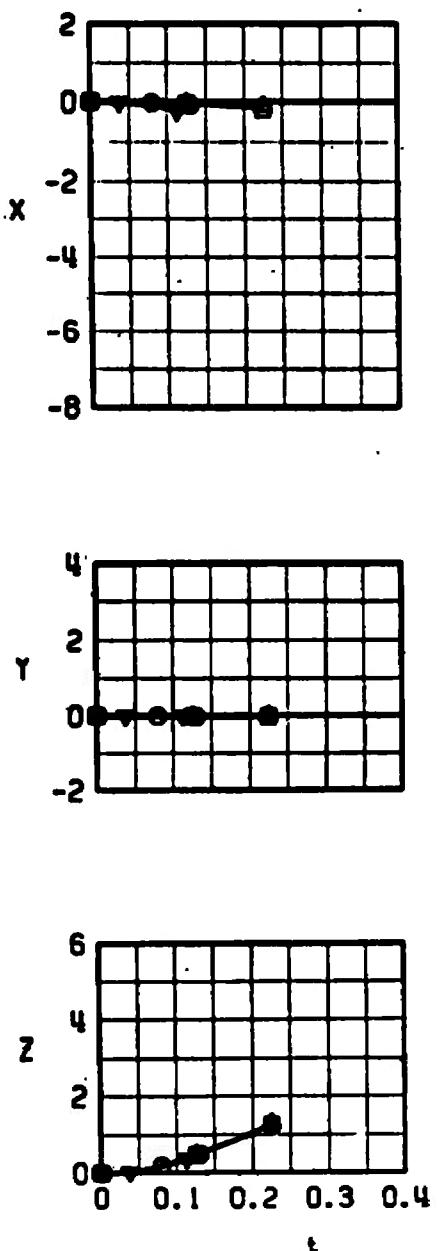
d. TER, Configuration 4H
Fig. 13 Continued

SYMBOL	M_∞	α
△	0.62	2.3
▣	0.70	1.4
◐	0.78	0.9
▷	0.86	0.5
▽	0.94	0.2
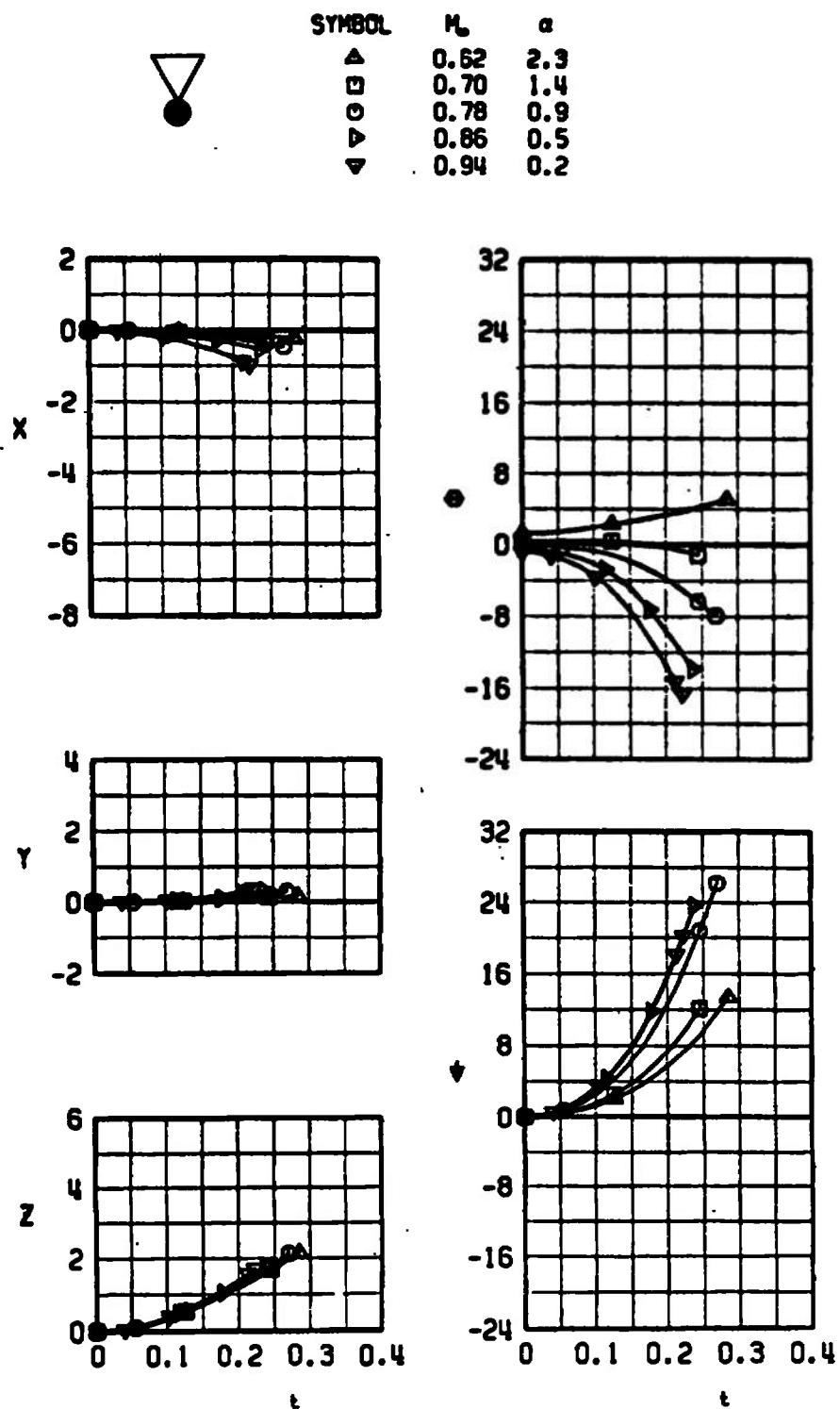
e. TER, Configuration 5H
Fig. 13 Continued

SYMBOL	M_∞	α
◇	0.53	3.5
△	0.62	2.3
◻	0.70	1.4
◔	0.78	0.9
▽	0.94	0.2
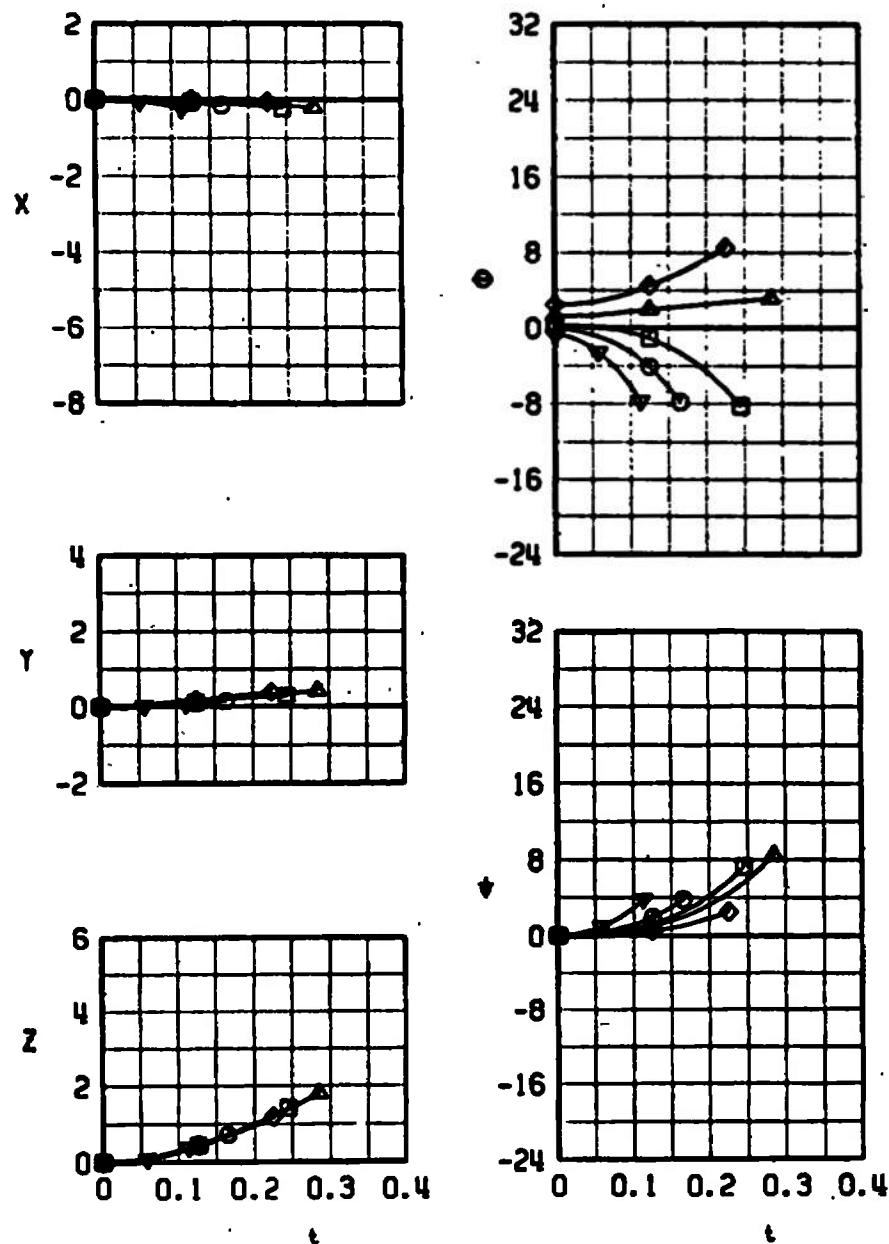
f. TER, Configuration 6H
Fig. 13 Continued
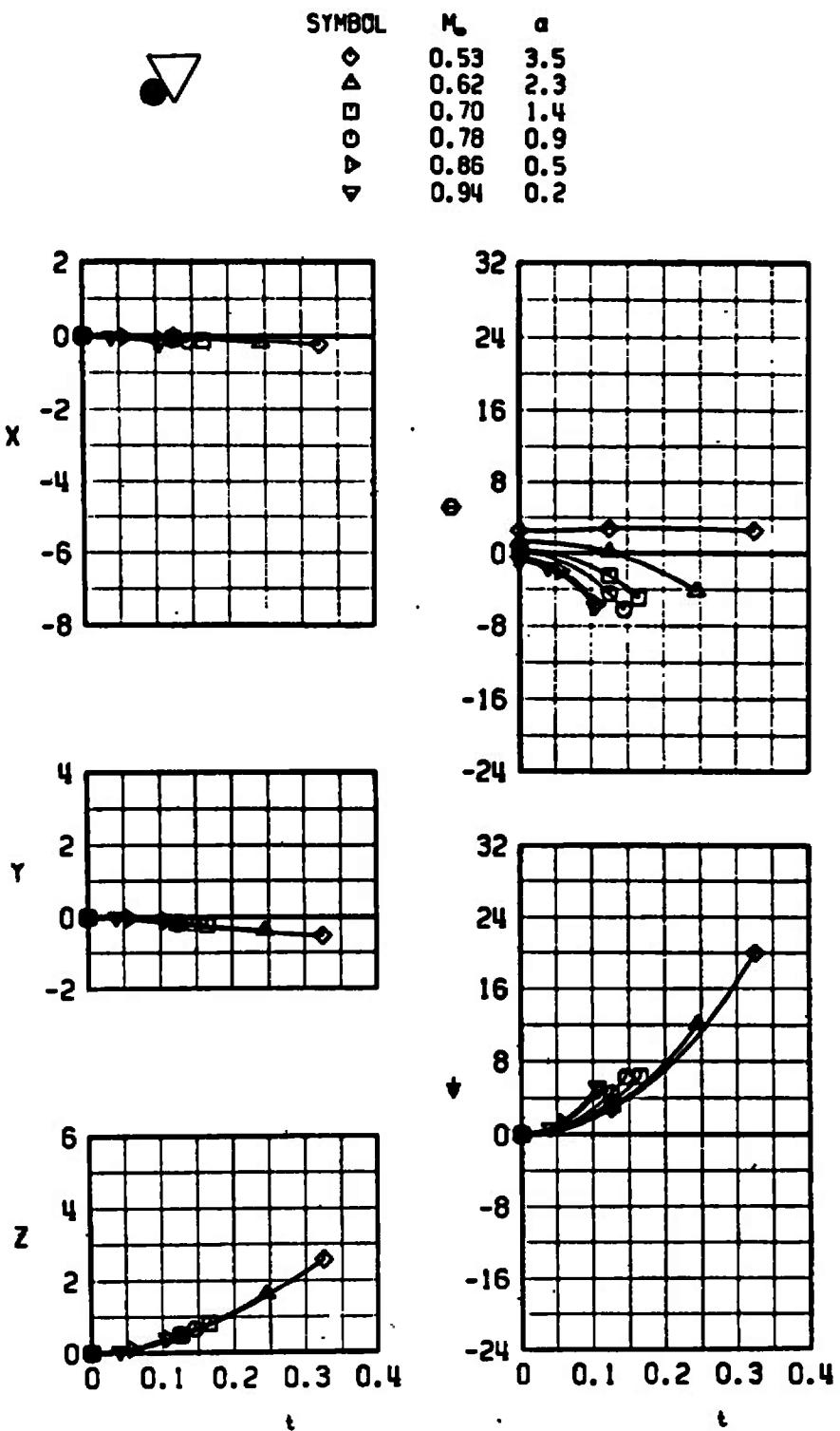
g. TER, Configuration 7H
Fig. 13 Continued

SYMBOL	M_∞	α
◇	0.53	3.5
△	0.62	2.3
⊟	0.70	1.4
◉	0.78	0.9
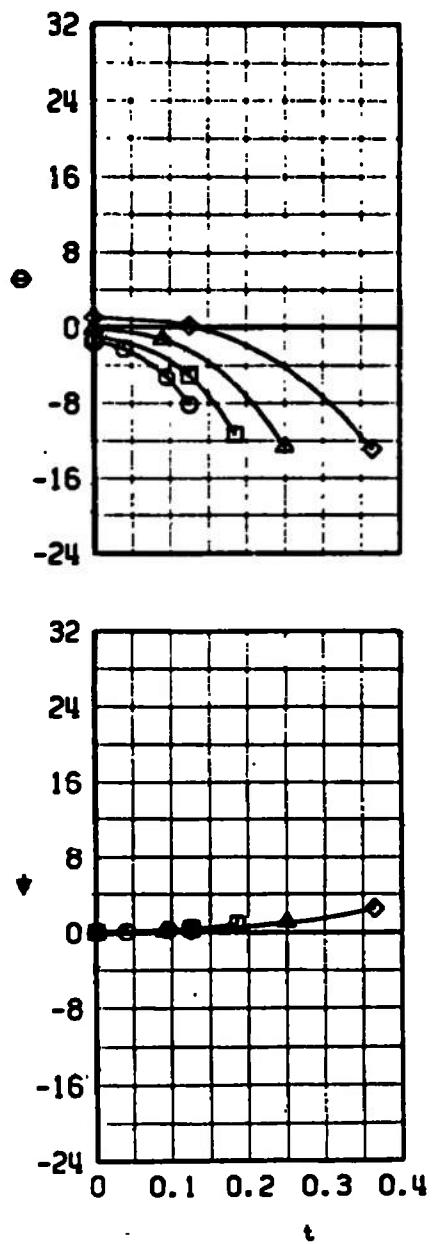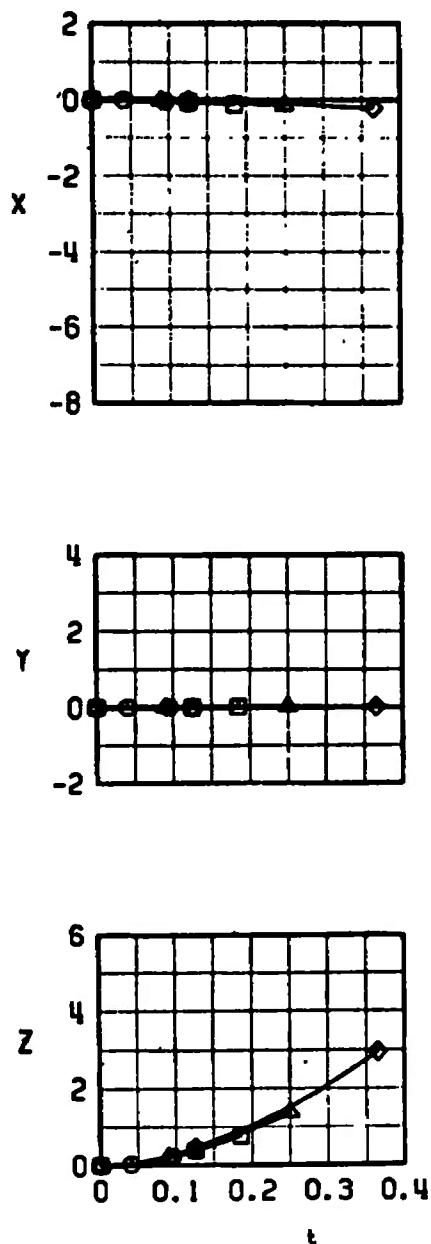
h. MER, Configuration 8H
Fig. 13 Continued
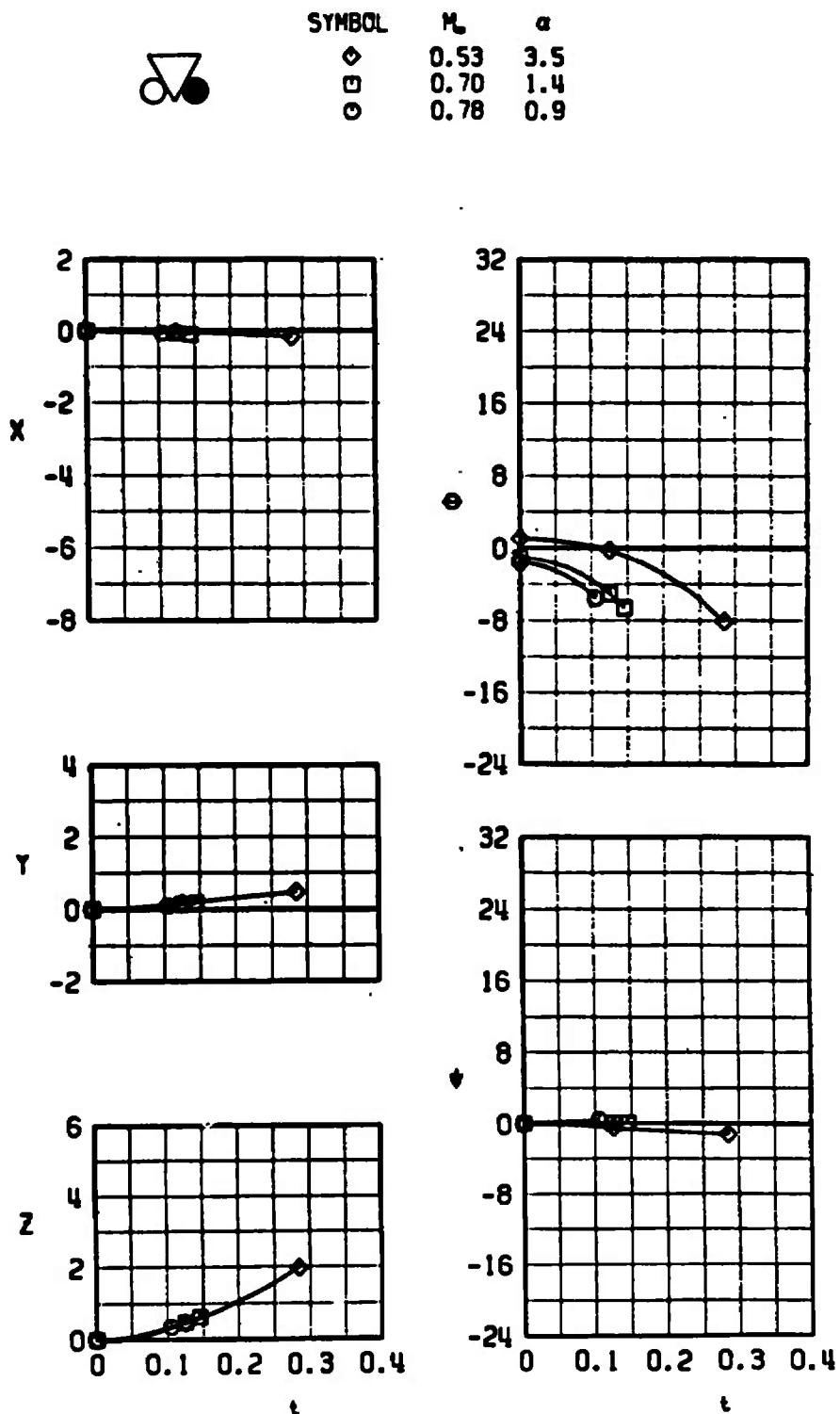
i. MER, Configuration 9H
Fig. 13 Concluded
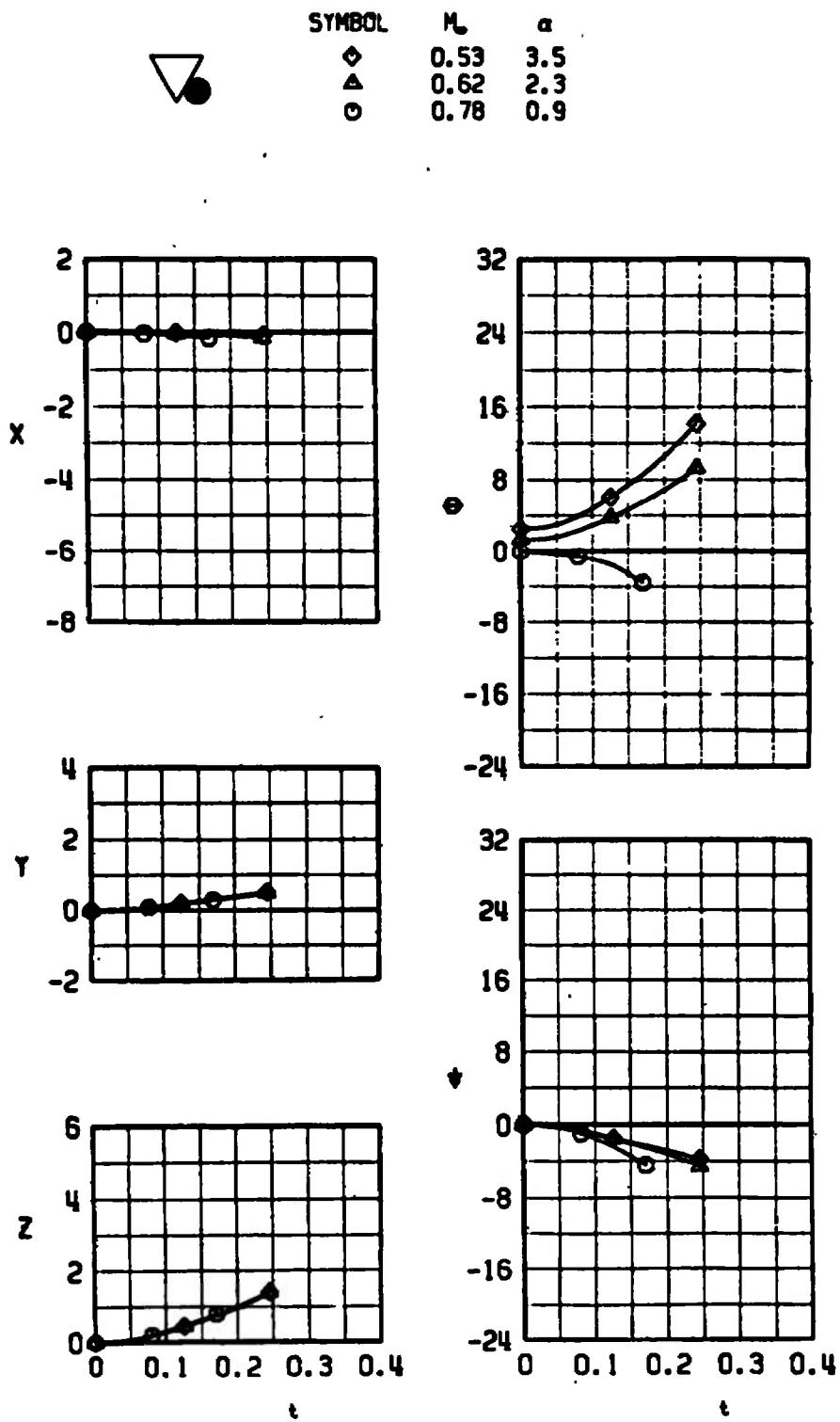
a. TER, Configuration 3H
Fig. 14 Effect of Mach Number on the Separation Characteristics of the
LAU-61/A (Full with the Heavy Warhead and Lugs Shifted 3 in.
Forward) from the Inboard TER
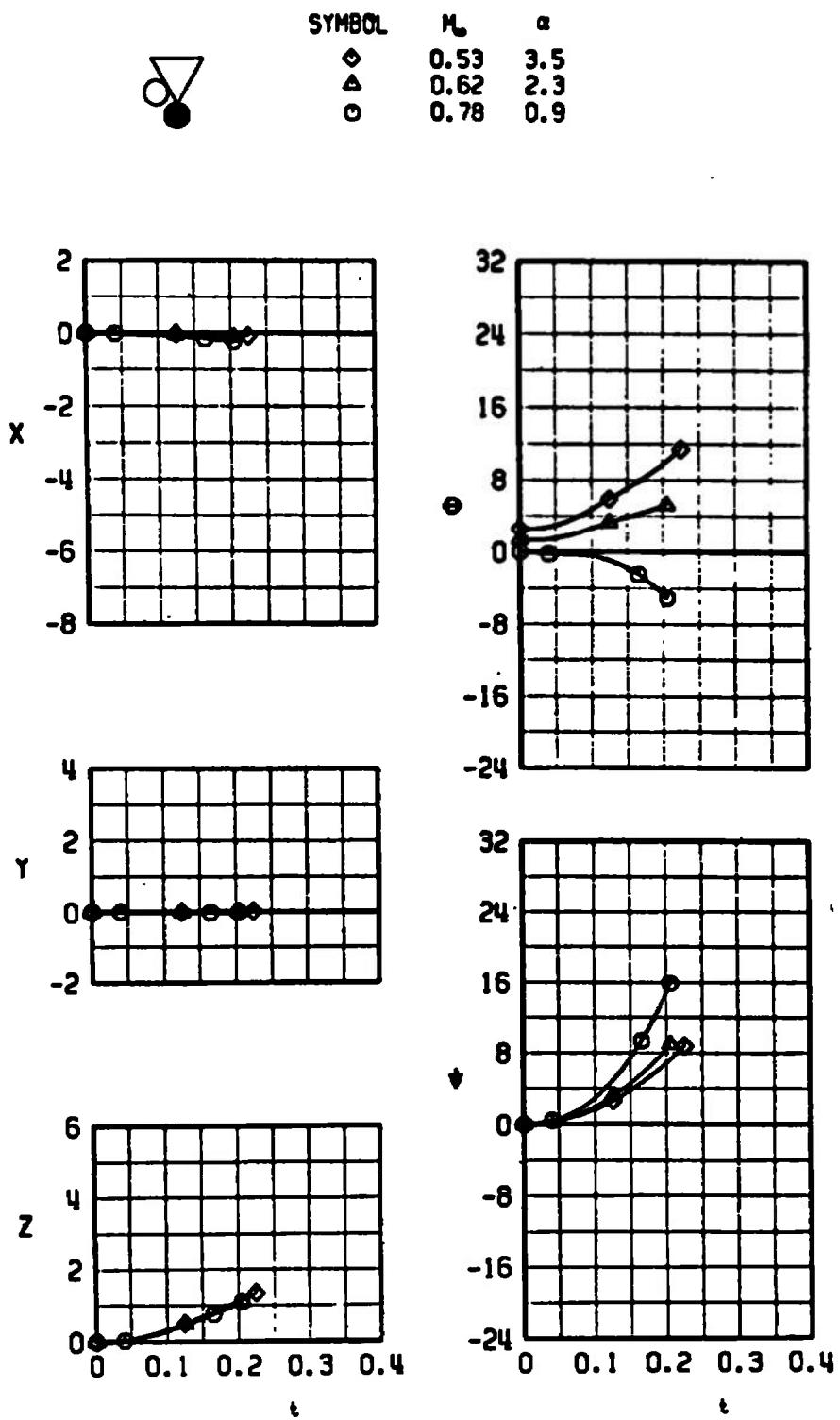
b. TER, Configuration 4H
Fig. 14 Continued
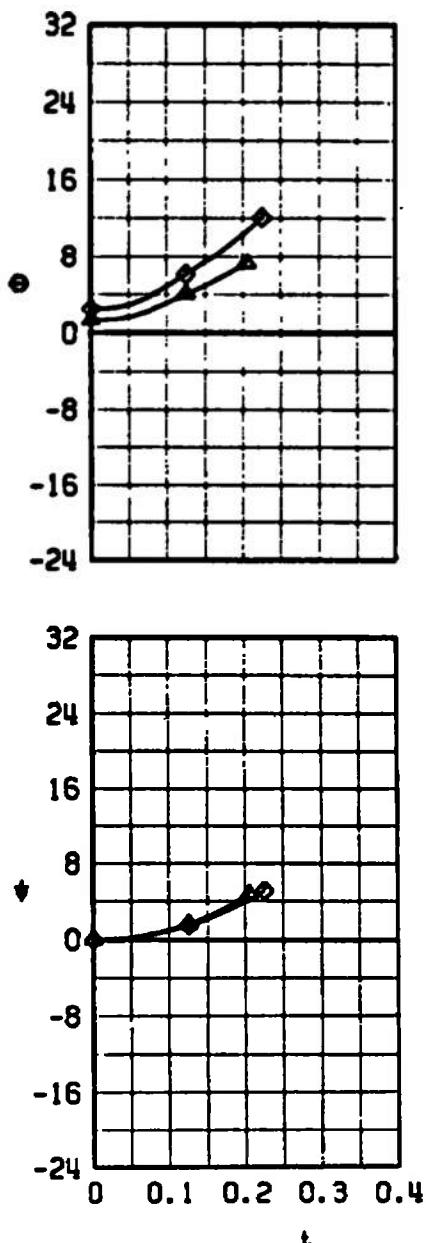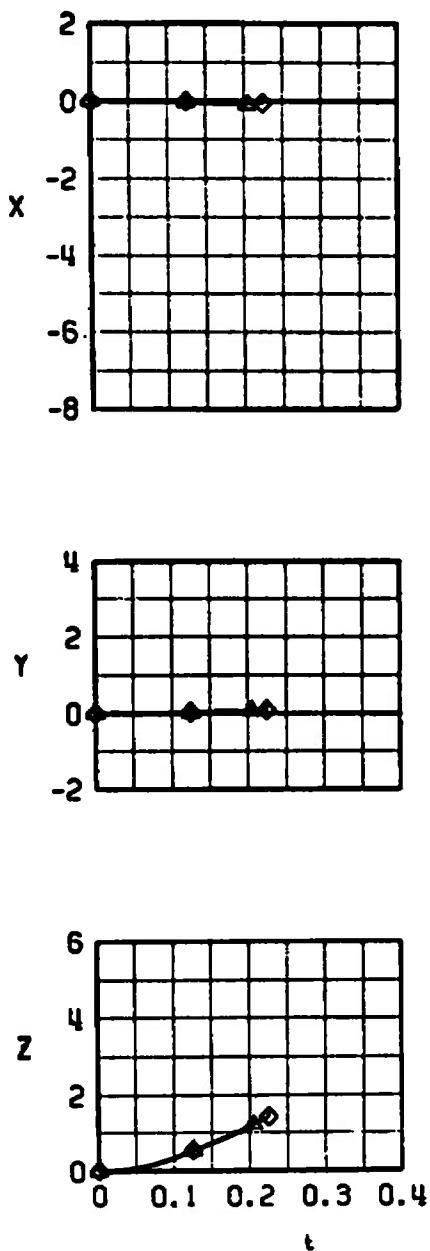
c. TER, Configuration 5H
Fig. 14 Continued
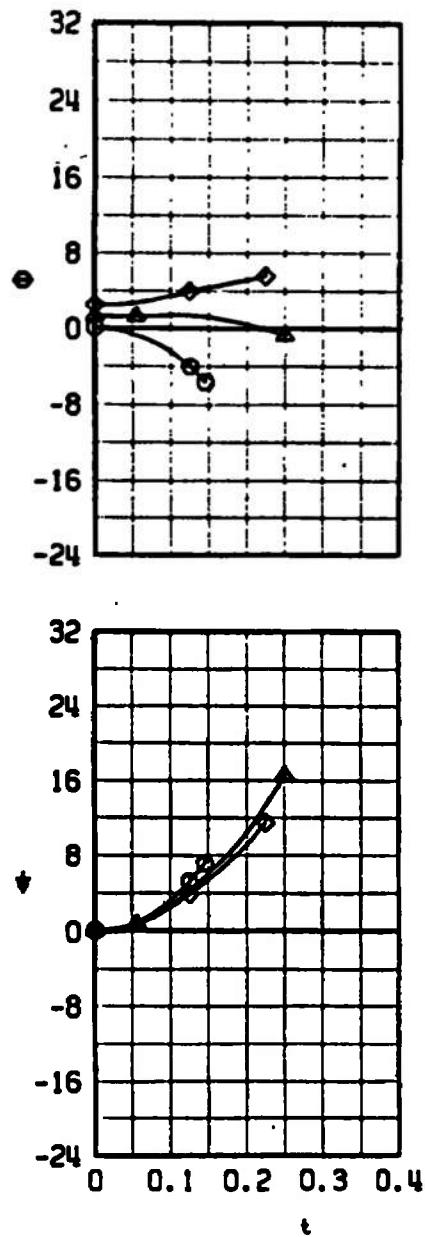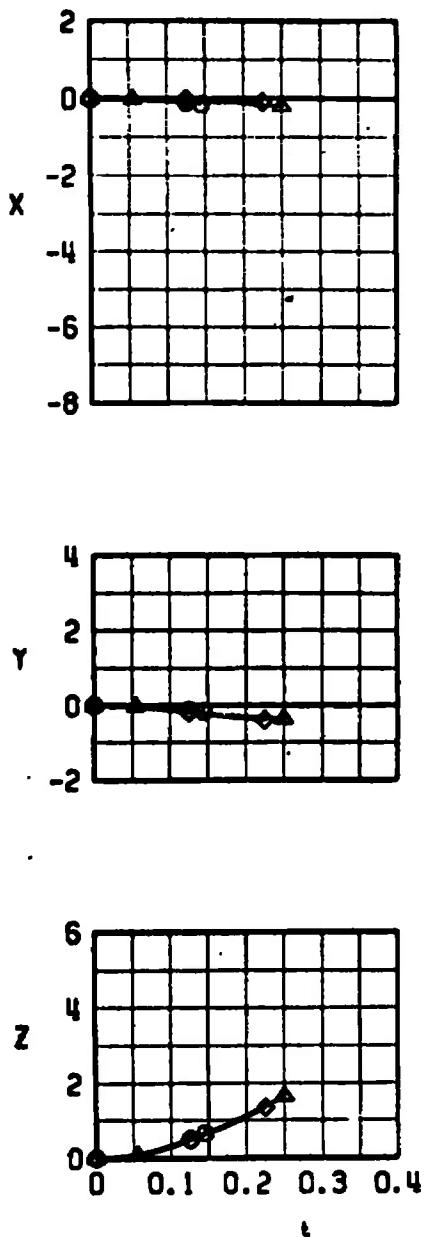
d. TER, Configuration 7H
Fig. 14 Concluded

37

SYMBOL	M_∞	α
◇	0.53	3.5
△	0.62	2.3
⊙	0.78	0.9
▽	0.94	0.2
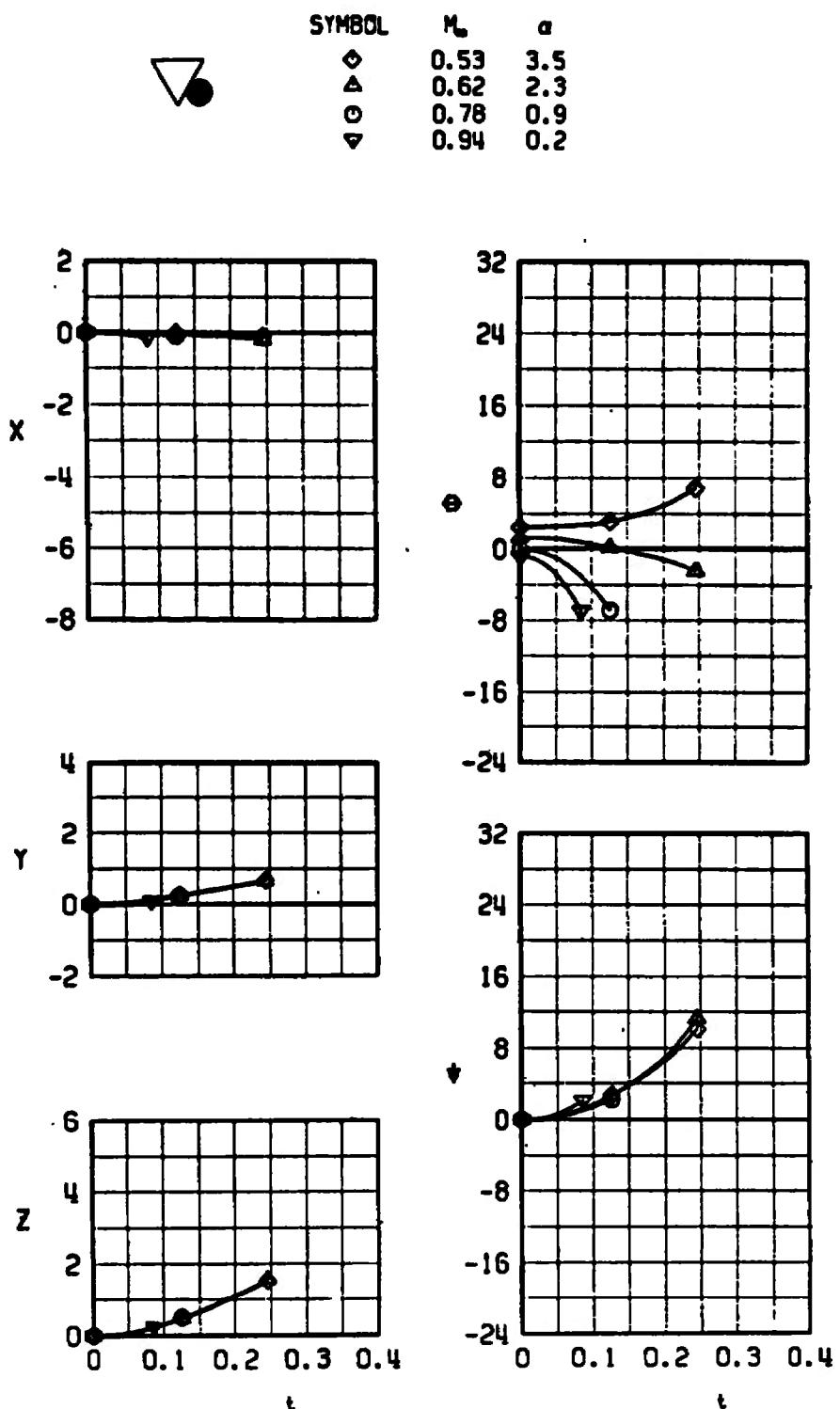
a. TER, Configuration 3L

Fig. 15 Effect of Mach Number on the Separation Characteristics of the LAU-61/A (Full with the Light Warhead and Lugs Shifted 6 in. Forward) from the Inboard TER

SYMBOL	M_∞	α
◇	0.53	3.5
△	0.62	2.3
○	0.78	0.9
▽	0.94	0.2
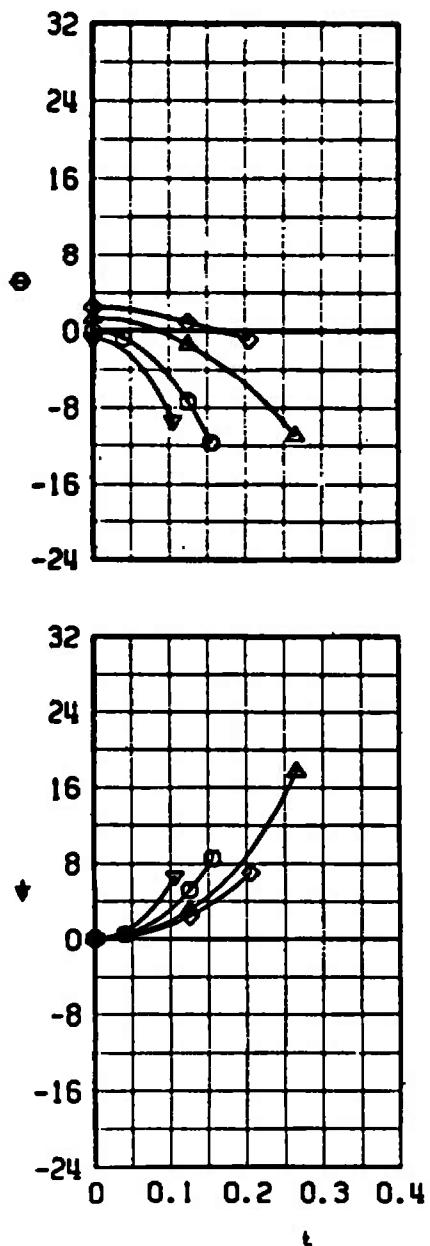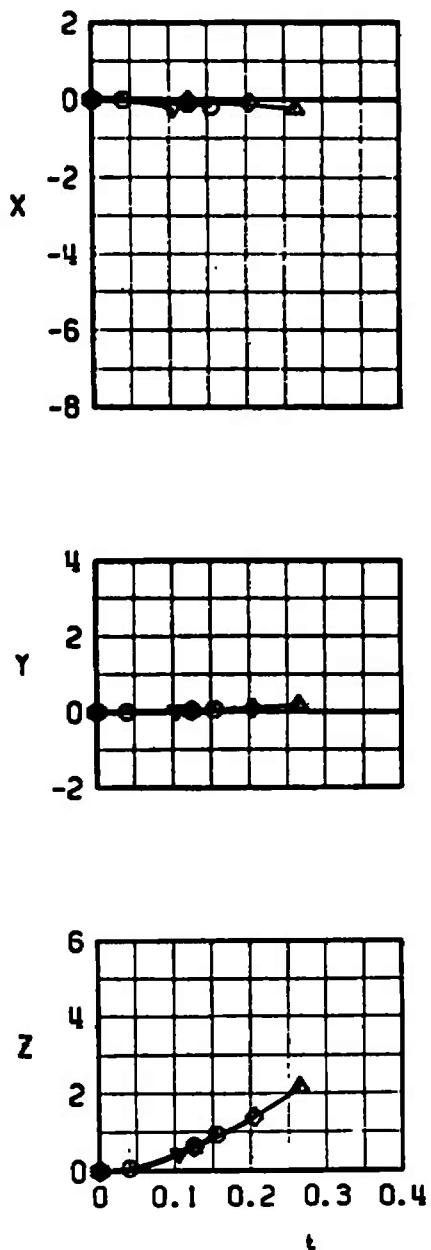
b. TER, Configuration 5L
Fig. 15 Continued

SYMBOL	M	α
◇	0.53	3.5
△	0.62	2.3
○	0.78	0.9
▽	0.94	0.2
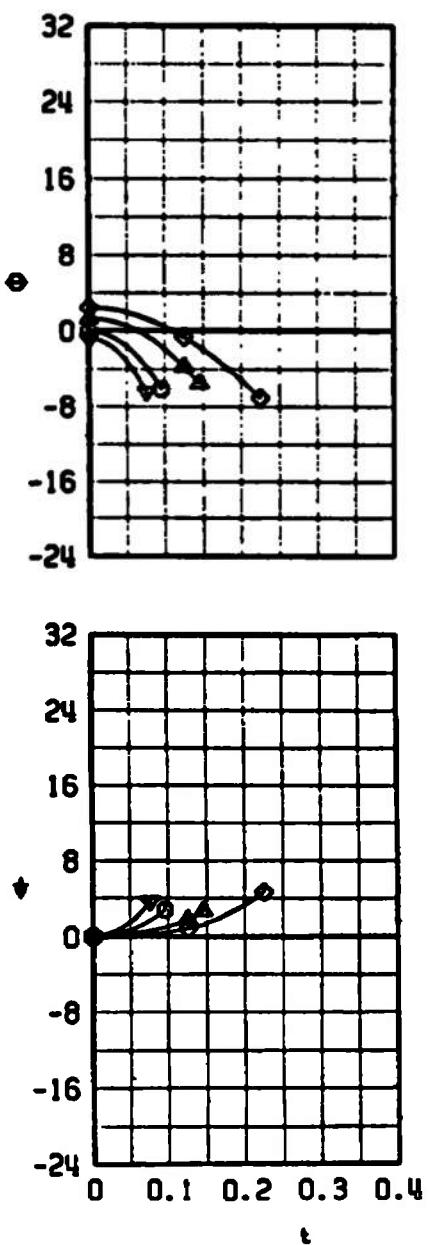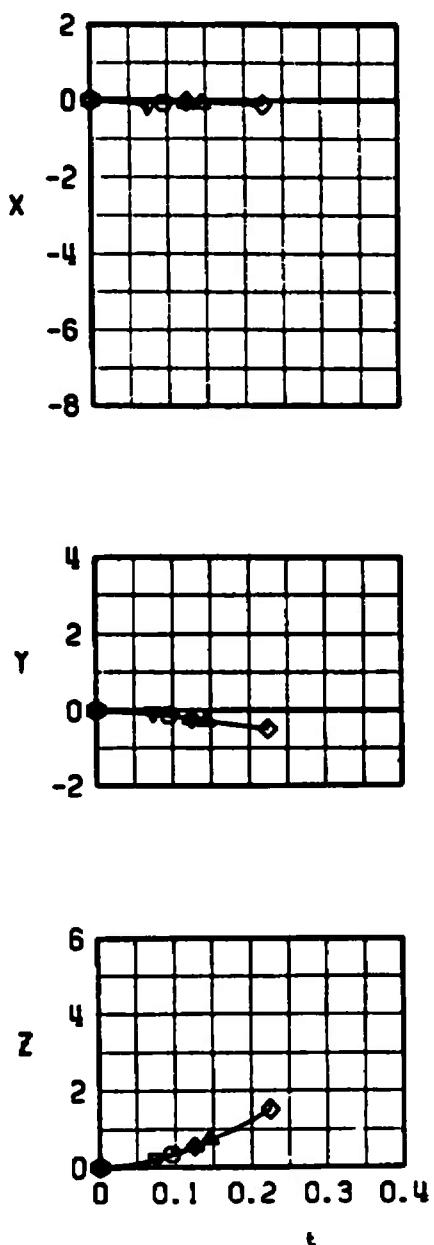
c. TER, Configuration 7L
Fig. 15 Concluded

40
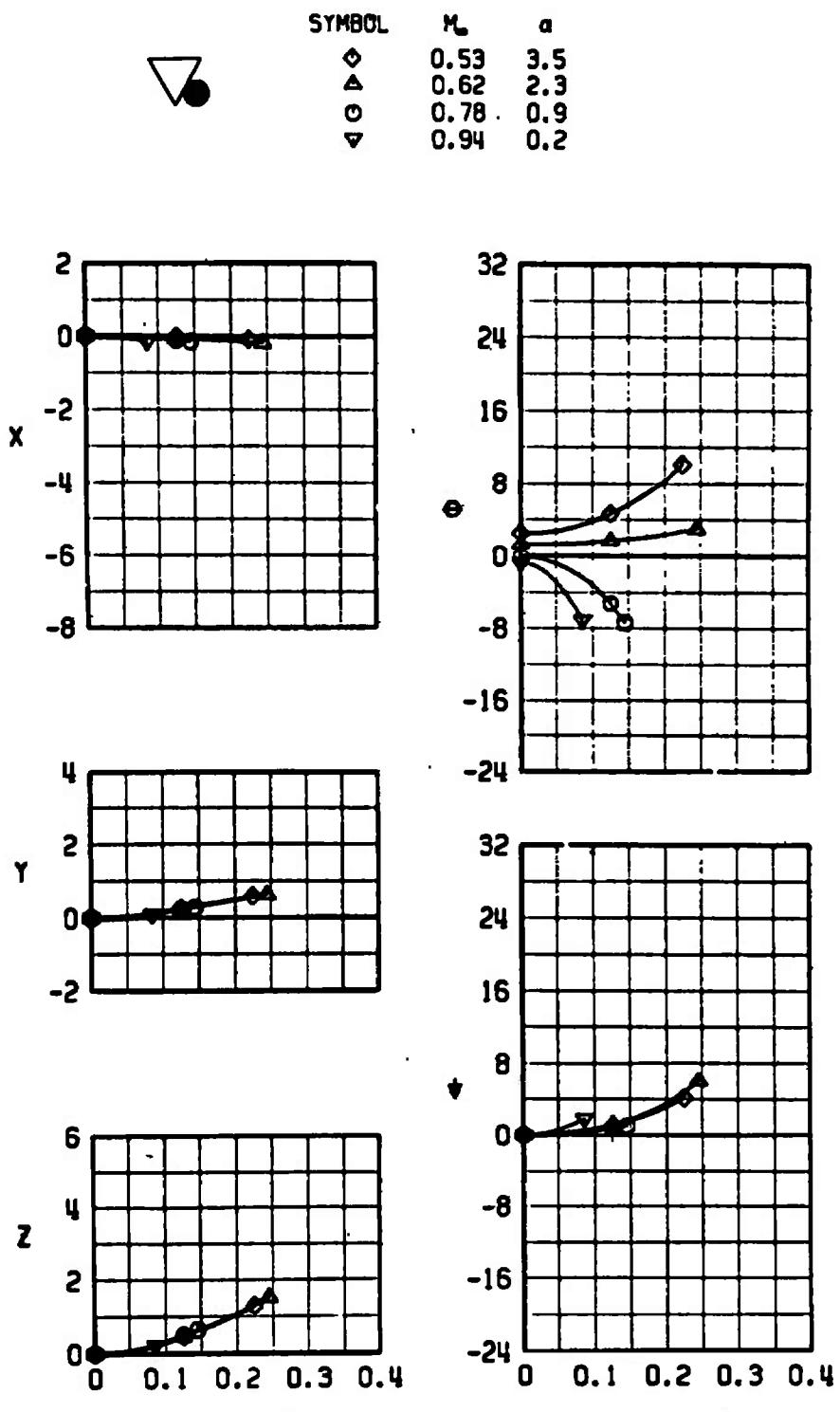
a. TER, Configuration 3L

Fig. 16 Effect of Mach Number on the Separation Characteristics of the LAU-61/A (Full with the Light Warhead and Lugs Shifted 3 in. Forward) from the Inboard TER
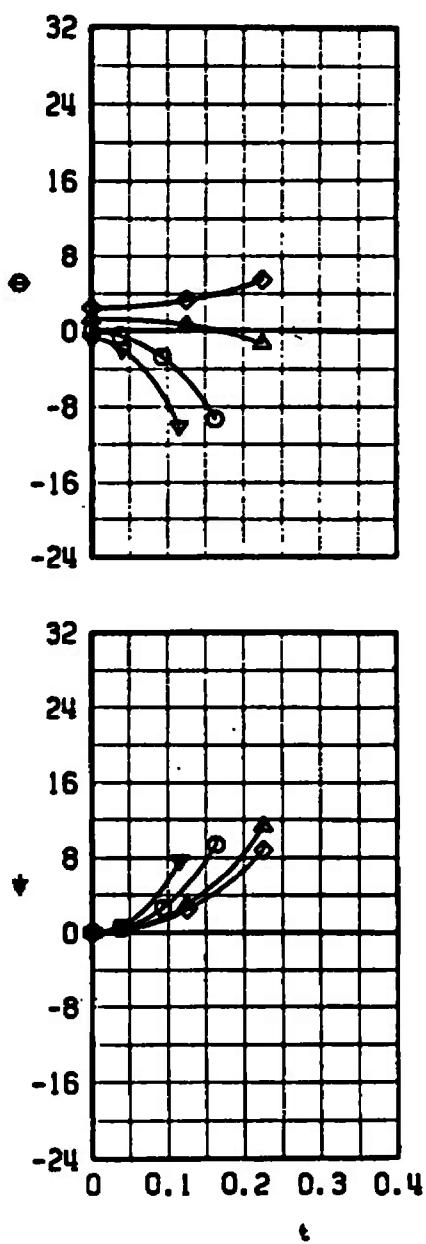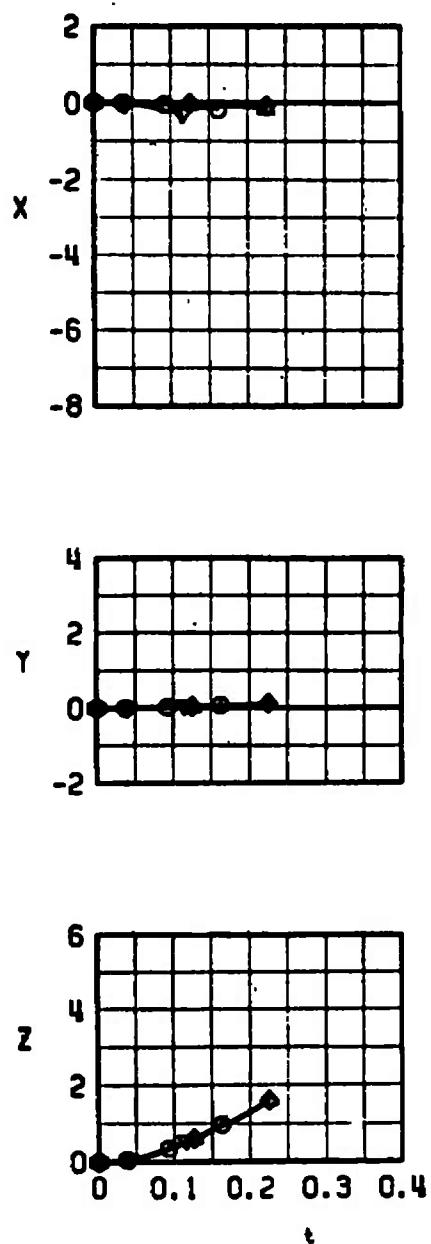
b. TER, Configuration 5L
Fig. 16 Continued

SYMBOL	M_∞	α
◇	0.53	3.5
△	0.62	2.3
⊙	0.78	0.9
▽	0.94	0.2
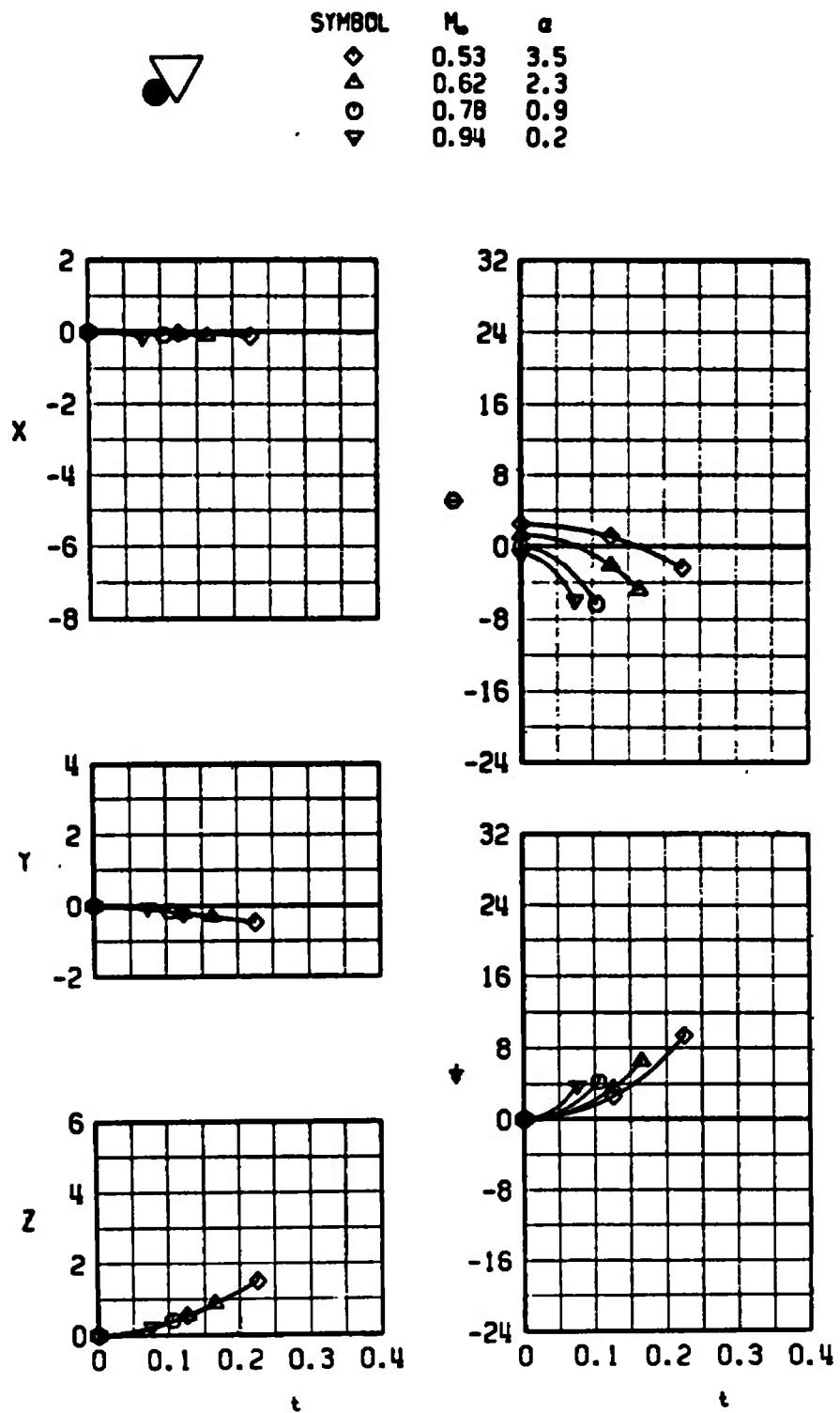
c. TER, Configuration 7L
Fig. 16 Concluded
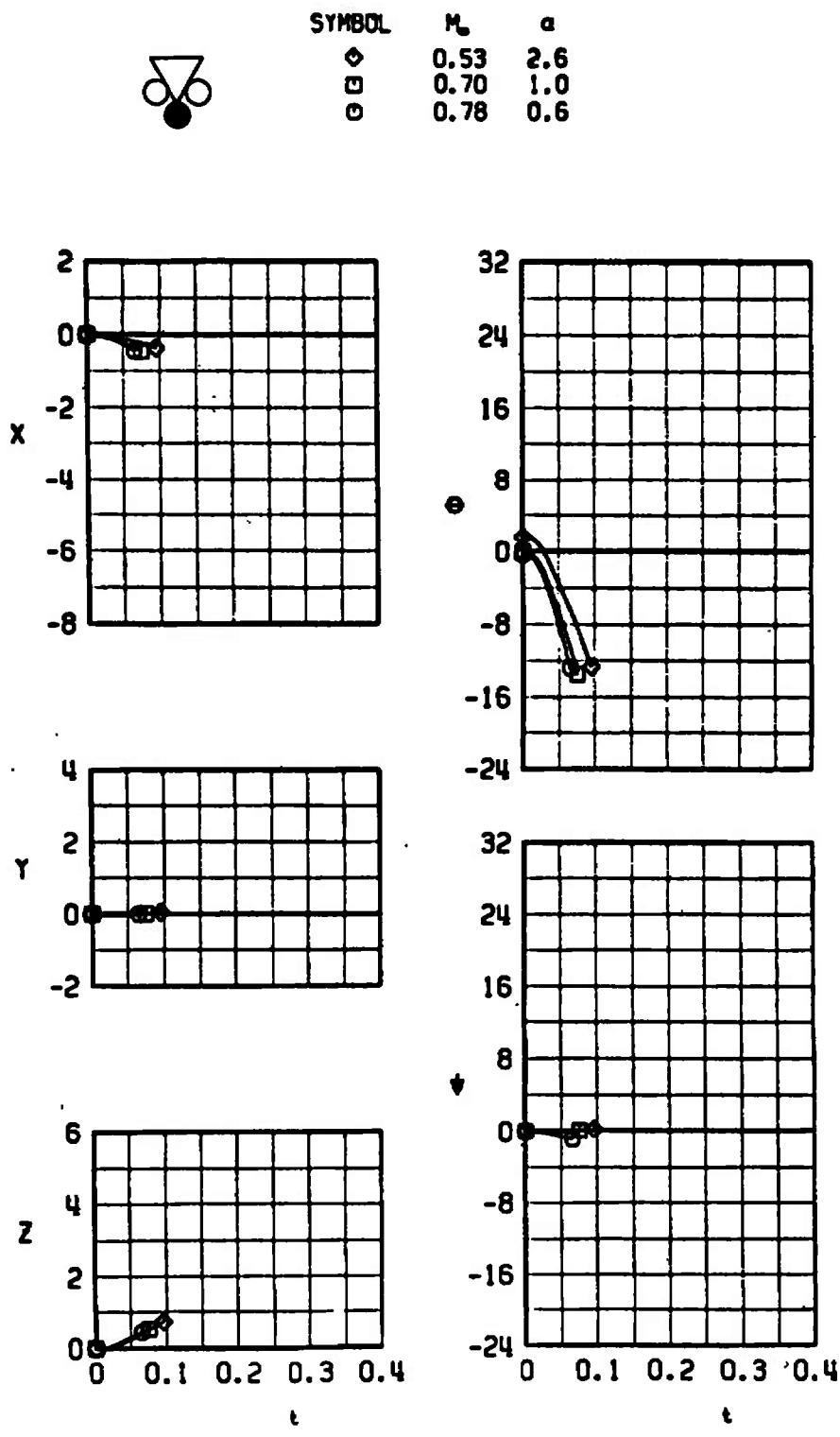
a. TER, Configuration 1E

Fig. 17 Effect of Mach Number on the Separation Characteristics of the LAU-61/A (Empty with Lugs Shifted 6 in. Forward) from the Inboard TER and Centerline MER
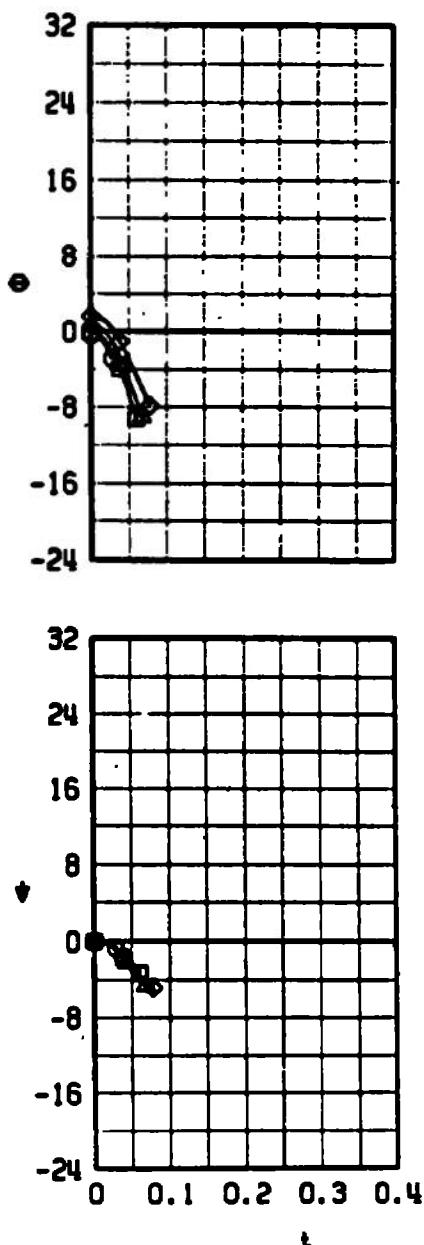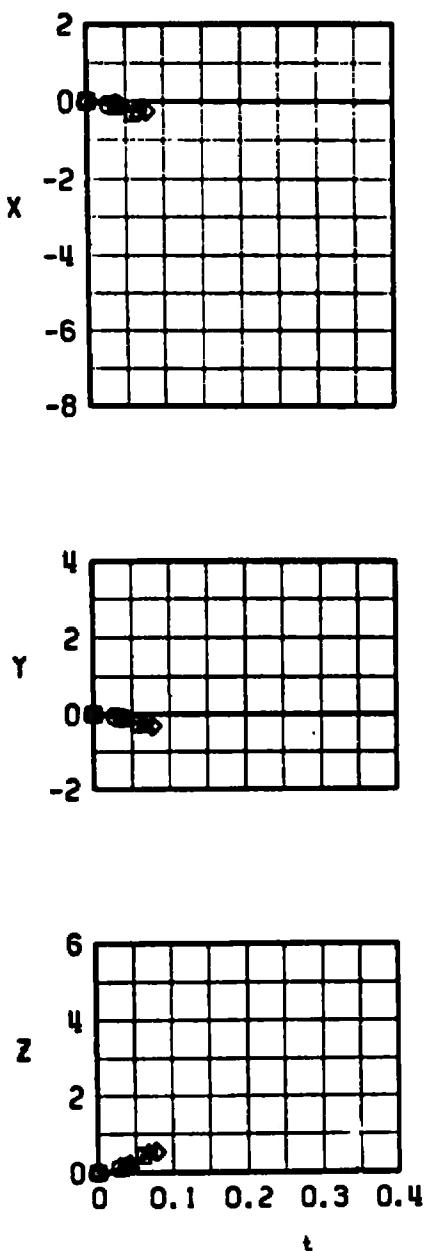
b. TER, Configuration 2E
Fig. 17 Continued

SYMBOL	M_∞	α
◇	0.53	2.6
△	0.62	1.6
▫	0.70	1.0
⊙	0.78	0.6
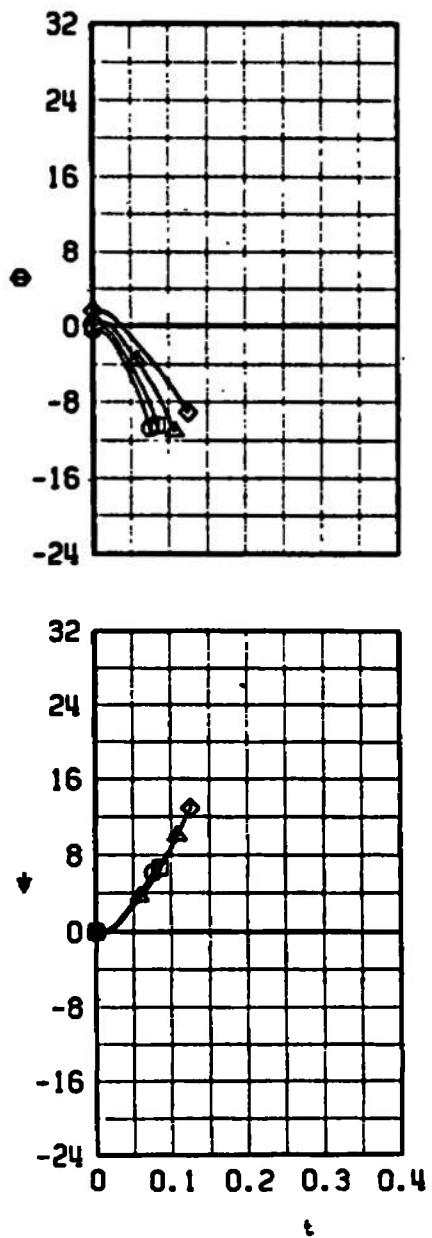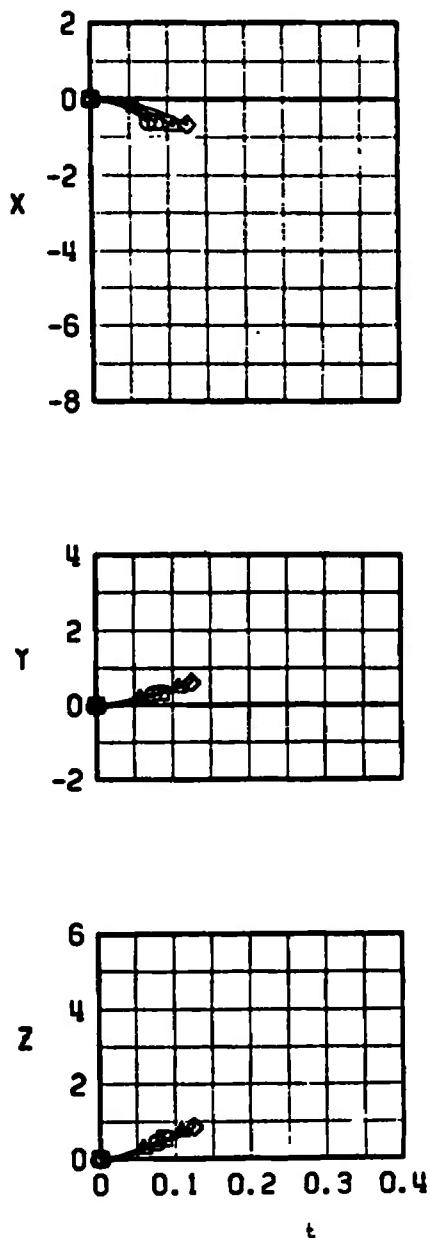
c. TER, Configuration 3E
Fig. 17 Continued
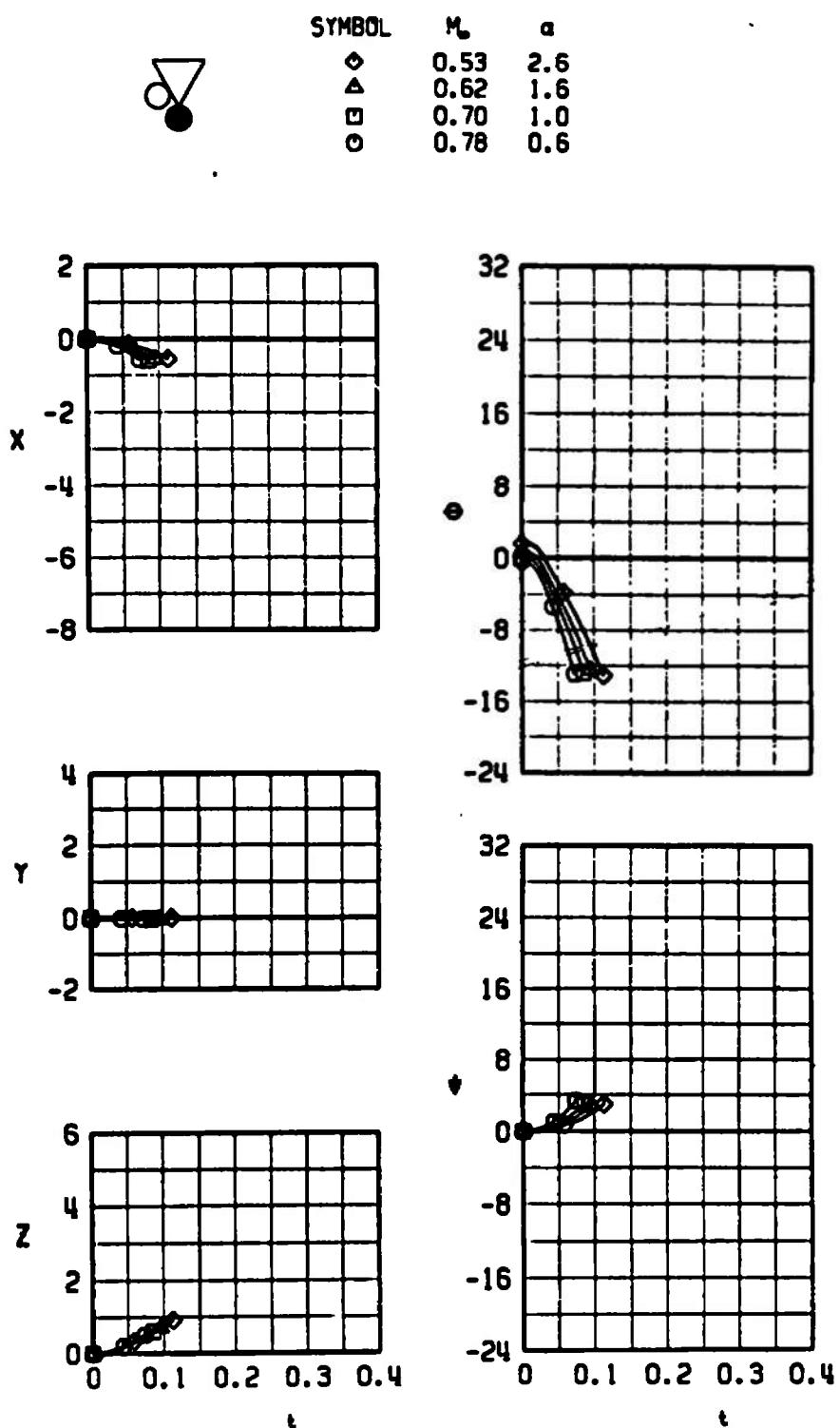
d. TER, Configuration 4E
Fig. 17 Continued

SYMBOL	M_∞	α
◇	0.53	2.6
△	0.62	1.6
▣	0.70	1.0
⊙	0.78	0.6
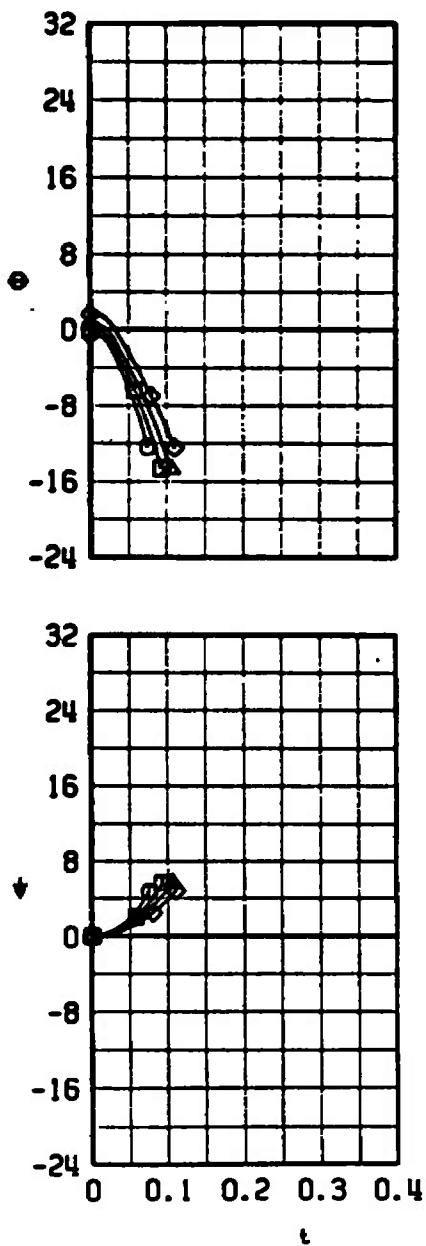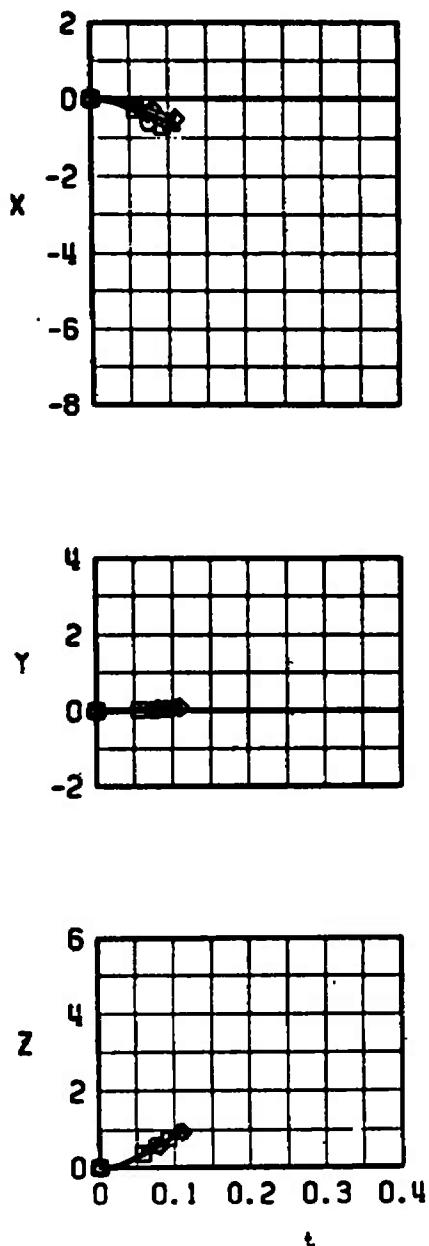
e. TER, Configuration 5E
Fig. 17 Continued

SYMBOL	M∞	α
◇	0.53	2.6
△	0.62	1.6
☉	0.78	0.6
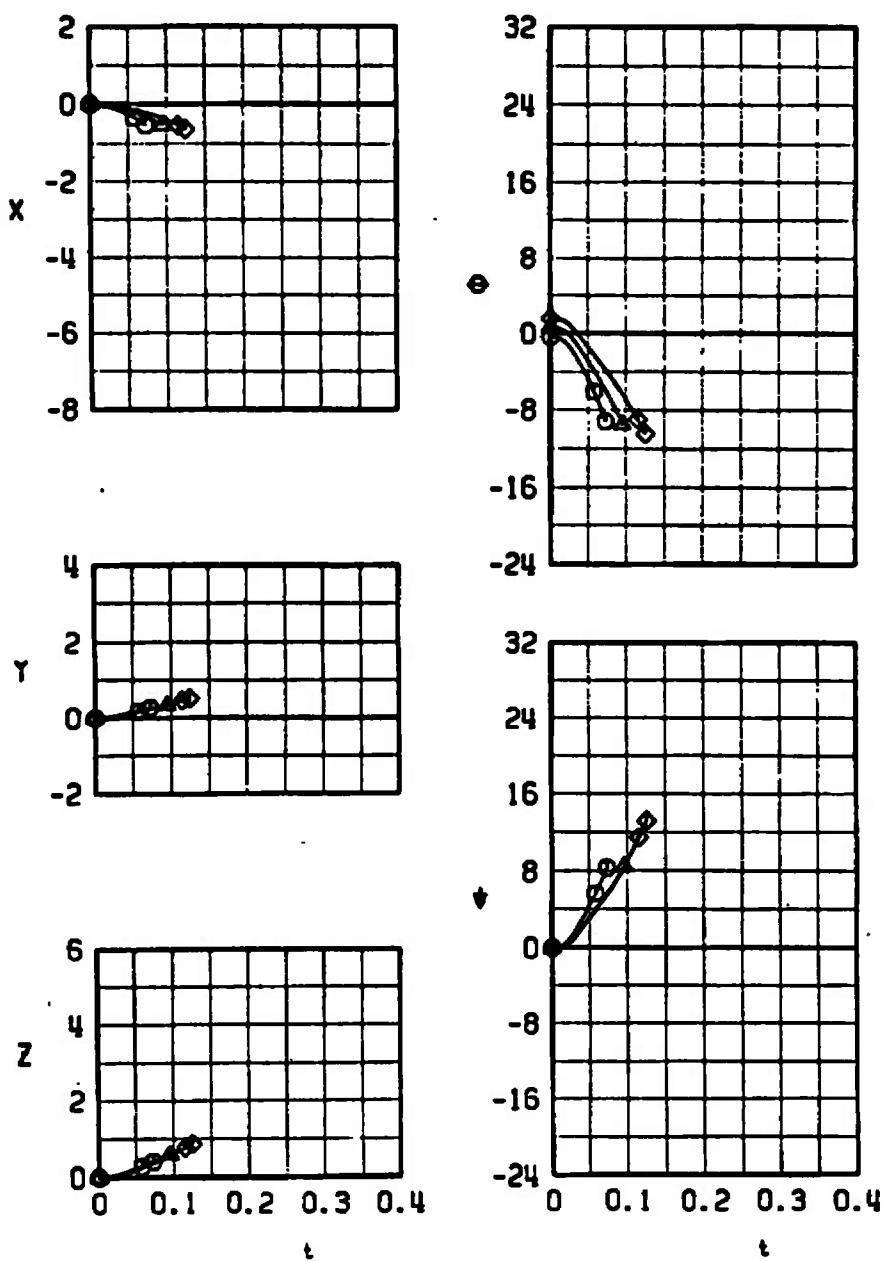
f. TER, Configuration 6E
Fig. 17 Continued

SYMBOL	M_∞	α
◇	0.53	2.6
▲	0.62	1.6
▥	0.70	1.0
◉	0.78	0.6
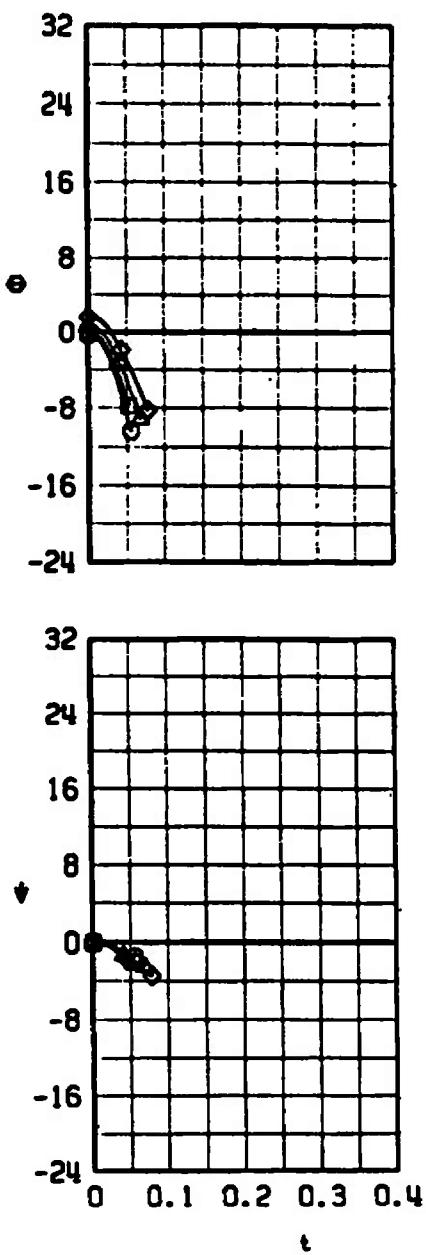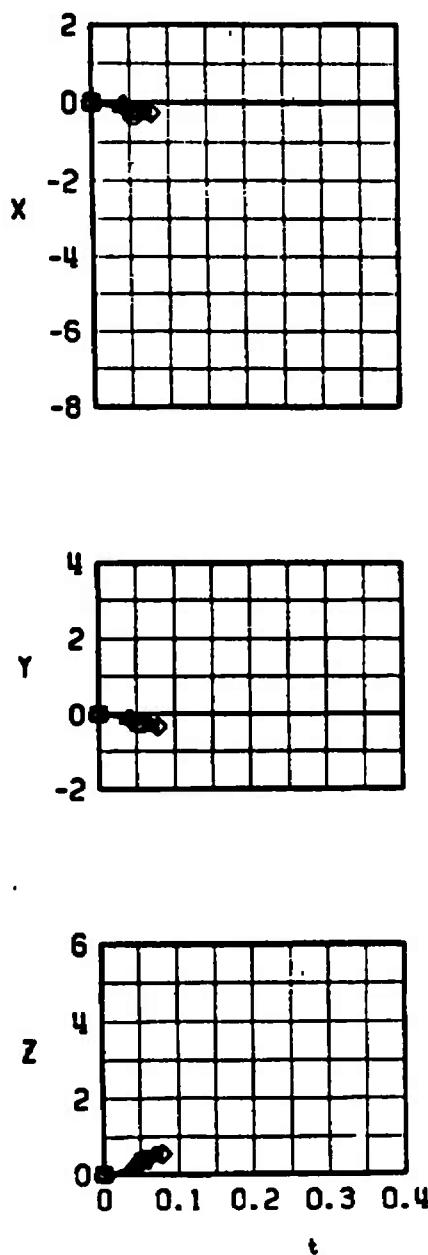
g. TER, Configuration 7E
Fig. 17 Continued

50

SYMBOL	M_∞	α
◇	0.53	2.6
☉	0.78	0.6
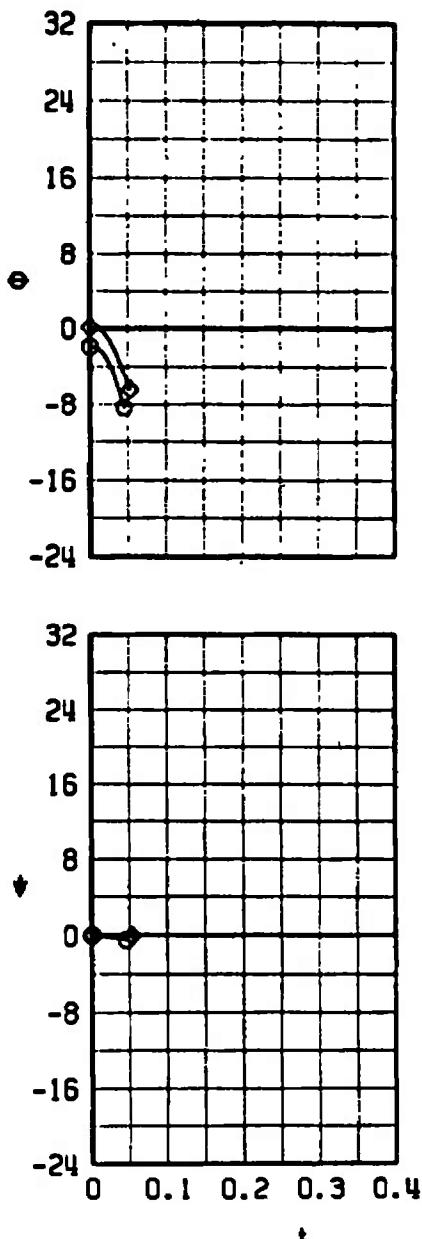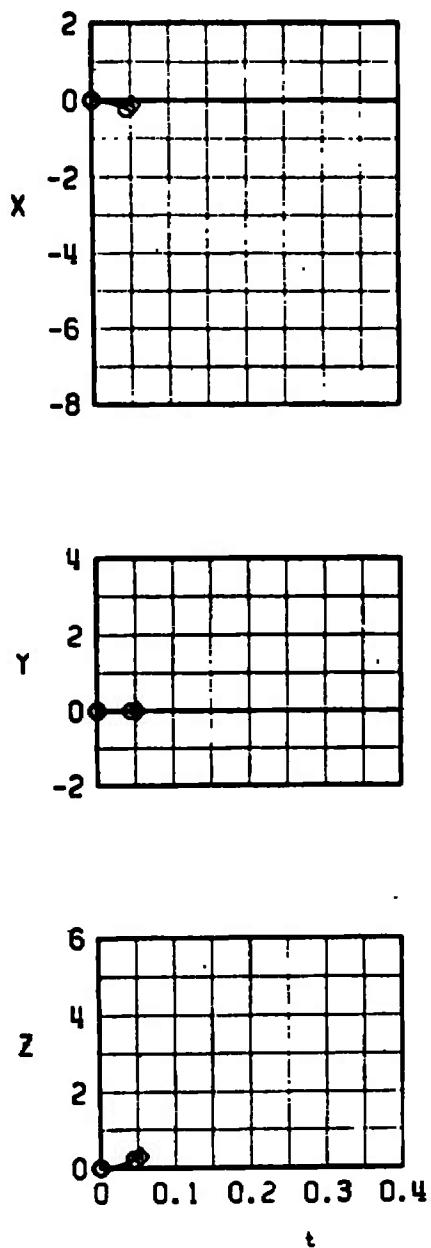
h. MER, Configuration 8E
Fig. 17 Continued
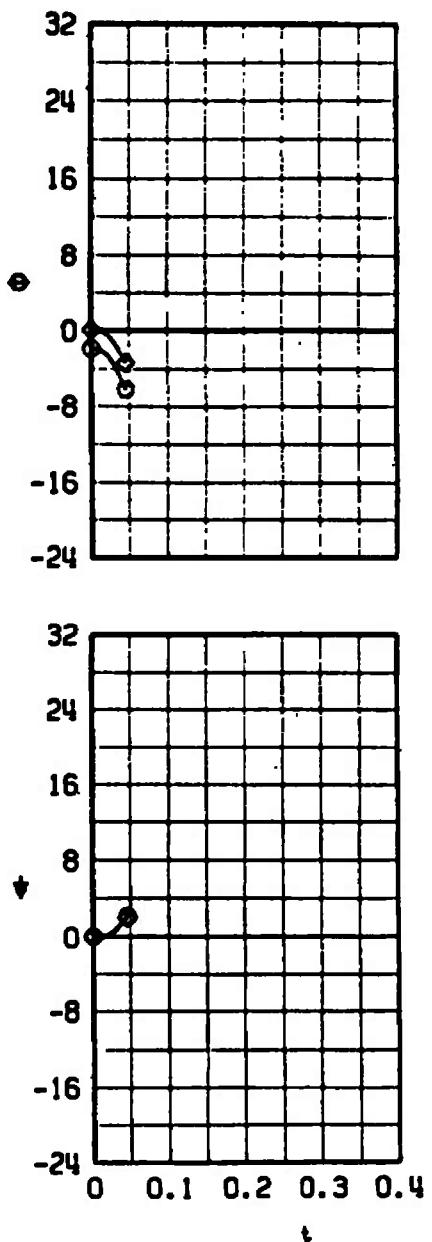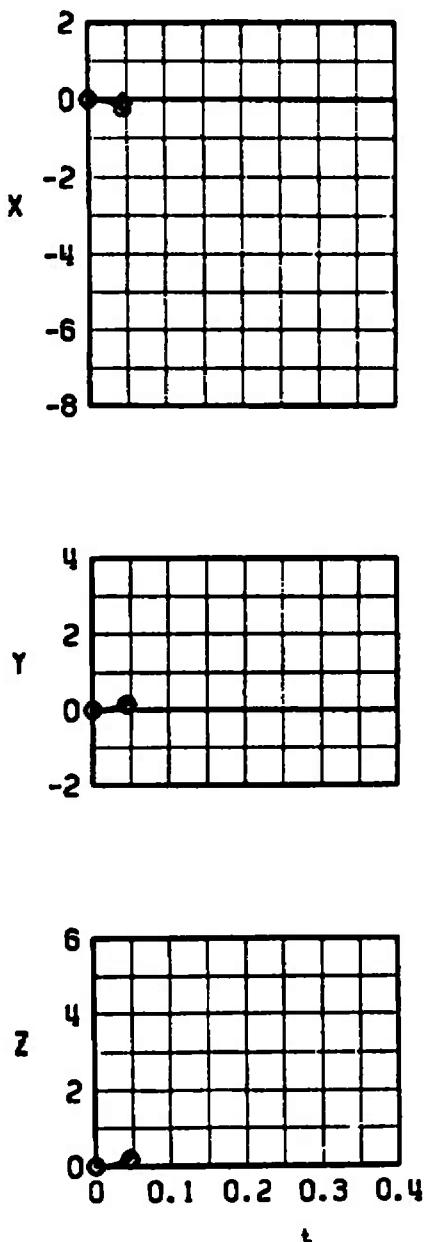
i. MER, Configuration 10E
Fig. 17 Concluded

| SYMBOL	M_∞	α
◇	0.53	2.6
△	0.62	1.6
⊡	0.70	1.0
⊙	0.78	0.6
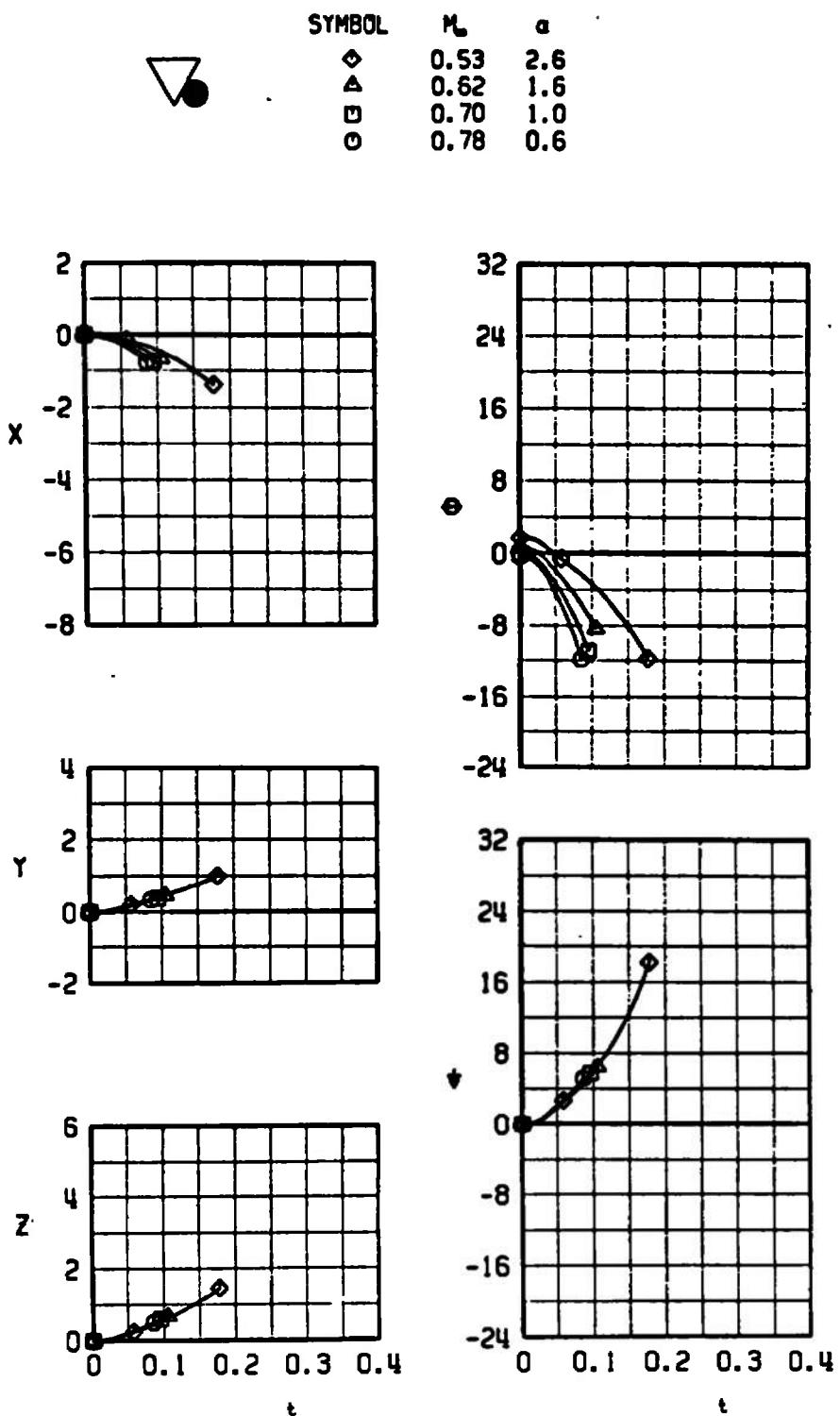
a. TER, Configuration 3E

Fig. 18 Effect of Mach Number on the Separation Characteristics of the LAU-61/A (Empty with Lugs Shifted 3-in. Forward) from the Inboard TER

SYMBOL	M_∞	α
◇	0.53	2.6
△	0.62	1.6
▣	0.70	1.0
○	0.78	0.6
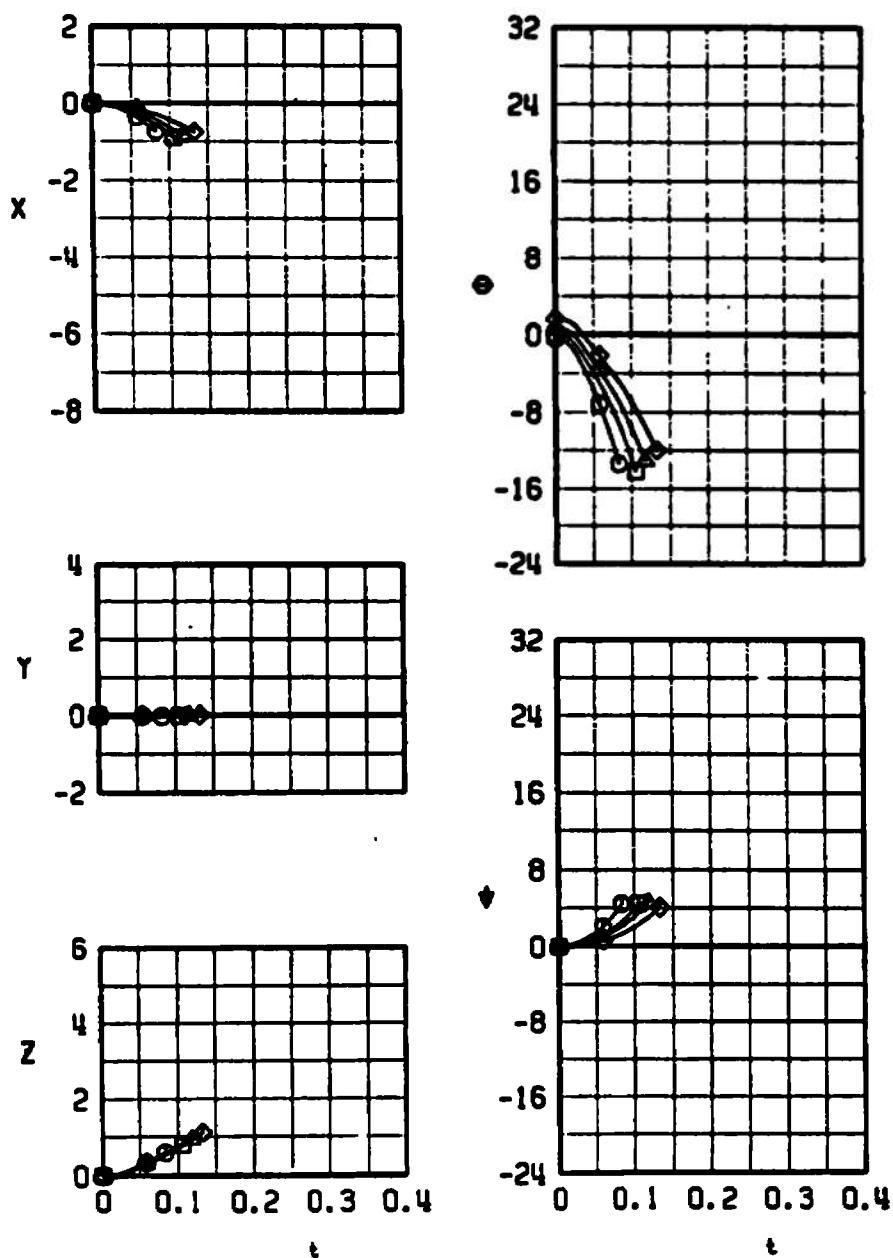
b. TER, Configuration 4E
Fig. 18 Continued

c. TER, Configuration 5E
Fig. 18 Continued

SYMBOL	M_∞	α
◇	0.53	2.6
△	0.62	1.6
⊡	0.70	1.0
⊙	0.78	0.6
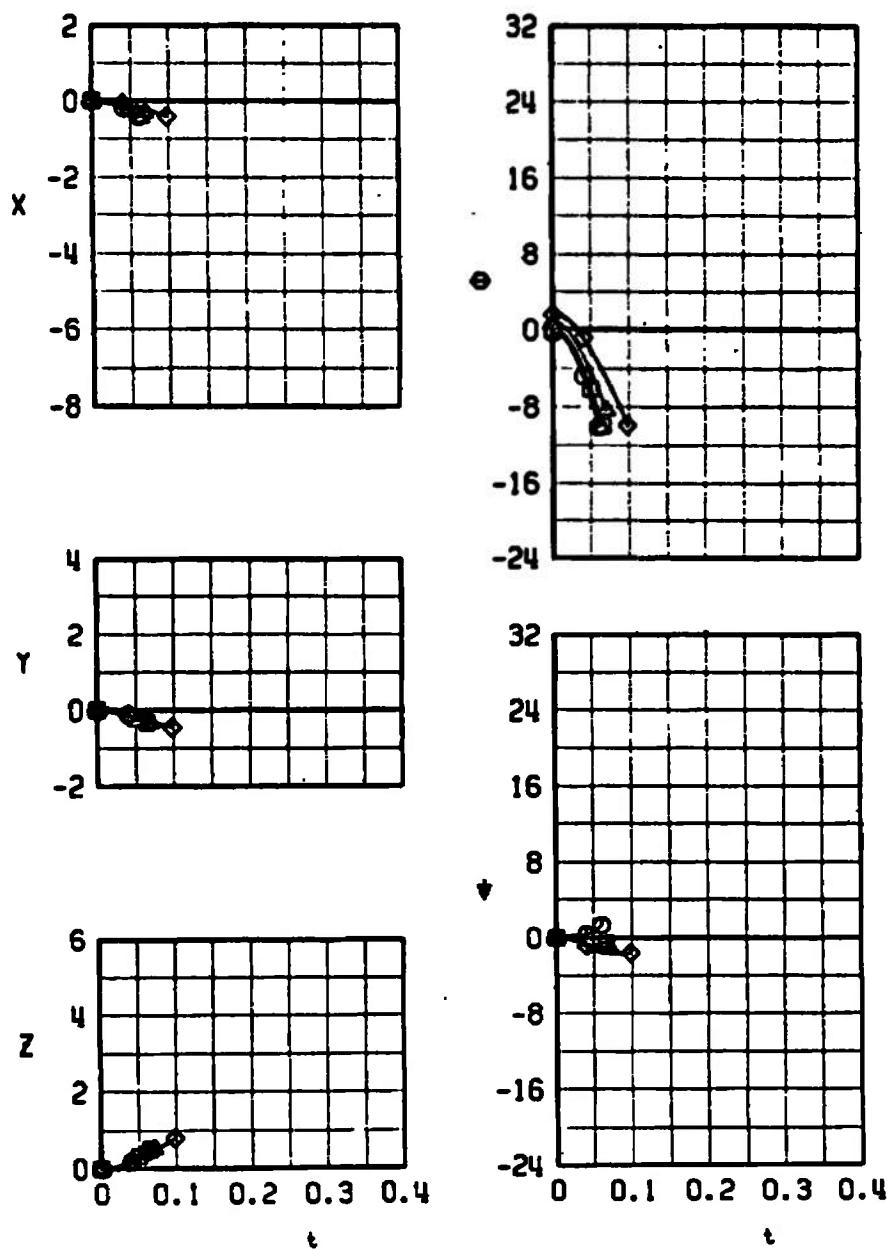
d. TER, Configuration 7E
Fig. 18 Concluded

SYMBOL	LUGS SHIFTED
O	6 IN.
Δ	3 IN.
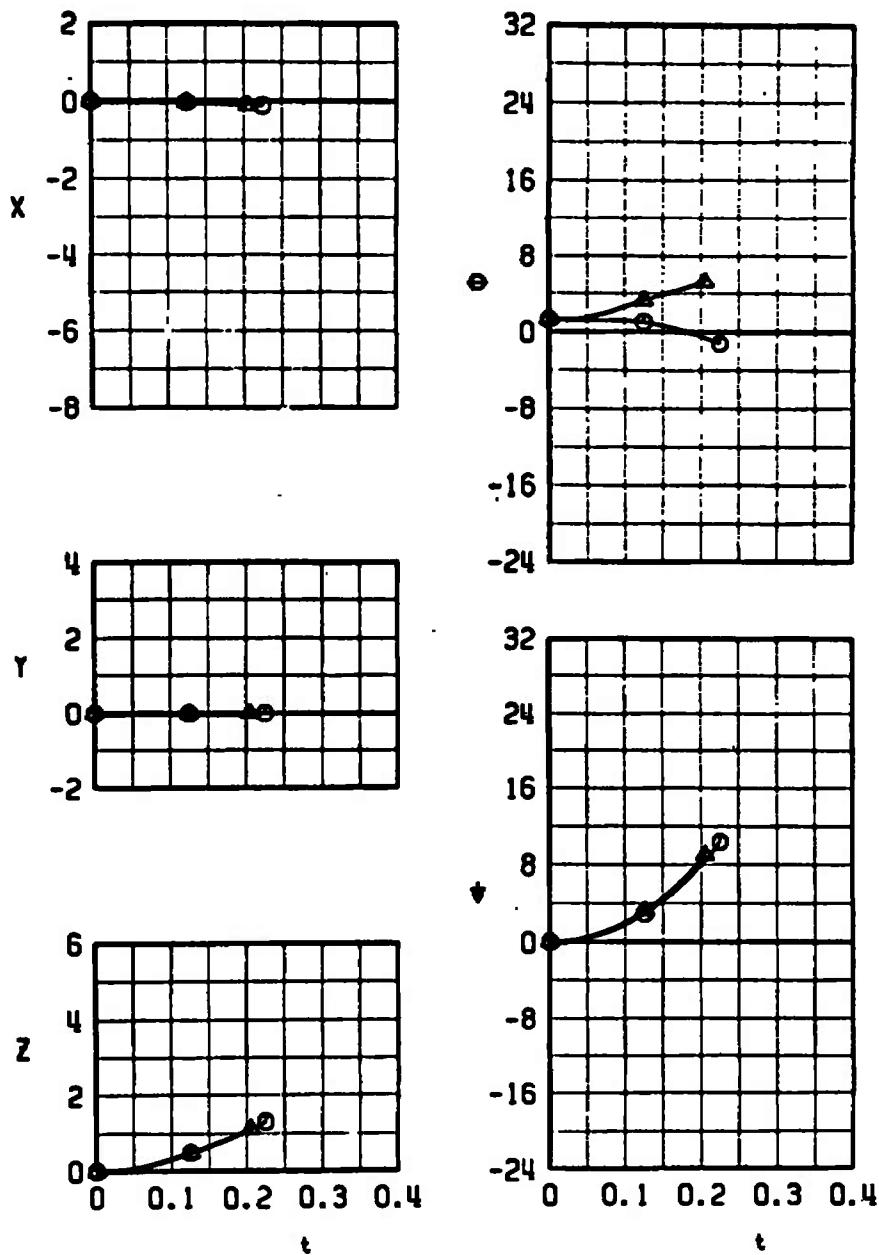
a. $M_\infty = 0.62$, Configuration 4H

Fig. 19 Comparison of Trajectories of the LAU-61/A (Full with the Heavy Warhead) from the Inboard TER with Lugs Shifted 6 and 3 in. Forward
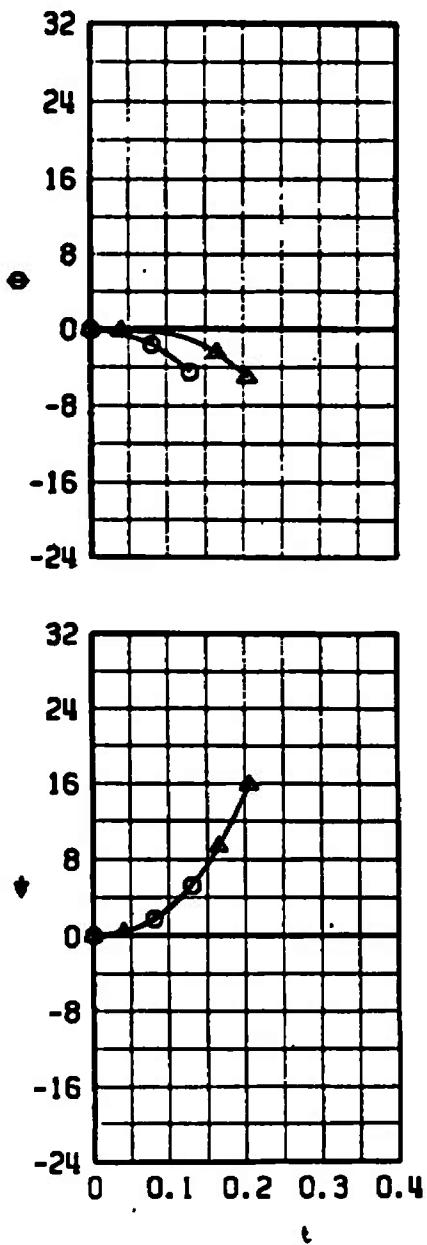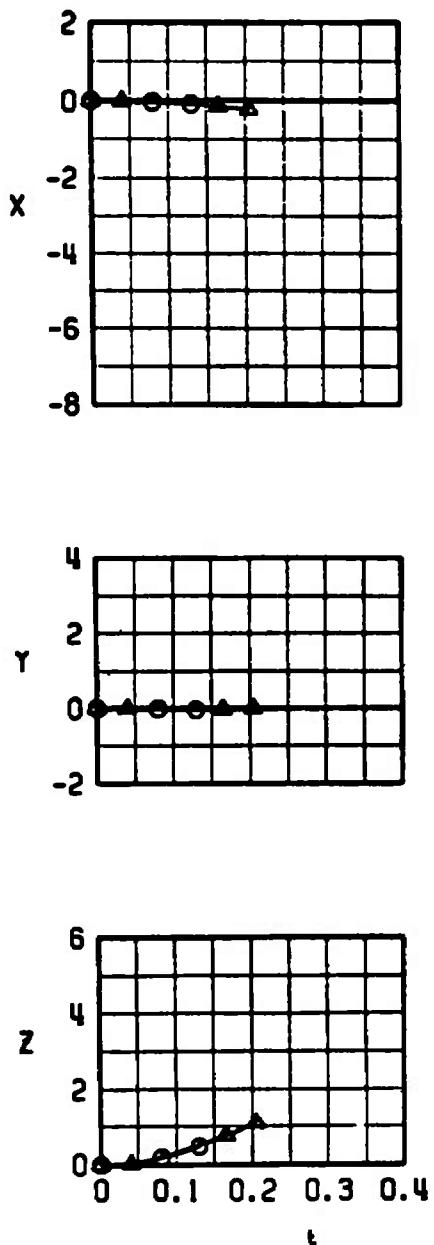
b. $M_\infty = 0.78$, Configuration 4H
Fig. 19 Concluded
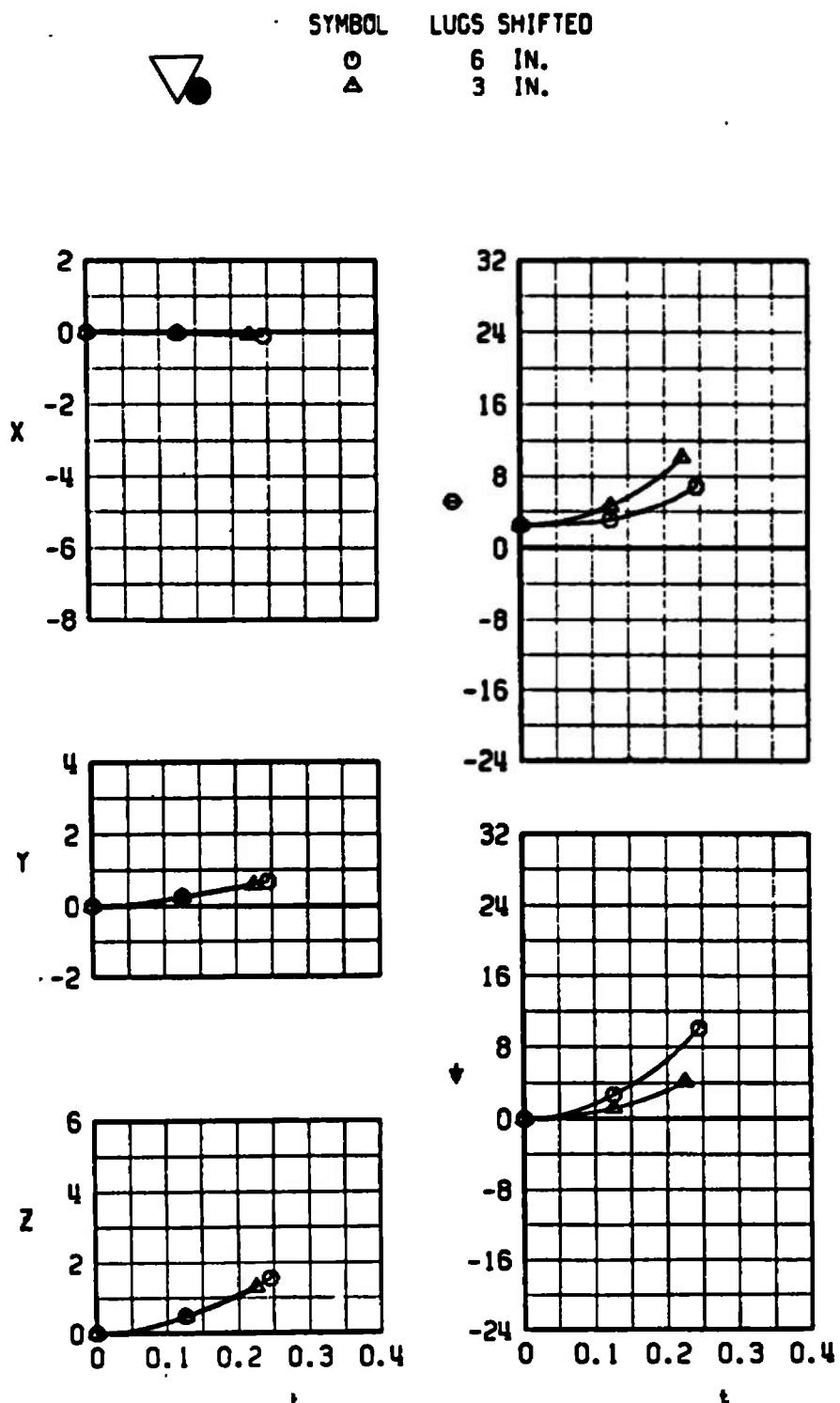
a. M∞ = 0.53, Configuration 3L

Fig. 20 Comparison of Trajectories of the LAU-61/A (Full with the Light
Warhead) from the Inboard TER with Lugs Shifted 6 and 3 in. Forward
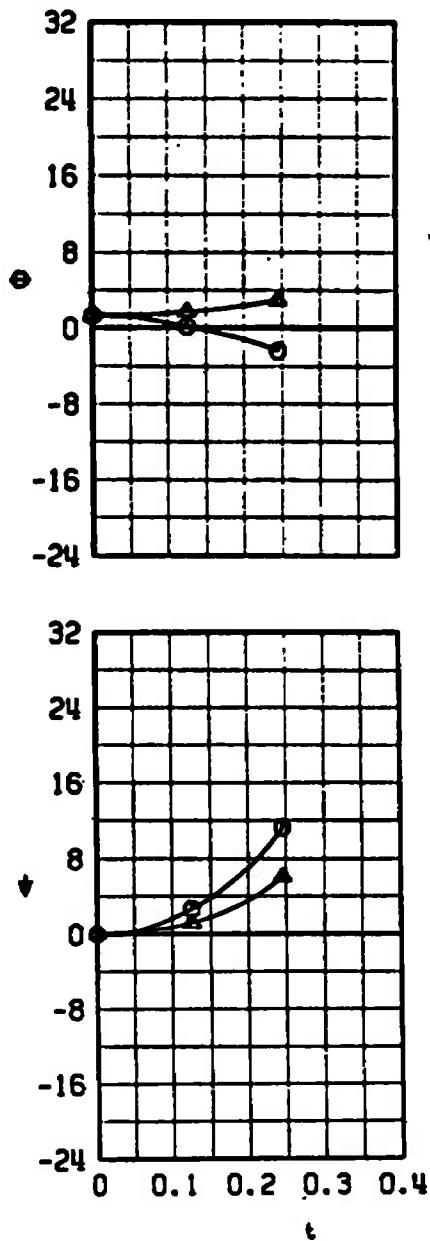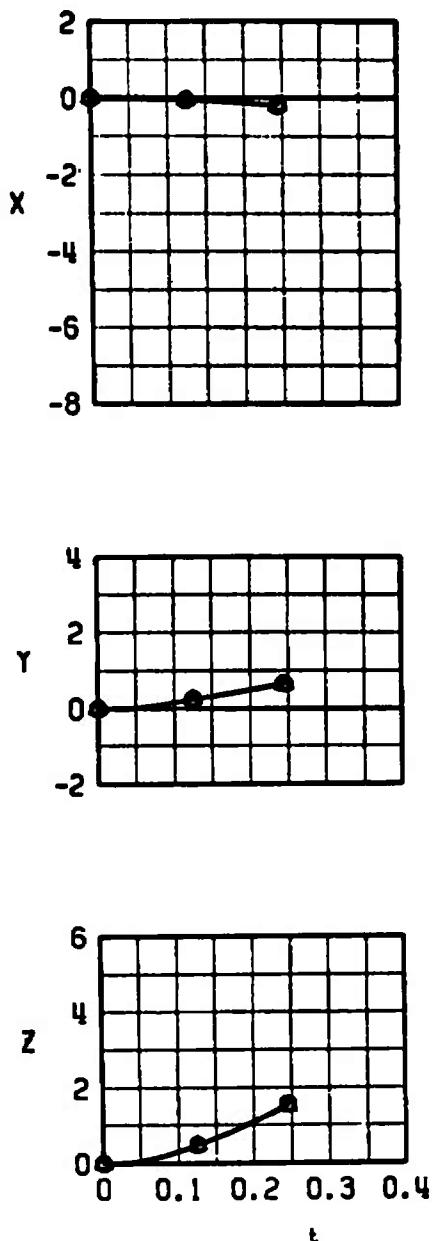
b. $M_\infty = 0.62$, Configuration 3L
Fig. 20 Concluded

a. M∞ = 0.53, Configuration 3E

Fig. 21 Comparison of Trajectories of the LAU-61/A (Empty) from the Inboard TER with Lugs Shifted 6 and 3 in. Forward
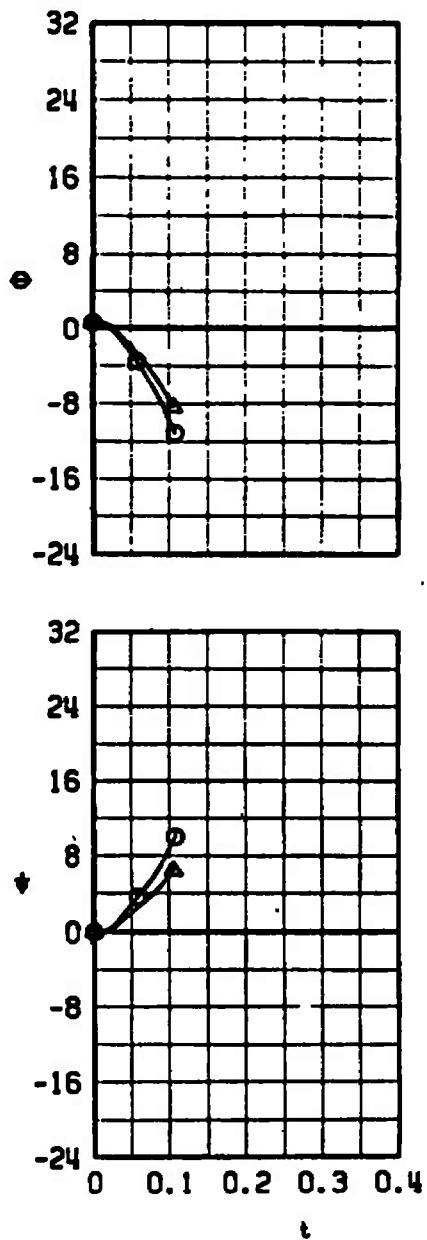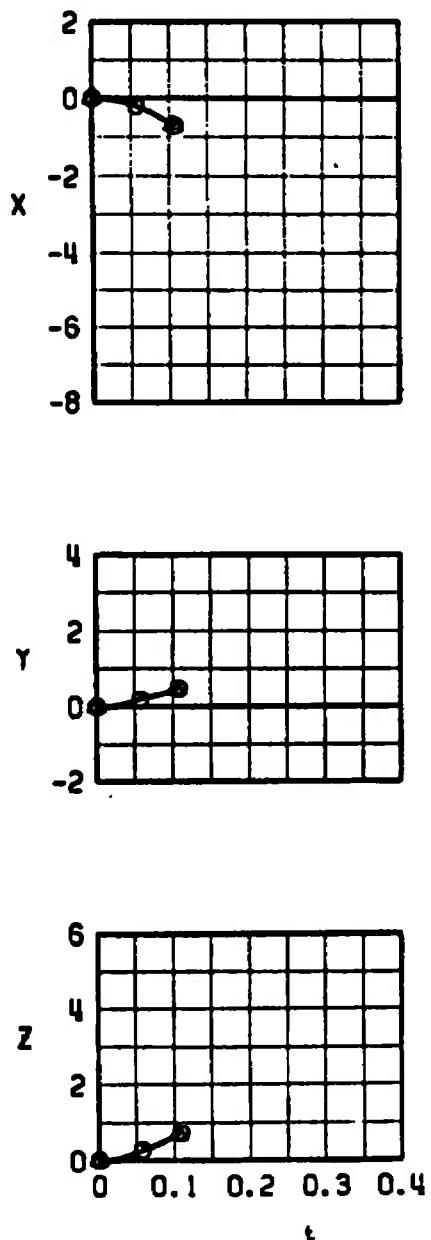
b. $M_\infty = 0.62$, Configuration 3E
Fig. 21 Concluded
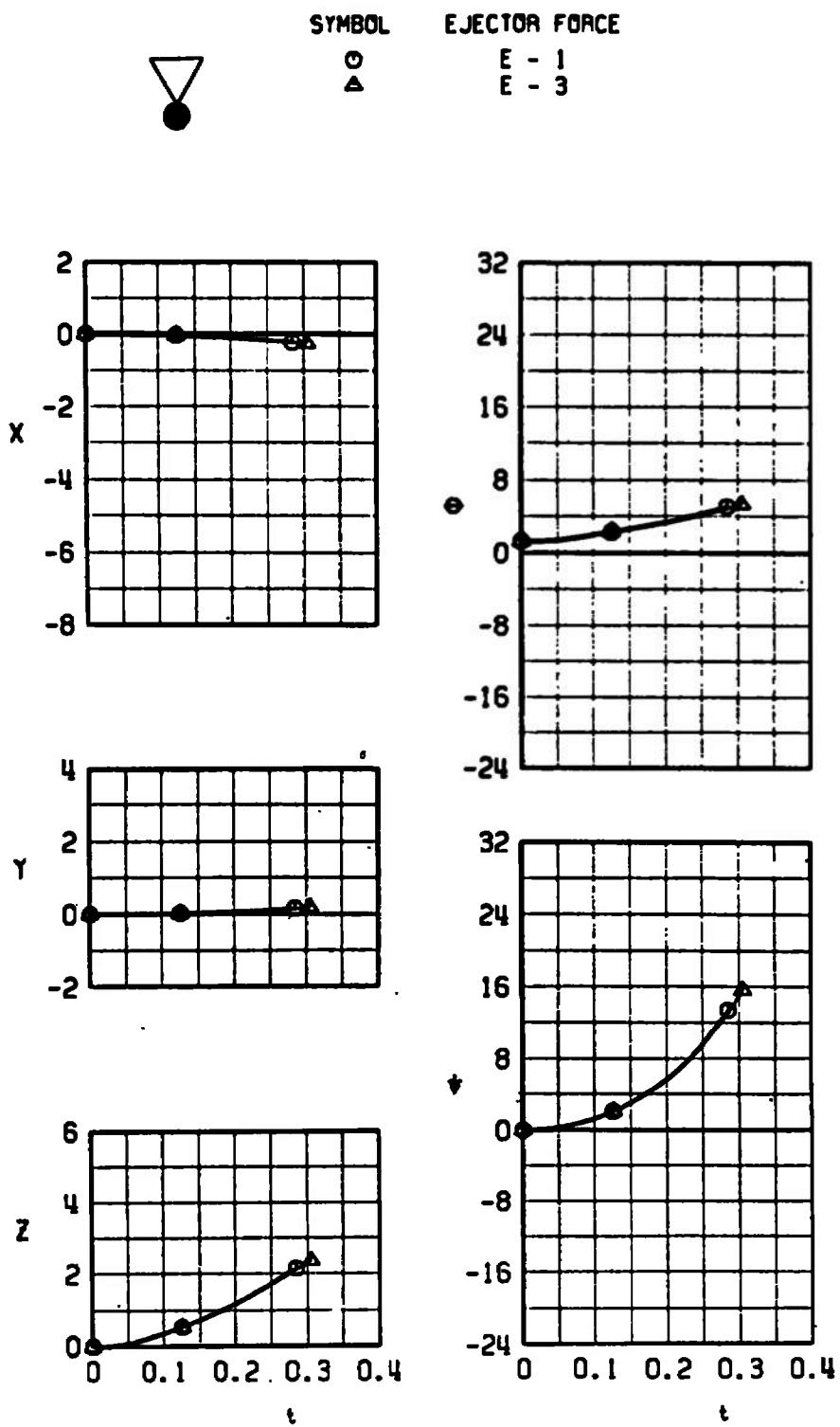
a. TER, M∞ = 0.62, Configuration 5H
Fig. 22 Comparison of Trajectories of the LAU-61/A (Full with the Heavy Warhead) from the Inboard TER and Centerline MER with Lugs Shifted 6 in. Forward for Ejector Forces E-1 and E-3
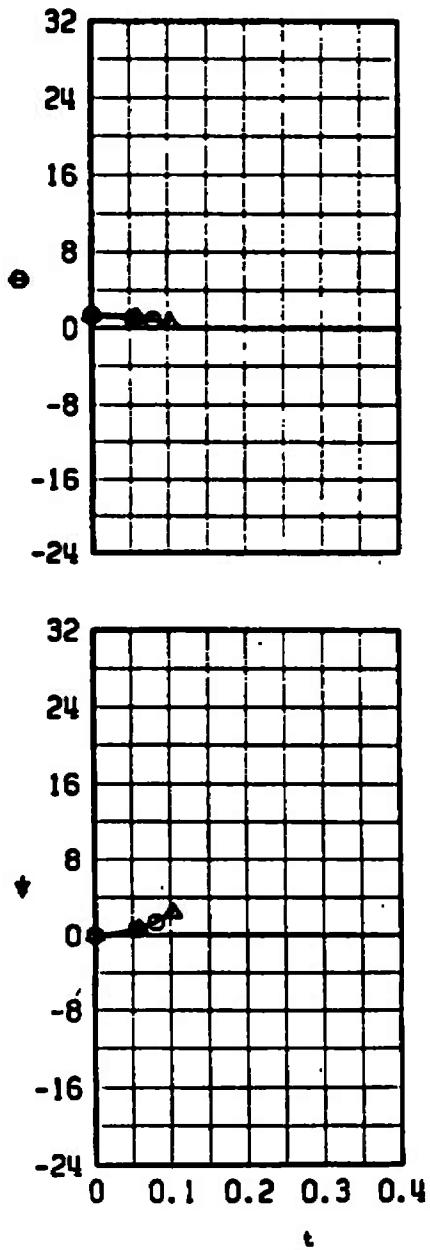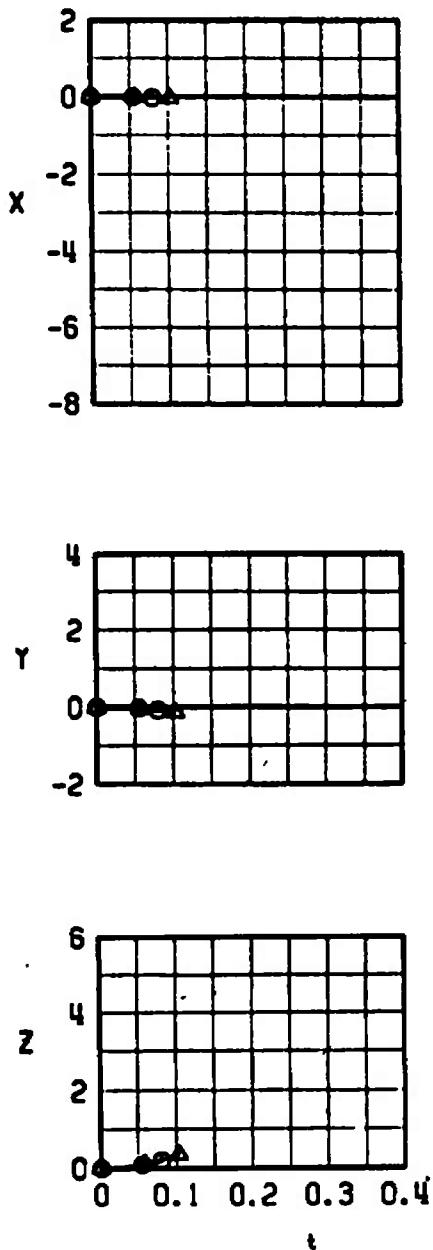
b. TER, $M_\infty = 0.62$, Configuration 7H
Fig. 22 Continued
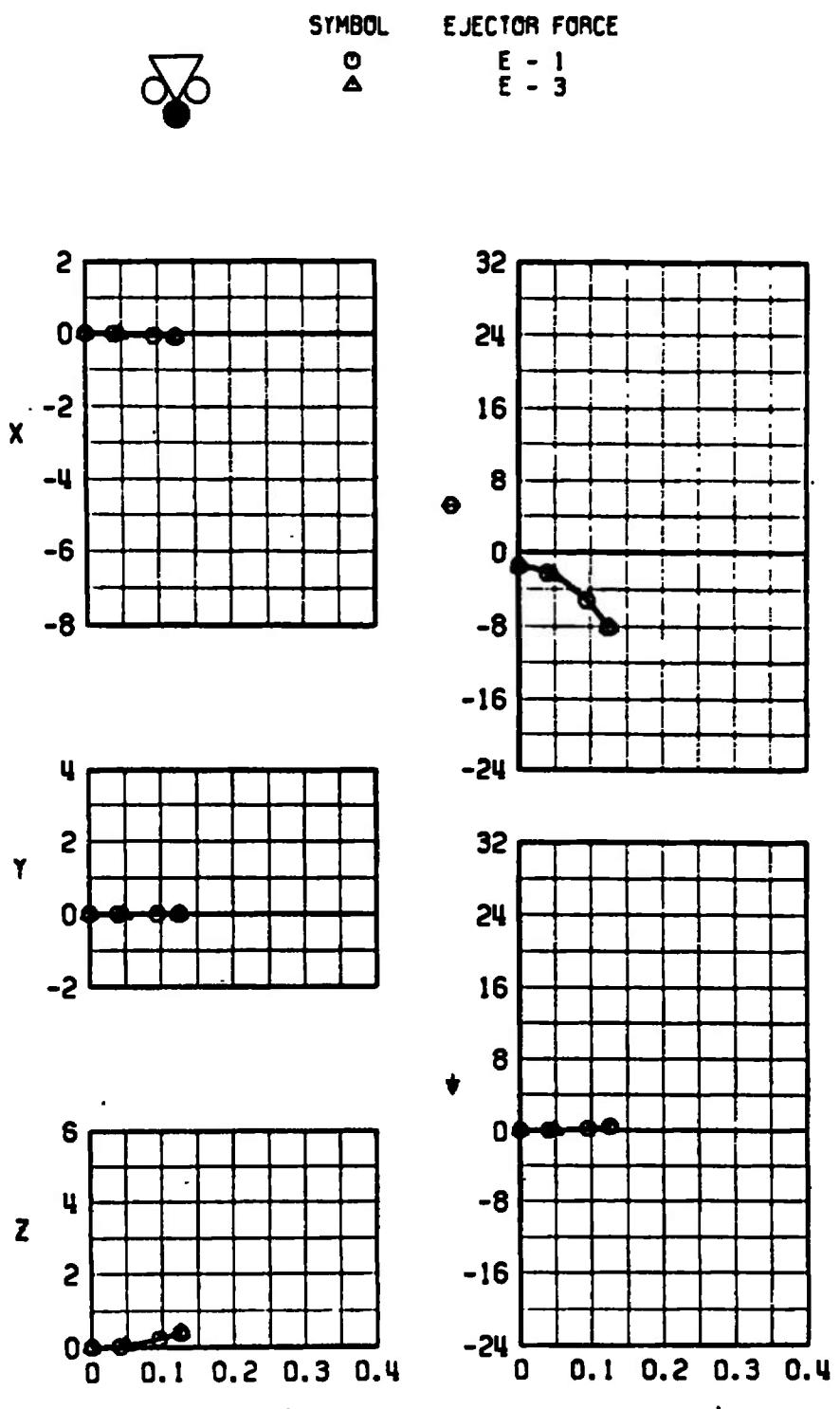
c. MER, M_∞ = 0.78, Configuration 8H

Fig. 22 Concluded

65
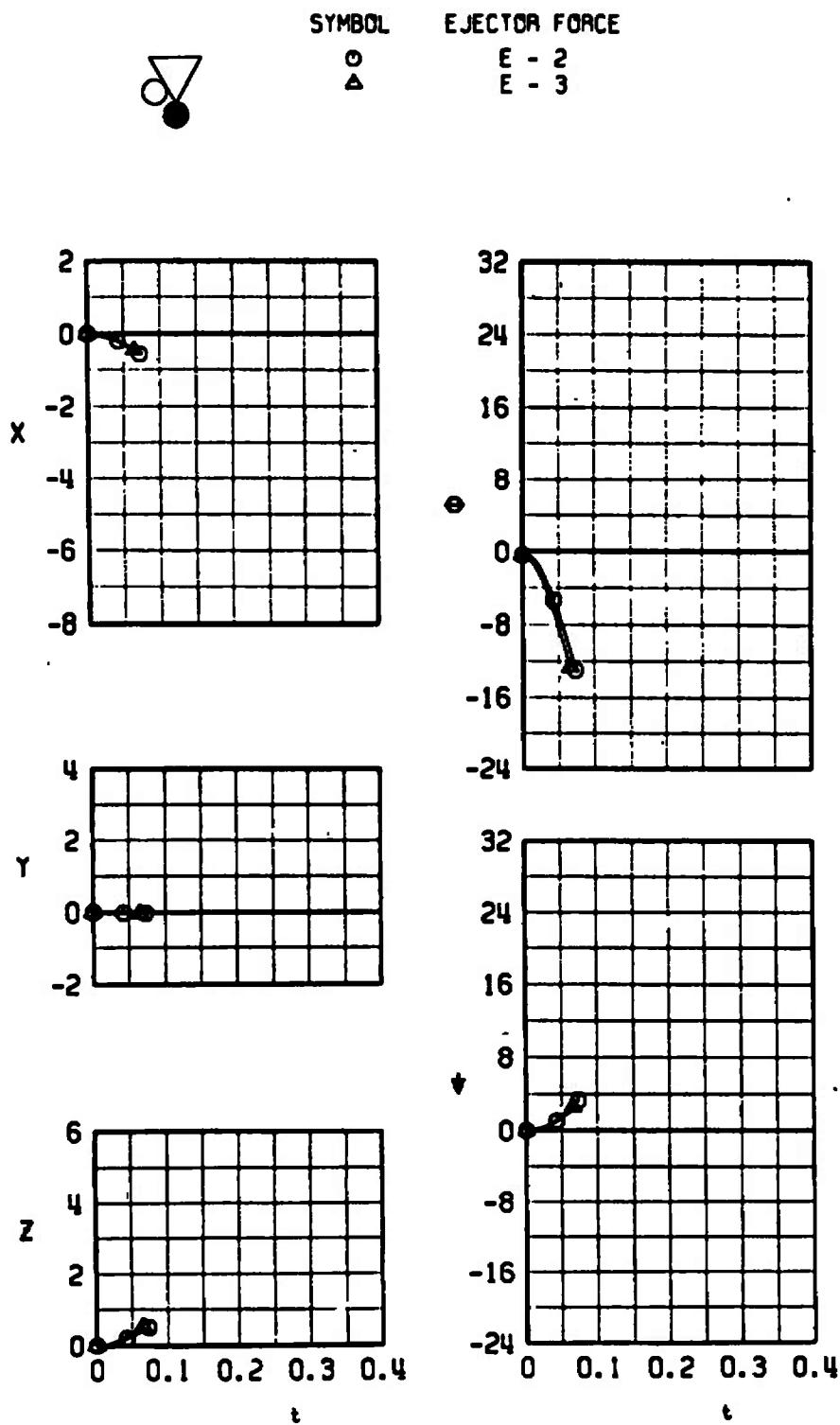
a. $M_\infty = 0.78$, Configuration 4E, Lugs Shifted 6 in.
Fig. 23 Comparison of Trajectories of the Empty LAU-61/A from the Inboard TER with Lugs Shifted 6 and 3 in. Forward for Ejector Forces E-2 and E-3
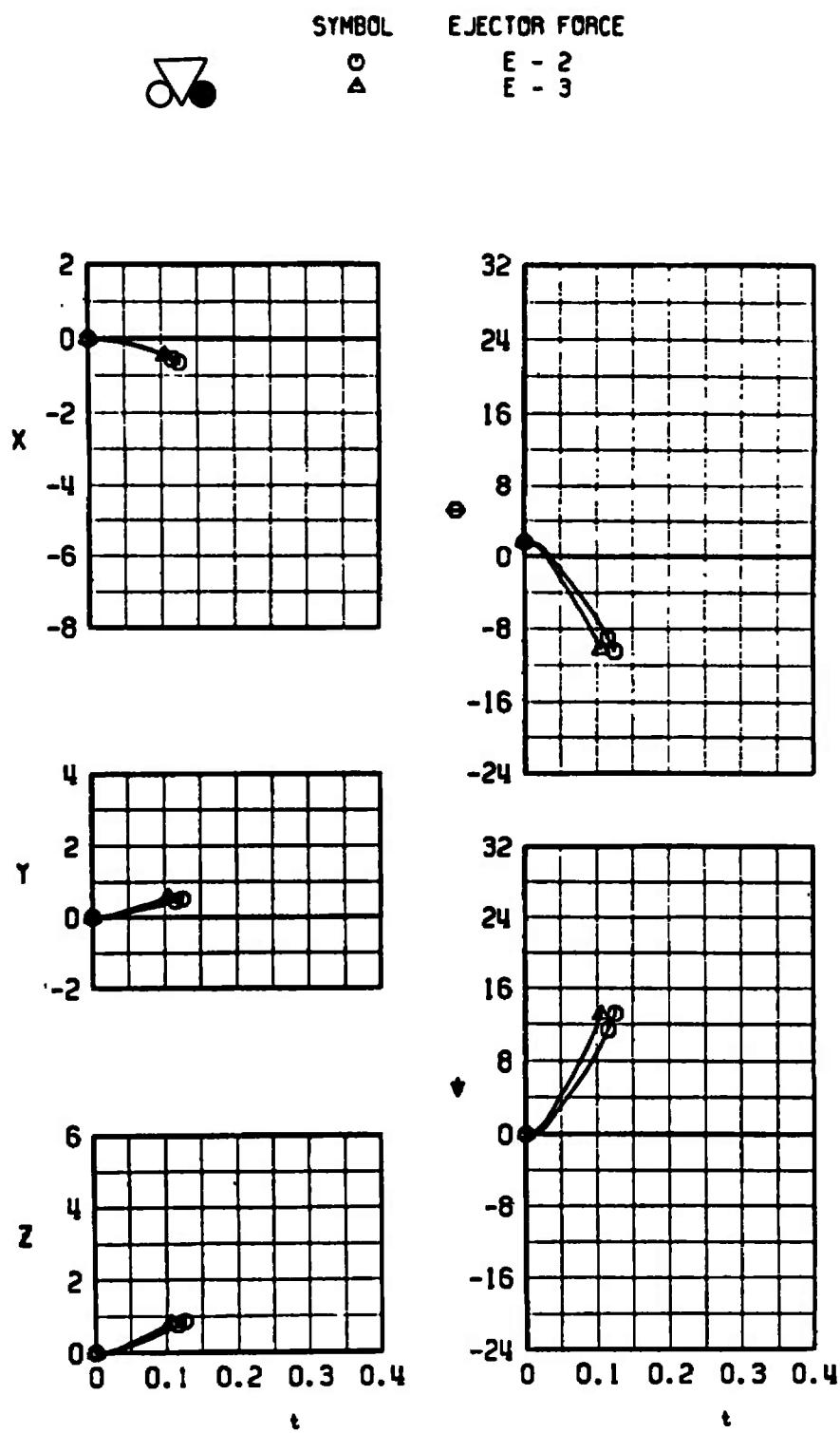
b. $M_\infty = 0.53$, Configuration 6E, Lugs Shifted 6 in.
Fig. 23 Continued
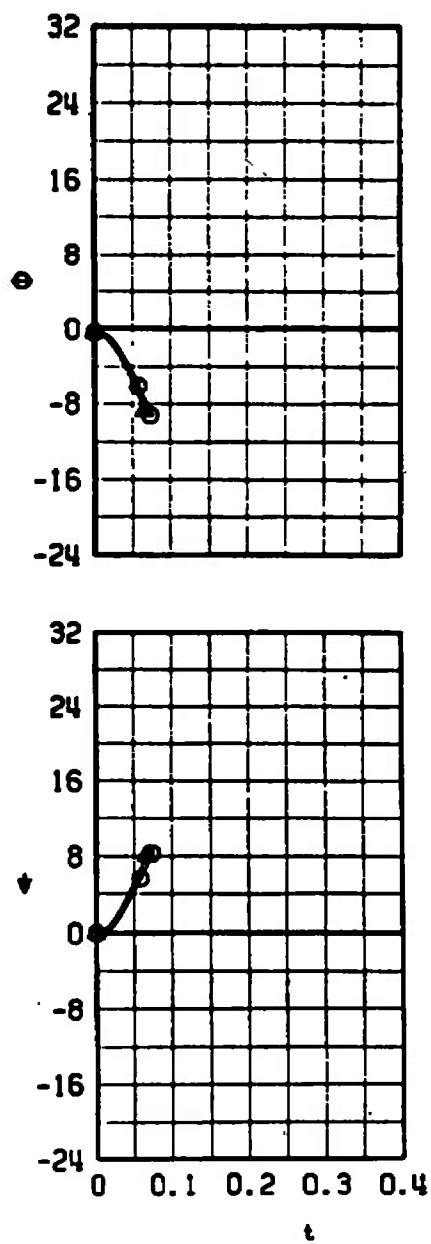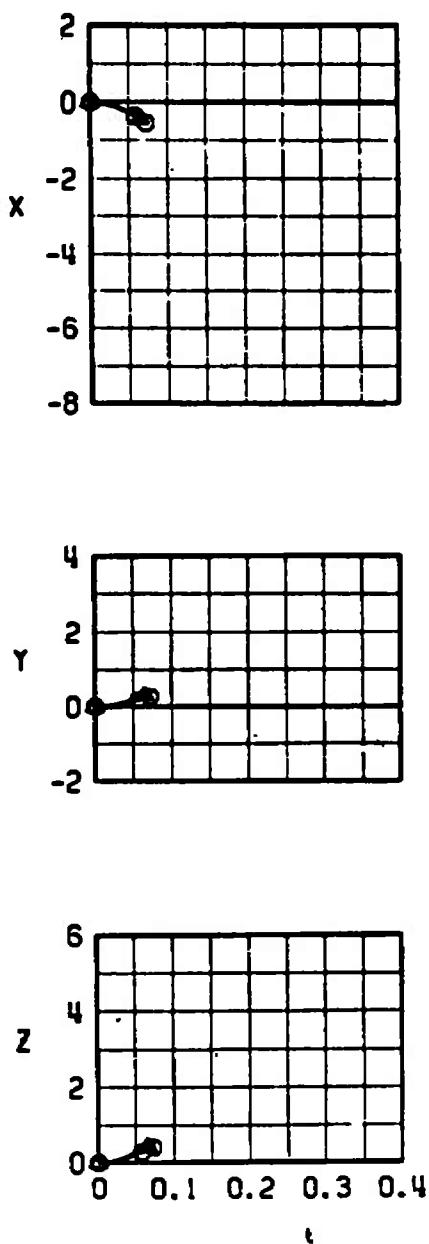
c. $M_\infty = 0.78$, Configuration 6E, Lugs Shifted 6 in.
Fig. 23 Continued
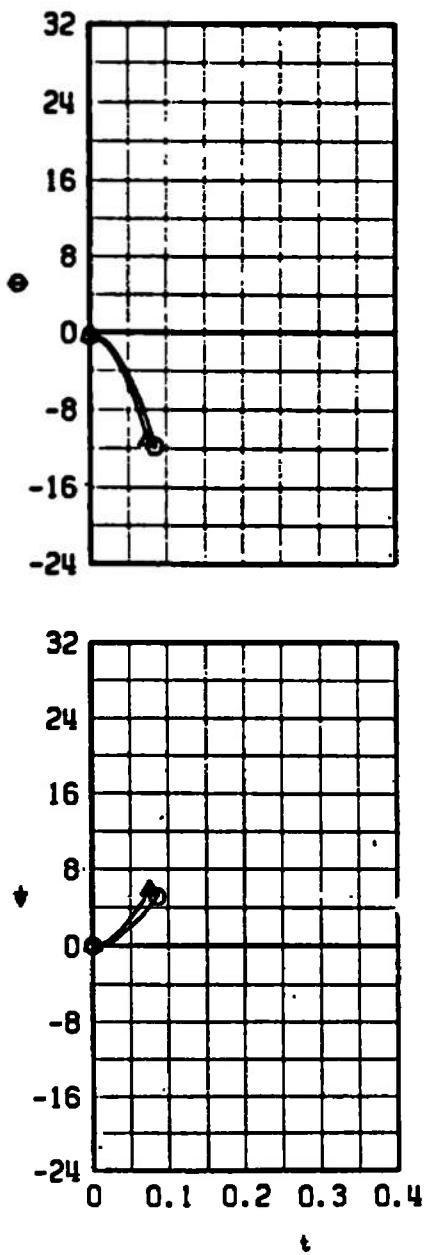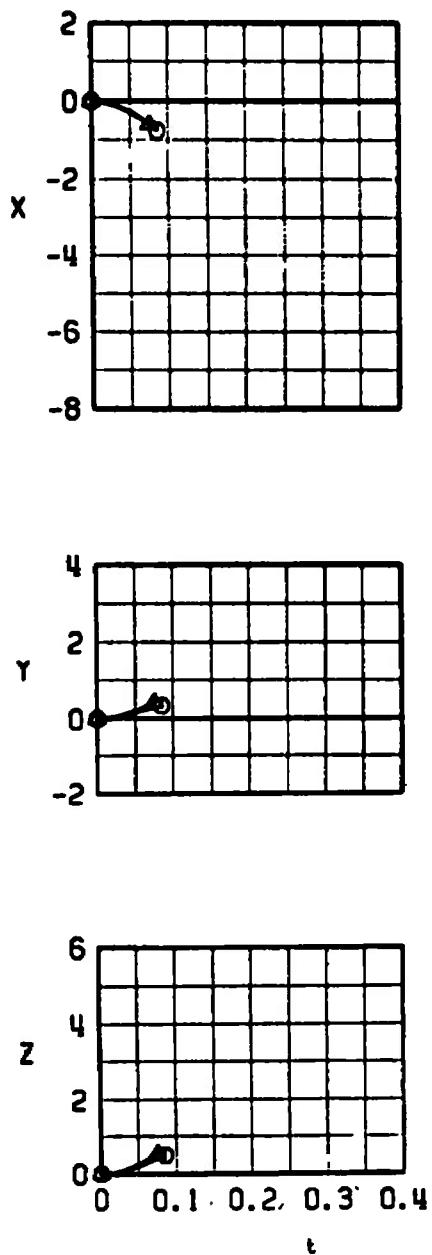
d. $M_\infty = 0.78$, Configuration 3E, Lugs Shifted 3 in.
Fig. 23 Continued
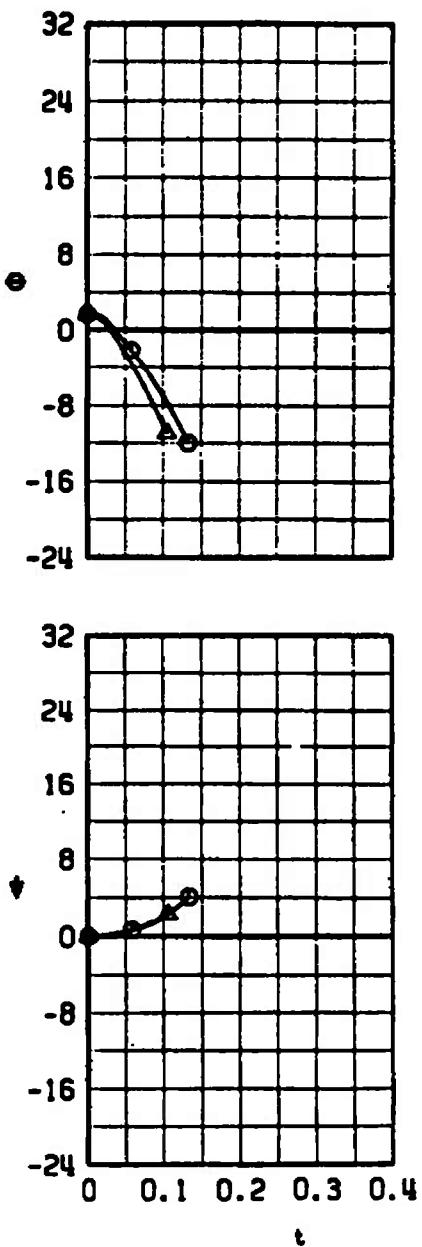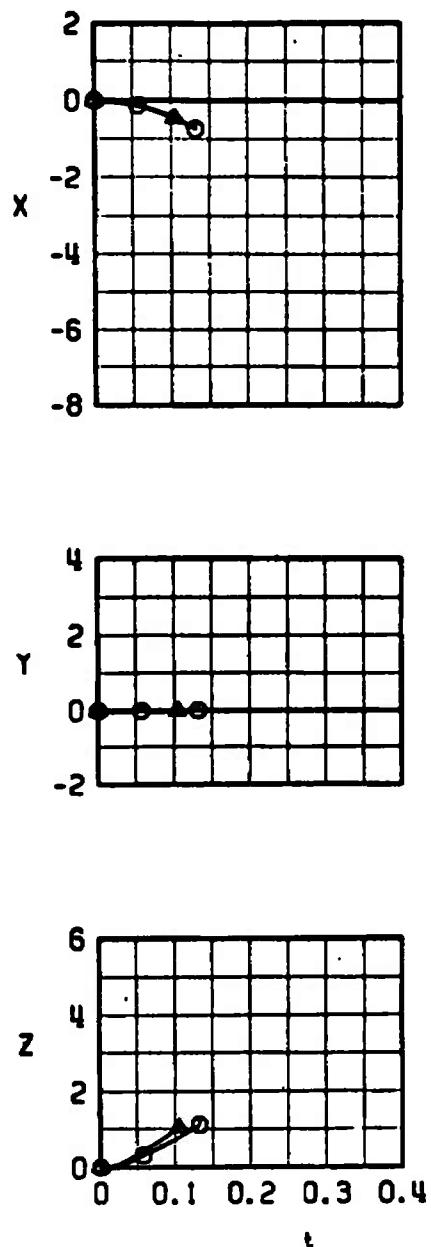
e. $M_\infty = 0.53$, Configuration 4E, Lugs Shifted 3 in.
Fig. 23 Continued
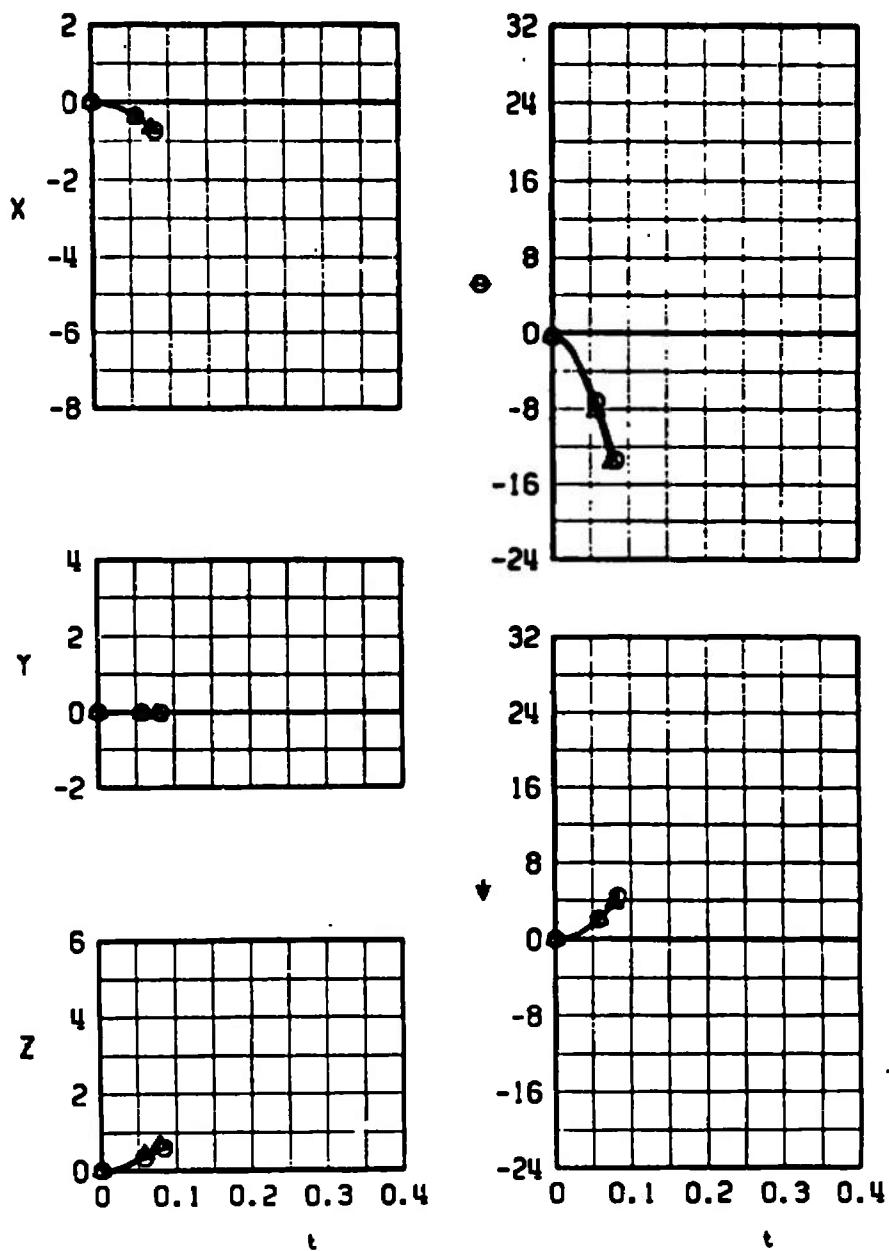
f. $M_\infty = 0.78$, Configuration 4E, Lugs Shifted 3 in.
Fig. 23 Continued
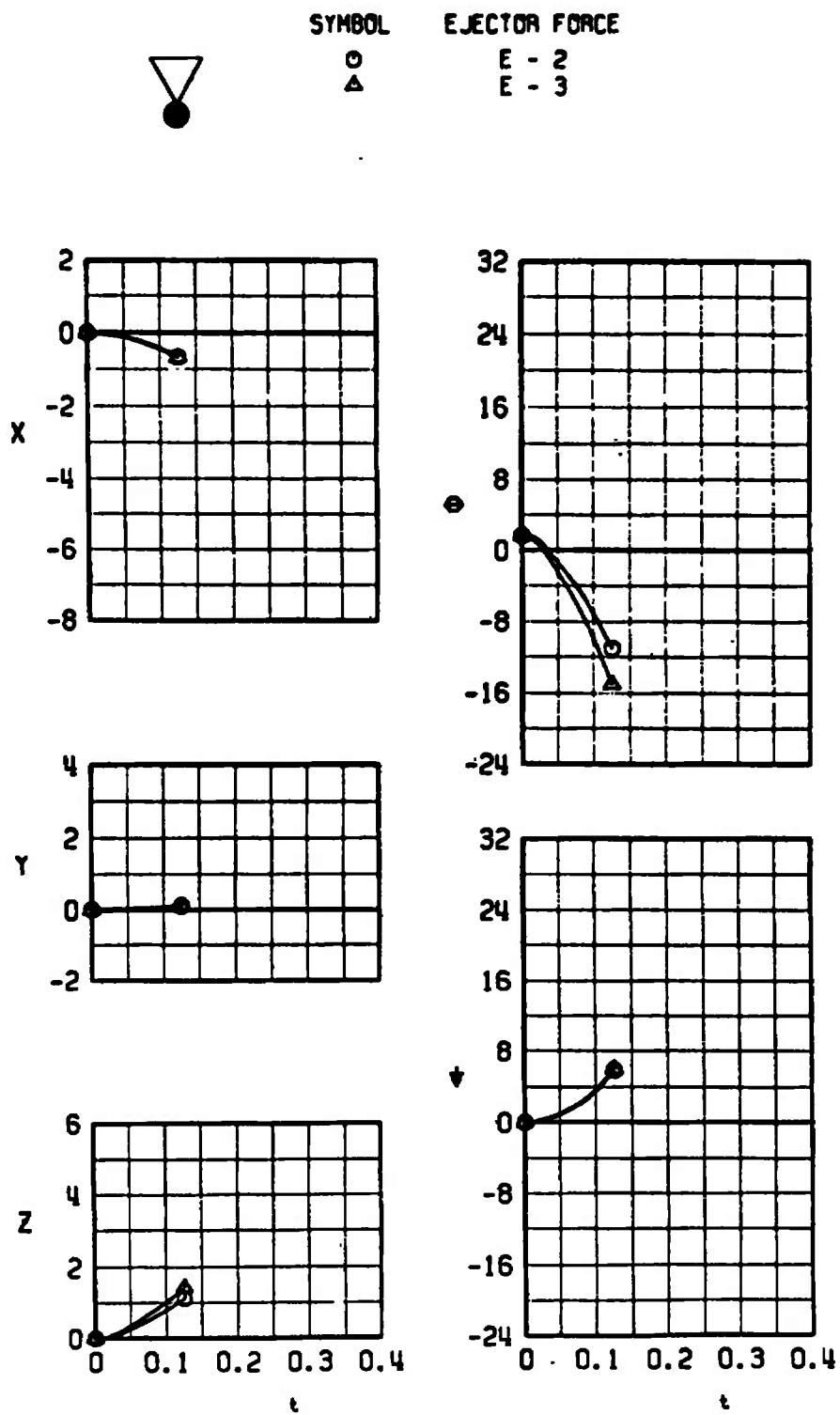
g. $M_\infty = 0.53$, Configuration 5E, Lugs Shifted 3 in.
Fig. 23 Continued
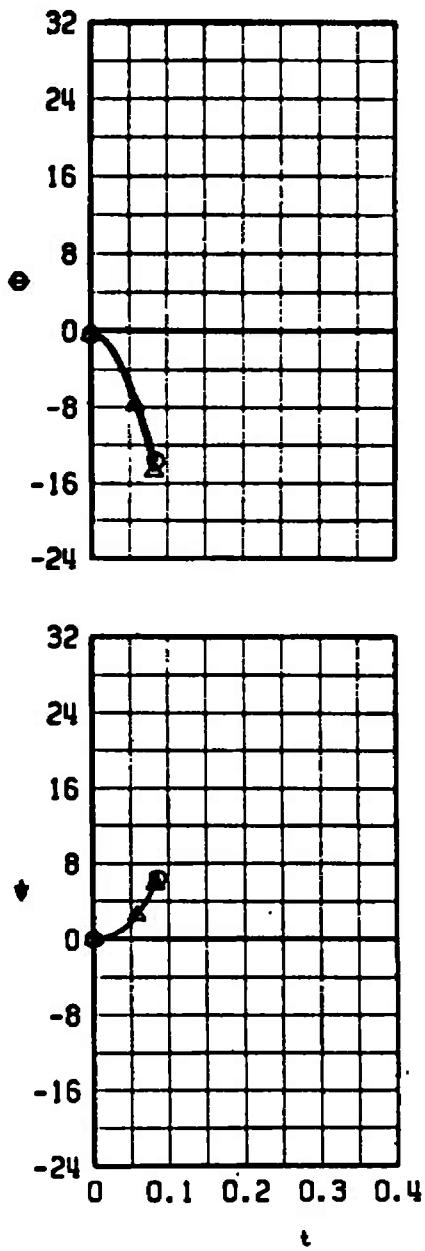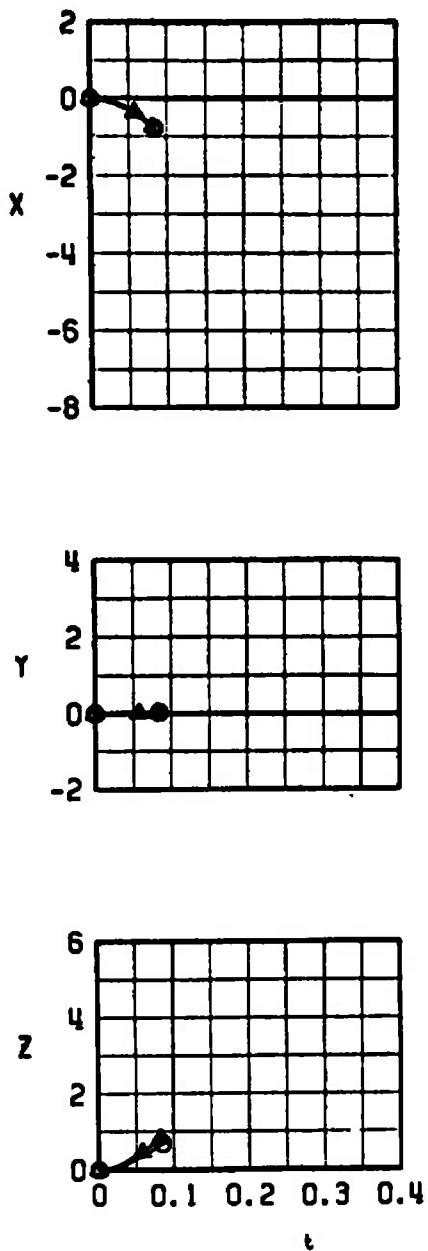
h. $M_\infty = 0.78$, Configuration 5E, Lugs Shifted 3 in.
Fig. 23 Concluded

TABLE I
FULL-SCALE LAU-61/A STORE PARAMETERS USED IN TRAJECTORY CALCULATIONS

Parameter	Full (Heavy)	Full (Light)	Empty
Pitch-Damping Derivative, C_{m_q}, per radian	-27	-27	-45
Yaw-Damping Derivative, C_{n_r}, per radian	-27	-27	-45
Mass, $\overline{m}$, Slugs	26.438	21.449	4.128
Center of Gravity with Respect to Store Nose, X_{cg}, ft	3.008	3.409	2.575
Store Reference Width, b, ft	1.308	1.308	1.308
Store Reference Area, S, ft^2	1.344	1.344	1.344
Ejector Piston Location Relative to Store cg, X_L, ft			
Lugs Shifted 6 in.	-0.205	0.1950	0.795
Lugs Shifted 3 in.	-0.455	-0.0545	0.545
Moment of Inertia, I_{xx}, Slug-ft^2	4.538	3.827	0.974
Moment of Inertia, I_{yy}, Slug-ft^2	56.516	41.375	10.396
Moment of Inertia, I_{zz}, Slug-ft^2	55.467	40.980	9.945

TABLE II
LAU-61/A LOAD CONFIGURATIONS

Configuration*	Centerline Pylon with MER	Inboard Pylon with TER	Outboard Pylon
1H, 1L, 1E	Dummy Sta. 2,6	Launch Sta. 1 Dummy Sta. 2,3	370-gal Fuel Tank
2H, 2L, 2E		Launch Sta. 2 Dummy Sta. 3	
3H, 3L, 3E		Launch Sta. 3	
4H, 4L, 4E		Launch Sta. 1 Dummy Sta. 2	
5H, 5L, 5E		Launch Sta. 1	
6H, 6L, 6E		Launch Sta. 3 Dummy Sta. 2	
7H, 7L, 7E		Launch Sta. 2	
8H, 8L, 8E	Launch Sta. 2 Dummy Sta. 4,6	Empty TER	
9H, 9L, 9E	Launch Sta. 6 Dummy Sta. 4		
10H, 10L, 10E	Launch Sta. 6		

*Suffixes H and L refer to heavy or light warhead, and E indicates an empty launcher.

DOCUMENT CONTROL DATA - R & D

(Security classification of title, body of abstract and indexing annotation must be entered when the overall report is classified)

1. ORIGINATING ACTIVITY *(Corporate author)*	2a. REPORT SECURITY CLASSIFICATION
Arnold Engineering Development Center Arnold Air Force Station, TN 37389	UNCLASSIFIED
	2b. GROUP N/A

3 REPORT TITLE

SEPARATION CHARACTERISTICS OF THE REDESIGNED LAU-61/A ROCKET LAUNCHER FROM THE F-4C AIRCRAFT AT MACH NUMBERS FROM 0.53 TO 0.94

4. DESCRIPTIVE NOTES *(Type of report and inclusive dates)*
Final Report – January 7 to 14, 1972

5. AUTHOR(S) *(First name, middle initial, last name)*

R. A. Paulk, ARO, Inc.

This document has been approved for public release ... distribution is ... Per TAB 16-6-72 D + d 12 mar ets

6. REPORT DATE	7a. TOTAL NO. OF PAGES	7b. NO. OF REFS
March 1972	84	3

8a. CONTRACT OR GRANT NO.	9a. ORIGINATOR'S REPORT NUMBER(S)
	AEDC-TR-72-47
b. PROJECT NO 2592	AFATL-TR-72-57
c. Program Element 64602F	9b. OTHER REPORT NO(S) *(Any other numbers that may be assigned this report)*
d. Task 04	ARO-PWT-TR-72-19

10. DISTRIBUTION STATEMENT Distribution limited to U.S. Government agencies only; this report contains information on test and evaluation of military hardware; March 1972; other requests for this document must be referred to Air Force Armament Laboratory (DLGC), Eglin AFB, FL 32542.

11. SUPPLEMENTARY NOTES	12. SPONSORING MILITARY ACTIVITY
Available in DDC.	Air Force Armament Laboratory (DLGC), Eglin AFB, FL 32542

13. ABSTRACT

A captive-trajectory store separation test was conducted using 0.05-scale models of the F-4C aircraft and the redesigned LAU-61/A rocket launcher(full and empty). The stores were launched from the Multiple Ejection Rack and the Triple Ejection Rack from the centerline pylon and the right-wing inboard pylon, respectively. For the redesigned LAU-61/A the support lugs will be shifted forward either 6 or 3 in. Both positions were used in these tests. The tests were run at Mach numbers 0.53 to 0.94 and at the parent-aircraft angle of attack to give level flight at a simulated altitude of 5000 ft. At selected conditions some of the trajectories were obtained for both constant and time-variant ejector forces.

DD FORM 1473
1 NOV 65

14. KEY WORDS	LINK A		LINK B		LINK C	
	ROLE	WT	ROLE	WT	ROLE	WT
F-4C						
jet aircraft						
external stores						
separation						
transonic wind tunnels						
subsonic flow						
flight simulation						
rocket launchers						

AFSC
Arnold AFS Tenn